Gdański Uniwersytet Medyczny

Małgorzata Juniewicz

Retrospektywna dozymetria promieniowania jonizującego w wybranych szkłach powszechnego użytku metodą spektroskopii EPR w zakresie dawek typowych dla wypadków radiacyjnych

Rozprawa doktorska

Praca została wykonana w Katedrze i Zakładzie Fizyki i Biofizyki
Gdańskiego Uniwersytetu Medycznego

Promotor: prof. dr hab. Bartłomiej Ciesielski

Promotor pomocniczy: dr n. med. Agnieszka Marciniak

Gdańsk 2023

PODZIĘKOWNIA

Pragnę złożyć podziękowania wszystkim osobom, dzięki którym powstanie tej pracy było możliwe.

W szczególności serdecznie dziękuję mojemu Promotorowi ***Panu prof. dr hab. Bartłomiejowi Ciesielskiemu*** *za nieocenioną pomoc przy realizacji niniejszej pracy, cenne uwagi, wyrozumiałość oraz życzliwość. Dziękuję za poświęcony czas i opiekę naukową, która cały czas motywowała mnie do dalszego zgłębiania wiedzy.*

Dziękuję mojej Promotor pomocniczej ***dr n. med. Agnieszce Marciniak*** *za nieocenioną pomoc, nieustanną motywację, nadzór nad harmonogramem oraz wspaniałą atmosferę w pracy naukowej i nie tylko.*

Chciałabym również podziękować fizykom z Katedry i Kliniki Onkologii i Radioterapii GUM, w szczególności ***mgr Anicie Prawdzik-Dampc*** *za wieloletnią współpracę oraz poświęcony czas.*

Słowa podziękowania kieruję również do całej mojej ***Rodziny oraz Przyjaciół*** *za ogromne wsparcie. W szczególności dziękuję mojemu* ***mężowi Marcinowi*** oraz ***córce Oliwii*** *i* ***synowi Aleksandrowi*** *za niezłomną cierpliwość, wyrozumiałość oraz wiarę w moje możliwości. Wasze wsparcie było nieocenione w chwilach zwątpienia.*

SPIS TREŚCI

WYKAZ ARTYKUŁÓW WCHODZĄCYCH W SKŁAD ROZPRAWY DOKTORSKIEJ

1. **Juniewicz M**, Ciesielski B, Marciniak A, Prawdzik-Dampc A. *Time evolution of radiation-induced EPR signals in different types of mobile phone screen glasses*. Radiation and Environmental Biophysics. 2019; 58(4): 493-500. DOI: https://doi.org/10.1007/s00411-019-00805-1

   IF: 1.321, MNiSW: 70.000

2. **Juniewicz M**, Marciniak A, Ciesielski B, Prawdzik-Dampc A, Sawczak M, Boguś P. *The effect of sunlight and UV lamp exposure on EPR signals in X-ray irradiated touch screens of mobile phones.* Radiation and Environmental Biophysics. 2020; 59(3):539-552. DOI: 10.1007/s00411-020-00858-7

   IF: 1.925, MNiSW: 70.000

3. Marciniak A, Ciesielski B, **Juniewicz M.** *EPR dosimetry in glass – a review.* Radiation and Environmental Biophysics. 2022; 61(2):179-203. DOI: 10.1007/s00411-022-00970-w

   IF: 2.017, MNiSW: 70.000

4. Marciniak A, **Juniewicz M**, Ciesielski B, Prawdzik-Dampc A, Karczewski J. *Comparison of three methods of EPR retrospective dosimetry in watch glass*. Frontiers in Public Health. 2022, 10. DOI: https://doi.org/10.3389/fpubh.2022.1063769

   IF: 6.461, MNiSW: 100.000

Sumaryczny wskaźnik Impact Factor: 11.724

Sumaryczna punktacja ministerstwa: 310.000

WYKAZ SKRÓTÓW

ADM –	metoda dawki dodanej	*ang. Added Dose Method*
AD&HM –	metoda dawki dodanej i wygrzewania	*ang. Added Dose&Heating Method*
ARS –	ostry zespół popromienny	*ang. Acute Radiation Syndrome*
BG –	sygnał tła	*ang. background signal*
IAEA –	Międzynarodowa Agencja Energii Atomowej	*ang. International Atomic Energy Agency*
CM –	metoda kalibracyjna	*ang. Calibration Method*
DF –	współczynnik zaniku	*ang. decay factor*
D_L –	minimalna wykrywalna dawka	*ang. Detection Limit*
EDS –	Spektroskopia Dyspersji Energii	*ang. Energy Dispersion Spectroscopy*
EPR –	elektronowy rezonans paramagnetyczny	*ang. Electron Paramagnetic Resonance*
g –	współczynnik rozszczepienia spektroskopowego	*ang. spectroscopic splitting factor*
GG –	szkło Gorilla Glass	*ang. Gorilla Glass*
ILC –	międzynarodowy projekt dozymetrii porównawczej	*ang. Inter-laboratory Comparison*
INES –	Międzynarodowa Skala Zdarzeń Jądrowych i Radiologicznych	*ang. International Nuclear and Radiological Event Scale*
IP –	szkło z telefonu iPhone 6S	*ang. glass from iPhone 6S*
LCF –	współczynnik korekcji wpływu światła	*ang. light correction factor*
LIS –	sygnał indukowany światłem	*ang. light-induced signal*
MG –	szkło mineralne	*ang. mineral glass*
RIS –	sygnał indukowany radiacyjnie, sygnał dozymetryczny	*ang. radiation-induced signal, dosimetric signal*
TG –	szkło ochronne	*ang. tempered glass*
WG –	szkło zegarkowe	*ang. watch glass*

STRESZCZENIE W JĘZYKU POLSKIM

WPROWADZENIE

Obecnie powszechne jest wykorzystanie źródeł promieniotwórczych w wielu dziedzinach działalności człowieka, m.in. w przemyśle, medycynie – zarówno w diagnostyce jak i terapii, badaniach naukowych oraz technikach pomiarowych. W Polsce w latach 2001-2015 nastąpił prawie trzykrotny wzrost liczby podmiotów, które wykorzystują promieniowanie jonizujące w różnych formach ich działalności. Pomimo stosowania wielu środków ostrożności dochodzi do przypadków napromieniowania ludzi niekontrolowanymi dawkami, które nie pozostają obojętne dla ich zdrowia i życia [1]. Wykorzystanie materiałów promieniotwórczych może również wystąpić podczas działań wojennych lub ewentualnych ataków terrorystycznych.

Zgodnie z definicją Międzynarodowej Agencji Energii Atomowej (*ang. International Atomic Energy Agency, IAEA*) wypadek radiacyjny określa się jako „zdarzenie, które doprowadziło do znaczących konsekwencji dla ludzi, środowiska lub obiektu". Przykładem poważnego „wypadku radiacyjnego" było uszkodzenie rdzenia reaktora i uwalnianie dużej ilości promieniowania, jak na przykład podczas katastrofy w Czarnobylu w 1986 roku czy w awarii elektrowni jądrowej w Fukushimie w 2011 roku [2]. Międzynarodowa Skala Zdarzeń Jądrowych i Radiologicznych (*ang. International Nuclear and Radiological Event Scale, INES*), stosowana w ponad 60 krajach, klasyfikuje zdarzenia radiacyjne na siedmiu poziomach: poziomy 1–3 nazywane są „incydentami", a poziomy 4–7 „wypadkami". Skala INES uwzględnia dawkę promieniowania dla ludzi i środowiska w pobliżu lokalizacji, rozprzestrzenianie się materiałów promieniotwórczych zamkniętych w instalacji oraz zdarzenia, w przypadku których nie zadziałały środki zapobiegawcze. Na przykład eksplozja reaktora w Czarnobylu została oceniona jako poważna awaria na poziomie 7. Ponadto, znaczący wypadek radiacyjny to taki, w którym ekspozycja osoby poszkodowanej na promieniowanie spełnia co najmniej jedno z następujących kryteriów:

(1) dawka na całe ciało jest równa lub przekracza 0,25 Gy,
(2) dawka na skórę jest równa lub przekracza 6 Gy,
(3) dawka pochłonięta (ze źródła zewnętrznego) przez inne tkanki lub narządy jest równa lub większa niż 0,75 Gy [3].

Główną konsekwencją wypadku radiacyjnego są szkody wyrządzone ludziom, którzy przebywali w miejscu zdarzenia oraz w jego sąsiedztwie. Zespół objawów klinicznych, które występują po napromieniowaniu całego ciała lub znacznej części ciała (ponad 60%) dawkami powyżej 1 Gy opisuje się terminem ostrego zespołu popromiennego (*ang. Acute Radiation Syndrome, ARS*) [4].

Masowe narażenie na promieniowanie ludności nie posiadającej w czasie wypadku osobistego dozymetru wymaga segregacji (tzw. triażu) poszkodowanych w celu wdrożenia odpowiednich procedur medycznych. Europejski konsensus dotyczący postępowania medycznego w przypadku masowego narażenia na promieniowanie uzyskano w 2005 roku podpisując protokół METREPOL (Medical Treatment Protocols for Radiation Accident) [5]. Zgodnie z tym protokołem w czasie pierwszych 48 godzin ofiary wypadku powinny być objęte systemem segregacji doraźnej, w którym poszkodowani są oceniani zarówno na podstawie danych klinicznych, jak i innych kryteriów pozwalających na ocenę pochłoniętej dawki. Narażenie całego ciała lub znacznej jego części na dawkę 4-5 Gy jest potencjalnie śmiertelne dla połowy napromieniowanych ludzi. Specjalistyczna opieka medyczna może znacznie zwiększyć prawdopodobieństwo przeżycia tych, którzy otrzymali dawki rzędu 3–7 Gy na całe ciało [2]. Ponadto, znajomość wielkości dawki pochłoniętej ma szczególne znaczenie przy ocenie ryzyka wystąpienia późnych powikłań oraz efektów stochastycznych.

W ocenie indywidualnych dawek nawet po wielu miesiącach od narażenia, w celu wsparcia diagnozy czy też wyboru sposobu leczenia, znajduje zastosowanie dozymetria retrospektywna. Termin ten odnosi się do metod określania dawki pochłoniętej po wystąpieniu zdarzenia radiacyjnego w sytuacjach, gdy konieczna lub wymagana jest ocena dawek u osób narażonych, a konwencjonalne dozymetry nie były dostępne lub były niewystarczające [6].

Metody dozymetrii retrospektywnej można podzielić na 2 grupy:

(1) fizyczne – oparte na metodach fizycznych, w szczególności wyróżniamy tu spektroskopię elektronowego rezonansu paramagnetycznego (*ang. Electron Paramagnetic Resonance, EPR*), techniki luminescencyjne – termoluminescencji (TL) i optycznie stymulowanej luminescencji (OSL),

(2) biologiczne – takie jak np. metody cytogenetyczne oceny zmian chromosomów w limfocytach krwi obwodowej (tworzenie chromosomów dicentrycznych, translokacji, mikrojąder).

Metody fizyczne wykorzystują do badań zarówno niektóre tkanki biologiczne (szkliwo zębów, kości, paznokcie) jak i materiały sztuczne znajdujące się w przedmiotach powszechnego użytku (telefony komórkowe, urządzenia elektroniczne, zegarki, okulary) w celu pomiaru zmian wywołanych promieniowaniem w tych materiałach. Spektroskopia EPR jest jedną z czułych metod wykrywających te zmiany. Pozwala na identyfikację oraz ilościową charakterystykę centrów paramagnetycznych (np. wolnych rodników) indukowanych przez promieniowanie jonizujące w badanych substancjach na podstawie pomiaru ich sygnałów EPR [7, 8]. Dla praktycznego zastosowania spektroskopii EPR w dozymetrii powypadkowej zasadnicze znaczenie ma wskazanie materiałów mogących pełnić funkcję detektora-dozymetru i określenie dokładności tej metody. Czułość takiego materiału na promieniowanie charakteryzuje minimalna wykrywalna dawka (*ang. Detection Limit,* D_L) dla określonej metody dozymetrycznej. Dla szkieł stanowiących materiał badawczy w tej pracy doktorskiej parametr D_L wynosił ok. 0,05-2,00 Gy, co jest wystarczające dla triażu osób poszkodowanych w wypadkach radiacyjnych przed podjęciem koniecznych działań medycznych. Uzasadnia to badania podejmowane przez wielu badaczy nad charakterystyką dozymetrii EPR w szkłach pozyskanych z zegarków lub z ekranów telefonów komórkowych (i innych przenośnych urządzeń elektronicznych), w tym w szkle Gorilla Glass (GG), które w ostatnich latach jest szeroko stosowane w produkcji ekranów dotykowych.

Dozymetria EPR w szkłach była dotychczas przedmiotem kilku międzynarodowych projektów dozymetrii porównawczej (*ang. Inter-laboratory Comparison,* ILC), w których uczestniczył również zespół badawczy Katedry i Zakładu Fizyki i Biofizyki w 2012 i 2021 roku [9, 10].

Telefony komórkowe prawdopodobnie stanowią jeden z najbardziej wszechobecnych przedmiotów osobistego użytku – na początku 2023 roku łączna liczba ich użytkowników na świecie wynosiła około 5,4 miliarda [11] – co odpowiada blisko 70% całej światowej populacji. Ponadto, telefony komórkowe często trzymane są blisko ciała, co jest dodatkowym atutem umożliwiającym wiarygodne odtworzenie dawki pochłoniętej przez ich użytkowników na podstawie dawki pochłoniętej przez szkło ekranów ich telefonów.

Szkło jest nieorganicznym, amorficznym, przezroczystym materiałem ceramicznym. Wykazuje potencjał jako materiał przydatny dla dozymetrii EPR ze względu na jego wszechobecność w środowisku człowieka, odporność na wodę i wiele chemikaliów, niską przewodność elektryczną i małe straty dielektryczne, co umożliwia szybkie pomiary EPR bez specjalnej, pracochłonnej preparatyki próbek. Jego właściwości zależą od metody

produkcji i składu chemicznego. Ponadto, w przeciwieństwie do próbek biologicznych, próbki szkła są zwykle dostępne w wystarczającej, optymalnej ilości, umożliwiającej czułe pomiary sygnałów EPR.

W skład widma EPR napromieniowanych próbek szkła wchodzą sygnały:

(1) BG (*ang. background signal*) – natywny sygnał tła próbki nienapromieniowanej, zazwyczaj złożony, szeroki i stabilny w temperaturze pokojowej, o wartości współczynnika rozszczepienia spektroskopowego g≈2,0 dla szkieł zegarkowych [12, 13, 14, 15, 16] i Gorilla Glass (GG) [17]. W szkle mineralnym (MG) i hartowanym (TG) z telefonów komórkowych szerokie linie zaobserwowano w zakresie g=1,98-2,01 [18, 19, 20]. Kształt widma BG jest indywidualny dla różnych rodzajów szkieł, a pochodzenie tego sygnału jest różne i jak dotąd nie zostało całkowicie wyjaśnione. Griscom [21] przypisał sygnały EPR w nienapromieniowanym szkle obecności jonów grup przejściowych, osadów ferromagnetycznych, centrów fotoindukowanych i defektów indukowanych mechanicznie. Również Bassinet i in. [22] oraz Trompier i in. [23] zasugerowali, że sygnał tła jest generowany podczas procesu produkcyjnego przez zanieczyszczenia w szkle. McKeever i in. [24] stwierdzili, że ekspozycja szkła na światło ultrafioletowe (UV) może być jednym z czynników wywołujących tło.

(2) LIS (*ang. light-induced signal*) – sygnał spowodowany naturalną ekspozycją telefonu/zegarka na światło słoneczne zawierające składową UV, bądź też na światło z lamp (np. wykorzystywanych do utwardzania kleju przy produkcji telefonów [24] lub z lamp UV stosowanych w solariach, gabinetach kosmetycznych itp.).

(3) RIS (*ang. radiation-induced signal*) – sygnał dozymetryczny indukowany przez promieniowanie jonizujące; centra paramagnetyczne będące źródłem tego sygnału są głównie przypisywane brakującemu wiązaniu tlenowemu między atomami krzemu (centra E'), niemostkowymi centrami dziur tlenowych (NBOHC) i rodnikami nadtlenowymi [21]. Stwierdzono brak wpływu mocy dawki na kształt i natężenie widm EPR indukowanych promieniowaniem jonizującym do 1,63 kGy/h [25].

Wyzwaniem dla dozymetrii metodą EPR jest częściowe lub całkowite nakładanie się tła na sygnały indukowane przez promieniowanie jonizujące. W pracach opisanych w tej rozprawie doktorskiej zastosowano metodę numerycznego rozkładu widm na ich składowe modelowe: sygnały BG, RIS oraz LIS – dla szkła eksponowanego na światło.

Wykazano, że zastosowanie tej metody umożliwia oddzielenie składowej dozymetrycznej (RIS) od pozostałych komponentów widma EPR (BG oraz LIS) i określenie jej wielkości. Ograniczeniem zastosowania tej metody w realistycznych scenariuszach wypadków radiacyjnych jest konieczność znajomości widm modelowych tych trzech komponentów. Dlatego też podjęto próbę (Artykuł 4) opracowania metody pozwalającej na rekonstrukcję pochłoniętej dawki bez konieczności posiadania informacji o sygnale tła natywnego badanej próbki. Sygnał modelowy RIS można uzyskać przez dopromieniowanie próbki znaną dawką – co jest niezbędne dla kalibracji sygnału dozymetrycznego względem dawki. Została ona nazwana przez autorów metodą dawki dodanej i wygrzewania (*ang. Added Dose&Heating Method, AD&HM*). W metodzie tej uzyskuje się widmo modelowe BG przez pomiar EPR napromieniowanych próbek szkła zegarkowego po ich wygrzewaniu w temperaturze 200℃ lub 250℃. Wygrzewanie powodowało zanik sygnału RIS pozwalając na odzyskanie sygnału natywnego próbki BG. Jednak konieczne jest przeprowadzenie dalszych badań w celu weryfikacji stosowalności AD&HM dla innych rodzajów szkieł oraz optymalizacji warunków wygrzewania próbek. Perspektywę dla dalszych badań stanowi również poszukiwanie „testu przesiewowego" wskazującego na obecność w badanych próbkach efektów wpływu światła (obecności sygnału LIS). Pominięcie tych efektów może silnie wpływać na wartość zrekonstruowanej dawki, a ich uwzględnienie znacznie komplikuje procedurę i czas potrzebny do oszacowania dawki pochłoniętej – co jest szczególnie istotne w przypadku pomiarów na dużą skalę. Jednym z kierunków badań na przyszłość jest również opracowanie rezonatorów umożliwiających pomiary EPR szkła bez konieczności separacji szkła ekranu (czyli bez uszkodzenia telefonu). Pojawiły się już pierwsze próby takich układów pomiarowych [26].

CELE PRACY

Przeprowadzone badania dotyczyły dozymetrii retrospektywnej opartej na detekcji i pomiarach względnych stężeń stabilnych wolnych rodników wygenerowanych przez promieniowanie jonizujące w szkłach ekranów telefonów komórkowych oraz szkła zegarkowego za pomocą spektroskopii elektronowego rezonansu paramagnetycznego (EPR).

Główne cele pracy:

(1) Zbadanie stabilności sygnałów EPR generowanych radiacyjnie w szkłach oraz określenie wpływu preparatyki próbki (kruszenia, wpływu wody) na sygnał tła i sygnał dozymetryczny EPR w szkłach ekranów smartfonów.

(2) Charakterystyka widm EPR generowanych radiacyjnie w różnych typach szkieł oraz weryfikacja możliwości ich zastosowania jako potencjalnego dozymetru do retrospektywnego określenia dawek pochłoniętych podczas wypadków radiacyjnych w zakresie do kilkudziesięciu Gy.

(3) Zbadanie efektów ekspozycji na światło naturalne i sztuczne szkieł nienapromieniowanych i napromieniowanych promieniowaniem jonizującym, określenie wpływu tych efektów na widma EPR i na wiarygodność dozymetrii oraz zaproponowanie sposobu zminimalizowania tych wpływów na zrekonstruowaną dawkę.

(4) Opracowanie metody pozwalającej na rekonstrukcję pochłoniętej dawki bez konieczności posiadania informacji o sygnale tła natywnego badanej próbki.

Hipotezą roboczą było wykazanie przydatności dozymetrii EPR w szkłach do wstępnego triażu osób napromieniowanych w wypadkach radiacyjnych.

MATERIAŁY I METODY

Materiał badawczy

Badania wykonano przy użyciu 5 typów próbek szkła: (1) Gorilla Glass (GG), (2) szkło mineralne (MG), (3) szkło ochronne (TG) oraz (4) szkło z telefonu iPhone 6S (IP) – pozyskanych z ekranów dotykowych telefonów komórkowych oraz (5) szkła zegarkowego (WG) stanowiącego materiał badawczy w międzynarodowym projekcie dozymetrii porównawczej RENEB ILC 2021 [11, 27]. Część próbek GG użytych do badań było wykorzystywanych również w międzynarodowym projekcie EURADOS Intercomparison 2012 [10].

Skład pierwiastkowy szkieł (Tab. 1) został określony metodą Spektroskopii Dyspersji Energii (EDS) w Instytucie Nanotechnologii i Inżynierii Materiałowej Politechniki Gdańskiej, z wyjątkiem szkła Gorilla Glass, którego skład pierwiastkowy został podany przez organizatorów projektu EURADOS [28].

Tabela 1. Skład pierwiastkowy szkieł.

	SiO_2[%]			**Al_2O_3 [%]**			**Na_2O [%]**	
Gorilla Glass (GG)*	60-80			13-20			nie określono ilościowo	
	w % (+/- 0,5)							
	Si	**Na**	**Mg**	**Al**	**K**	**P**	**Ca**	**O****
szkło mineralne (MG)	23,0	2,5	2,0	7,5	8,0	-	-	57,0
szkło ochronne (TG)	28,0	7,0	2,5	2,5	2,0	-	3,5	54,5
iPhone 6S (IP)	17,5	4,5	1,0	10,5	7,0	4,5	-	55,0
szkło zegarkowe (WG)	27,5	11,0	2,5	1,0	1,0	-	3,0	54,0

* Skład pierwiastkowy szkła GG został podany przez organizatorów projektu EURADOS [28].

**Dokładność pomiaru wynosiła 0,5% dla wszystkich badanych pierwiastków z wyjątkiem tlenu, dla którego dokładność była na poziomie 3,0%.

Preparatyka próbek

Próbki szkieł pozyskano z dotykowych ekranów smartfonów przez ich mechaniczne oddzielenie od pozostałych części telefonu. Szkło zegarkowe otrzymano w postaci całych tarcz zegarkowych od organizatorów projektu RENEB ILC 2021, którego zespół Katedry Fizyki i Biofizyki GUMed był uczestnikiem. Uzyskane fragmenty szkieł pokruszono na mniejsze kawałki, tak aby mieściły się w pomiarowej rurce kwarcowej (o wewnętrznej średnicy 4 mm) umieszczanej we wnęce spektrometru EPR. Próbki szkła oczyszczono z pozostałości klejów, farb oraz innych warstw adhezyjnych i na końcu przemyto etanolem. Tak przygotowane próbki przechowywano w ciemności między kolejnymi pomiarami EPR, poza okresami celowej, kontrolowanej ekspozycji na światło sztuczne lub naturalne, co opisano w częściach poświęconych metodyce badań w artykułach załączonych do niniejszej rozprawy doktorskiej.

Pomiary EPR

Pomiary EPR wykonane zostały przy użyciu spektrometru Bruker EMX 6/1, pracującego w paśmie X (9,85 GHz). Próbki szkła były umieszczone w kwarcowych rurkach o średnicy wewnętrznej 4 mm i mierzone w temperaturze pokojowej. Pomiar pojedynczej próbki wykonywany był w 3 pozycjach, następnie widma te uśredniano. Pomiary EPR wykonywano przy następujących parametrach akwizycji widm: moc mikrofalowa – 22,30 i 32 mW, amplituda modulacji – 0,15 i 0,5 mT, szerokość skanu – 10 mT, czas konwersji

– 81,92 ms, stała czasowa – 163,84 ms i liczba uśrednianych skanów dla jednej pozycji od 5 do 10.

Widma EPR mierzono w obecności standardu wewnątrzwnękowego w postaci niewielkiej ilości proszku MgO naturalnie zanieczyszczonego jonami Mn^{2+} umieszczonego przy dnie wnęki lub korzystając z komercyjnie dostępnego standardu ER 4119HS-2100 Marker Accessory (Bruker BioSPin GmbH, Niemcy). Widma szkieł normalizowano względem masy próbek i względem średniej amplitudy linii standardu.

Napromieniowanie

Napromieniowania próbek dokonano w Katedrze i Klinice Onkologii i Radioterapii Gdańskiego Uniwersytetu Medycznego. Napromieniowano je promieniami X przy użyciu przyspieszacza medycznego Clinac 2300 o napięciu 6 MV w warunkach równowagi elektronowej. Część próbek szkła zegarkowego (Artykuł 4) zostało napromieniowanych aparatem Maxishot SPE 240 kV (Hamburg, Niemcy) o efektywnej wartości energii 75 keV.

Wpływ światła

W pracy (Artykuł 2) badano wpływ ekspozycji szkieł na cztery źródła światła, których charakterystykę przedstawiono w Tabeli 2.

Tabela 2. Charakterystyka źródeł światła.

Źródło światła	**Opis**	**Natężenie promieniowania**
bezpośrednie światło słoneczne	Naświetlenia były wykonywane około południa w słoneczne dni. Całkowita fluencja (w J/m^2) została obliczona przez pomnożenie zmierzonej wartości natężenia promieniowania i czasu trwania ekspozycji.	800 W/m^2
lampa CLEO Advantage 80W-R (Philips)	Układ dwóch równoległych lamp powszechnie stosowanych w solariach o mocy 80 W każda.	48 W/m^2

lampa Ultraviolet Radiant Lamp AP-111 (Alle Paznokcie)	Lampa ultrafioletowa powszechnie stosowana w gabinetach kosmetycznych do utwardzania lakierów do paznokci z 4 żarówkami o mocy 9 W każda.	164 W/m^2
żarówki fluorescencyjne Duluxstar (OSRAM)	Układ 6 żarówek o mocy 24 W każda.	110 W/m^2

Natężenie promieniowania źródeł światła mierzono za pomocą miernika mocy ORION-TH (OPHIR) w punktach umieszczenia próbek. Widma emisyjne dla sztucznych źródeł światła analizowano z wykorzystaniem monochromatora 0,3-m (SR303i, Andor) wyposażonego w siatkę 600 linii/mm i detektora ICCD (DH740, Andor) (Artykuł 2, Rys. 1).

Wpływ temperatury – wygrzewanie

Wyżarzanie próbek (Artykuł 4) nienapromieniowanych i napromieniowanych wykonywane było w suszarce VWR VENTI-Line z wymuszoną konwekcją (VL 53, VL 115) w temperaturze 200℃ oraz w elektrycznym piekarniku kuchennym w temperaturze 250℃.

Analiza ilościowa widm i analiza statystyczna

Analizę ilościową widm EPR (justowanie względem pozycji standardu, odejmowanie tła, pomiar amplitudy linii widmowych) oraz obliczenia dozymetryczne wykonano za pomocą oprogramowania producenta spektrometru (Bruker), programu SlideWrite Plus v.7.7 oraz programu Excel z pakietu Microsoft Office 2019. Rozkład numeryczny widm EPR został przeprowadzony przy użyciu procedury Reglinp w programie Excel z pakietu Microsoft Office 2019. W analizie danych stosowano metody statystyki opisowej i niepewności pomiarowe przedstawione na rysunkach w postaci tzw. słupków błędów, które odnoszą się do jednego odchylenia standardowego i odzwierciedlają niepewność pomiaru masy próbek i powtarzalność pomiarów EPR przy zmiennej geometrii próbki we wnęce spektrometru.

OMÓWIENIE ARTYKUŁÓW WCHODZĄCYCH W SKŁAD ROZPRAWY

Artykuł 1. Ewolucja w czasie napromieniowanych sygnałów EPR w różnych typach szkieł ekranów telefonów komórkowych.

Juniewicz M, Ciesielski B, Marciniak A, Prawdzik-Dampc A. *Time evolution of radiation-induced EPR signals in different types of mobile phone screen glasses*. Radiation and Environmental Biophysics. 2019; 58(4): 493-500.

Celem tej pracy była ocena przydatności wykorzystania szkieł z dotykowych ekranów telefonów komórkowych pod względem ich potencjalnego zastosowania w retrospektywnej dozymetrii promieniowania jonizującego. Badania przeprowadzono na 4 różnych typach szkieł: Gorilla Glass (GG) – pozyskane w ramach międzynarodowego projektu dozymetrii porównawczej Intercomparison 2012 [10], szkło mineralne (MG) z telefonu Sony Xperia L, szkło hartowane (TG) – stosowane powszechnie jako ochrona ekranu telefonu komórkowego oraz szkło ekranu telefonu iPhone 6S (IP).

Wpływ kruszenia szkła (co jest niezbędne w przygotowaniu próbek do pomiarów EPR) na sygnał EPR został sprawdzony dla szkła mineralnego (MG) oraz szkła hartowanego (TG). Badanie wykonano w 2 etapach: najpierw zmierzono większe kawałki szkła (około 12×3 mm^2), a następnie pokruszono na mniejsze fragmenty (ziarna o wielkości 0,3–4 mm). Uzyskane wyniki wykazały brak wpływu kruszenia na intensywność i kształt widma EPR (Rys. 2a–c) zarówno dla próbek nienapromieniowanych, jak i napromieniowanych. Nie wykazano również relacji pomiędzy przemywaniem próbki wodą a zmianą kształtu jej sygnału EPR.

Zaobserwowano istotne różnice w widmach nienapromieniowanych szkieł (tzw. sygnałach tła) (Rys. 3). Ta zmienność międzypróbkowa sygnałów BG może stanowić istotne ograniczenie w praktycznym wykorzystaniu szkieł ekranów telefonów komórkowych w dozymetrii EPR w wypadkach radiacyjnych, gdy próbki referencyjne w postaci nienapromieniowanego szkła tego samego rodzaju co próbka badana nie są dostępne.

Zbadano również wpływ promieniowania jonizującego na sygnały EPR dla badanych rodzajów szkieł (Rys. 3). Podobieństwo widm napromieniowanych próbek MG, GG oraz w pewnym stopniu dla IP (Rys. 3), wskazuje na podobieństwo centrów paramagnetycznych generowanych w tych szkłach przez promieniowanie jonizujące.

Na podstawie kształtu widm i dominującej linii widmowej o współczynniku $g < 2{,}00$ zidentyfikowano centra paramagnetyczne typu E (elektrony) w szkłach, zgodnie z doniesieniami literaturowymi [24, 29]. Natomiast składnik widma o mniejszej intensywności (o wartości współczynnika $g > 2{,}00$) wskazuje na obecność centrów paramagnetycznych typu H. Odmienny kształt widma RIS dla szkła TG, z pojedynczą szeroką linią o współczynniku $g > 2{,}00$, pozwala na przypisanie go do jednej z dziur paramagnetycznych, prawdopodobnie centrum H2.

Przedstawione na Rys. 4 krzywe kalibracji w zakresie dawek 0-20 Gy dla 3 rodzajów szkła wykazują liniową zależność natężenia sygnału RIS od dawki. Nachylenie linii regresji dla pomiarów wykonanych 15 dni po napromieniowaniu było mniejsze niż dla tych wykonanych po 6 dniach (Rys. 4a), co sugeruje zanik sygnału indukowanego radiacyjnie (RIS) w czasie między tymi pomiarami dla szkła GG. Efekt ten potwierdzono dla szkła TG (Rys. 5b), dla którego zaobserwowano największy spadek RIS w ciągu pierwszych 10 dni po napromieniowaniu.

Ostatnim etapem pracy było szczegółowe określenie kinetyki zaniku sygnału EPR dla dwóch zakresów czasowych: w ciągu miesiąca po napromieniowaniu dla szkła TG (Rys. 5b) oraz w czasie 1,5 roku dla szkła GG (Rys. 5a). Po znormalizowaniu wyników do jednego punktu czasowego (20 dzień po napromieniowaniu), przedstawiono je w postaci wspólnej krzywej kinetyki zaniku (Rys. 5d). Wynika z niej, że w ciągu pierwszych 10 dni po napromieniowaniu spadek sygnału RIS w tych szkłach wyniósł ok. 50% i w następnym roku spadł do ok. 25% wartości początkowej.

W artykule tym pokazano, że szkła ekranów telefonów komórkowych mogą stanowić dobry materiał dla celów dozymetrii powypadkowej. Naprężenia mechaniczne spowodowane przez cięcie i kruszenie próbek szkła oraz wpływ wody nie powodują zmian kształtu ich sygnałów EPR. Największy spadek sygnału indukowanego radiacyjnie zaobserwowano w ciągu 5-10 dni po napromieniowaniu, a następnie proces zaniku spowalnia, w związku z czym wykorzystanie szkła jako dozymetru jest możliwe co najmniej do 18 miesięcy po napromieniowaniu. Zwrócono również uwagę na potencjalne trudności w wykorzystaniu tego materiału w dozymetrii wypadkowej spowodowane zróżnicowaniem kształtu sygnału tła pomiędzy różnymi typami szkieł. Uniemożliwia to zastosowanie jednego uniwersalnego modelowego sygnału tła w analizie ilościowej widm EPR w celu wiarygodnej rekonstrukcji pochłoniętej dawki.

Artykuł 2. Wpływ naświetlania światłem słonecznym i lampą UV na sygnały EPR w napromieniowanych promieniowaniem rentgenowskim ekranach dotykowych telefonów komórkowych.

Juniewicz M, Marciniak A, Ciesielski B, Prawdzik-Dampc A, Sawczak M, Boguś P. *The effect of sunlight and UV lamp exposure on EPR signals in X-ray irradiated touch screens of mobile phones*. Radiation and Environmental Biophysics. 2020; 59(3):539-552.

W pracy tej opisano wpływ ekspozycji 4 rodzajów szkieł (GG, MG, TG oraz IP) pochodzących z ekranów telefonów komórkowych na światło dwóch typów lamp emitujących światło ultrafioletowe (lampy CLEO oraz lampy kosmetycznej), światło w zakresie widzialnym z żarówek fluorescencyjnych oraz bezpośrednie światło słoneczne. Opis źródeł światła znajduje się w podrozdziale „Materiały i metody". Zbadano wpływ światła na sygnały EPR szkieł nienapromieniowanych oraz napromieniowanych promieniowaniem jonizującym.

Na Rys. 2a przedstawiono zmiany kształtu widm EPR próbek nienapromieniowanego szkła mineralnego (MG) spowodowane ekspozycją (5-75 min.) na bezpośrednie światło słoneczne oraz na sztuczne światło z lamp zawierające składową UV. Na Rys. 2b przedstawiono wyekstrahowany sygnał EPR generowany światłem (LIS) otrzymany jako różnicę dwóch sygnałów: mierzonego w szkle nienapromieniowanym promieniowaniem jonizującym po naświetlaniu go światłem UV i sygnału tła (BG).

W badaniach przedstawionych w tej pracy zastosowano dwie procedury numerycznego rozkładu widm w celu ilościowego wyodrębnienia zawartego w nich sygnału dozymetrycznego: (1) standardową, oznaczoną jako B-R – uwzględniającą obecność w nich sygnału BG oraz składowej dozymetrycznej (RIS), (2) niestandardową, oznaczoną jako B-R-L, uwzględniającą dodatkowo udział składowej indukowanej światłem (LIS). Wykazano, że wyodrębnione procedurą B-R-L składowe widmowe BG z nienapromieniowanych próbek szkła danego rodzaju nie zmieniają się wraz ze wzrostem fluencji światła lampy kosmetycznej (Rys. 2c).

W następnej części artykułu poddano analizie widma próbek napromieniowanego szkła MG eksponowanego na światło słoneczne (Rys. 3a) oraz na światło UV z lampy CLEO (Rys. 4a). Natomiast szkło Gorilla Glass było naświetlane jedynie lampą CLEO (Rys. 5a). Przedstawiony na Rys. 3b, 4b i 5b sygnał radiacyjny (RIS) różni się wyraźnie kształtem od sygnału tła (BG) oraz sygnału indukowanego światłem (LIS). Zależność sygnału RIS od fluencji uzyskana w procedurze B-R (Rys. 3c, 4c i 5c) pokazuje zanik sygnału RIS

pod wpływem nawet krótkiego czasu ekspozycji na światło UV. Podobny jakościowo wniosek wynika z zastosowania procedury B-R-L (Rys 3e, 4e i 5c). Sygnał dozymetryczny był stabilny w czasie po ekspozycji na światło nawet do ok. 170 dni dla szkła GG (Rys. 5d), w przeciwieństwie do obserwowanych zmian sygnału RIS w próbkach nie poddanych działaniu światła, w których zanik RIS obserwowano przez co najmniej 600 dni (Artykuł 1, Rys. 5a). Ponowne napromieniowanie naświetlonych próbek dawką 10 Gy spowodowało odbudowę sygnału RIS, co pokazuje, że wcześniejsza ekspozycja na światło nie wpływa na ich czułość na promieniowanie jonizujące. Dodatkowo, próbki MG_1_10Gy (Rys. 3c) oraz MG_10Gy (Rys. 4d) ponownie napromieniowano dawką 10 Gy i poddano 15 minutowej ekspozycji na światło. W obu przypadkach zaobserwowano podobny, co do wielkości, spadek RIS. Pokazuje to, że na radioczułość sygnału RIS nie ma wpływu ekspozycja próbek na światło przed ich napromieniowaniem promieniowaniem jonizującym.

Dla szkła MG uwzględnienie w numerycznym rozkładzie widm składowej LIS, generowanej przez bezpośrednie światło słoneczne i światło UV pochodzące z lampy CLEO, ma niewielki wpływ na zrekonstruowaną wielkość sygnału dozymetrycznego (Rys. 3e, 4e). Dla szkła Gorilla Glass (GG) pominięcie obecności składowej LIS w procedurze rozkładu widm może powodować przeszacowanie (nawet o około 90%) wartości RIS (Rys. 5c). Może to być wynikiem znacznej różnicy kształtu składowych BG oraz LIS dla szkła GG (Rys. 5b). W widmach napromieniowanych próbek poddanych działaniu światła UV, wzrostowi składnika LIS towarzyszy spadek składowej RIS. Maksymalna wartość LIS i jednocześnie minimalna wartość RIS są widoczne już po około 5-15 min. ekspozycji na światło, co odpowiada fluencji równej 700 kJ/m^2 (światło słoneczne) oraz 20 kJ/m^2 (lampa CLEO) (Rys. 3f, 4f oraz 5e). W konsekwencji, zależności między RIS i LIS (Rys. 3g, 4g i 5g) można wykorzystać do wprowadzenia korekty niwelującej wpływ światła na RIS. Przy znanej (np. wyznaczonej eksperymentalnie dla innej próbki tego samego szkła) monotonicznej zależności między RIS a LIS, można wyznaczyć wartość sygnału skorygowanego RIS_{cor}, czyli takiego, który byłby mierzony jeśli próbka nie byłaby wystawiona na światło, na podstawie poniżej zależności:

$$RIS_{cor} = RIS/LCF$$

(gdzie: *LCF* jest współczynnikiem korekcji wpływu światła *(ang. light correction factor)* wyznaczonym na podstawie zależności RIS od LIS jak pokazano na Rys. 4g i 5g[1]).

Analiza ilościowa wpływu światła na sygnał dozymetryczny dla szkieł TG oraz IP została przeprowadzona przy użyciu procedury B-R. Zaobserwowano, że ekspozycja napromieniowanych próbek szkła TG na światło pochodzące z lampy CLEO (Rys. 6a) jak i światło słoneczne (Rys. 6b) nie spowodowała wyraźnych zmian kształtu widm. Wykazano, że jest to szkło mniej wrażliwe na światło od pozostałych zbadanych w tym artykule – dopiero 30-minutowa ekspozycja na światło powodowała ok. 50% spadek sygnału RIS. Podobnie jak w przypadku szkieł MG oraz GG, sygnał RIS był stabilny po ekspozycji na światło, a ponowne napromieniowanie spowodowało ponowny wzrost sygnału RIS (Rys. 6d).

Ekspozycja na światło widzialne nie zawierające składowej UV (Rys. 7b) nie spowodowała wyraźnych zmian wartości sygnału RIS szkła IP (próbka iP2_6S_10Gy naświetlona żarówką fluorescencyjną DULUXTAR). Ekspozycja tego szkła na światło zawierające ultrafiolet, spowodowała znaczny spadek wartości RIS (próbka iP1_6S_10Gy), podobnie jak dla szkieł MG i GG. Wartość sygnału dozymetrycznego RIS po naświetleniu była stabilna co najmniej do około 45 dnia po ekspozycji na światło (Rys. 7c).

Podsumowując, w tym artykule wykazano, że we wszystkich typach zbadanych szkieł ekspozycja na światło ze składową UV powoduje spadek wartości sygnału dozymetrycznego RIS uzyskanego poprzez numeryczny rozkład widm EPR na modelowe składowe widmowe – BG, RIS i LIS. Nawet kilkuminutowe działanie światła słonecznego może spowodować kilkudziesięcioprocentowy zanik mierzonego sygnału dozymetrycznego. Wykazano, że RIS w szkle ochronnym (TG) ekranu jest najmniej wrażliwy na światło. Zaobserwowano, że pominięcie LIS w rozkładzie numerycznym widm może powodować znaczną (ok. 90%) niedokładność w rekonstrukcji dawki metodą EPR. Zaproponowano metodę ilościowej korekty wartości sygnału dozymetrycznego w szkłach poddanych działaniu zarówno promieniowania jonizującego jak i światła,

[1] W omawianym artykule u dołu strony 547 jest pomyłka w sformułowaniu: „Consequently, the corrected magnitudes of the RIS (i.e. which would be measured if the glass was not exposed to light) are 0.62/0.4=1.55 and 0.42/0.5=0.84, respectively." Oczywiście wartość RIS_{cor} wyznaczamy na podstawie storunku $\frac{RIS}{LCF}$, a nie $\frac{LIS}{LCF}$, więc w tym przypadku, tj. dla próbki wykorzystanej do uzyskania zależności RIS vs LIS, dostajemy przy $LCF = 0{,}5$ dla RIS_{cor} wartość $0{,}5/0{,}5 = 1{,}0$. Dla innej próbki np. szkła GG, analizowanej za pomocą tych samych widm modelowych BG, RIS i LIS, dla której zmierzono by inne wartości RIS i LIS, np. $RIS = 0{,}7$ i $LIS = 0{,}42$, wartość współczynnika korekcji można by odczytać z Rys. 5g jako $LCF = 0{,}5$ i ostatecznie wyliczyć $RIS_{cor} = 0{,}7/0{,}5 = 1{,}4$.

na podstawie zaobserwowanej zależności pomiędzy składowymi widmowymi RIS i LIS, o ile obie te składowe charakteryzują się różnym kształtem widma EPR.

Artykuł 3. Dozymetria EPR w szkle - przegląd.

Marciniak A, Ciesielski B, Juniewicz M. *EPR dosimetry in glass – a review.* Radiation and Environmental Biophysics. 2022; 61(2):179-203.

Omawiany artykuł stanowi przegląd opublikowanych dotąd prac dotyczących pomiarów sygnałów EPR w szkle. Zawiera informacje szczególnie istotne w odniesieniu do zastosowania spektroskopii EPR w dozymetrii retrospektywnej dla dawek typowych dla wypadków radiacyjnych.

We wstępie podkreślono istotność doboru metody pomiarowej, która pozwoli na osiągnięcie zadowalającej dokładności. Zwrócono uwagę na potrzebę opracowania metod rekonstrukcji dawki mających zastosowanie w sytuacji nieoczekiwanego napromieniowania ludzi, mającego miejsce podczas wypadku radiacyjnego bądź też, gdy potrzeba zweryfikowania pochłoniętej dawki pojawia się po zaplanowanym napromieniowaniu. Przedstawiono zalety szkła jako potencjalnego materiału na detektor w dozymetrii retrospektywnej. Opisano szczegółowo strukturę i skład chemiczny szkieł (Tab. 1). Różnice w składzie pierwiastkowym szkła i tkanek mają istotne znaczenie dla ostatecznej oceny dawki pochłoniętej w materiale biologicznym na podstawie dawki zmierzonej w innym materiale. Do przybliżonej oceny dawki należy zastosować stosunek masowych współczynników pochłaniania (*ang. mass absorption coefficients*) i zdolności hamowania (*ang. stopping power*) dla danego typu szkła i tkanki miękkiej. Obliczenia tych stosunków dla szerokiego zakresu energii fotonów i elektronów wykonano na podstawie składu pierwiastkowego z Tabeli 1 i współczynników oddziaływania z Bazy Danych NIST Standard Reference Database 124 i 126 (https://www.nist.gov).

W pracy przedstawiono charakterystykę sygnałów EPR obserwowanych w szkłach: sygnałów tła natywnego (BG), sygnałów indukowanych światłem (LIS) oraz sygnałów indukowanych promieniowaniem jonizującym (RIS). Zestawiono widma teł z widmami napromieniowanych próbek różnych rodzajów szkieł (Rys. 2). Zwrócono uwagę na konieczność wyizolowania sygnału indukowanego radiacyjnie z pozostałych składowych widma w celu dokładnej rekonstrukcji dawki pochłoniętej podczas zdarzenia radiacyjnego. Zestawiono informacje o centrach paramagnetycznych w różnych rodzajach szkła mineralnego wykorzystywanego do produkcji przedmiotów z otoczenia

człowieka (np. szkło laboratoryjne, okienne, zegarkowe oraz pochodzące z ekranów urządzeń elektronicznych, w szczególności smartfonów), odpowiedzialnych za obecność sygnału tła oraz sygnału dozymetrycznego (Tab. 2). Odrębnie przedstawiono sygnały EPR w szkle Gorilla Glass (GG) (Rys. 4). Charakteryzuje się ono wysoką odpornością na pękanie i zarysowania, co spowodowało wszechobecność jego zastosowania w ekranach urządzeń elektronicznych codziennego użytku.

W artykule opisano trzy metody ilościowego określenia zmian wywołanych przez promieniowanie jonizujące w widmach EPR szkieł:

(1) Pomiar różnicy odchyleń linii widmowej od linii bazowej w zakresie widma EPR, w którym występuje sygnał RIS – tzw. metoda amplitudowa (Rys. 5). Zwrócono uwagę na wady zastosowania tej popularnej metody, gdy sygnał RIS pokrywa się z sygnałem BG lub niepożądanym sygnałem LIS.

(2) Wyznaczenie drugiej całki widma EPR, która odzwierciedla całkowitą liczbę centrów paramagnetycznych tworzących sygnał EPR. Metoda ta była stosowana przez niektórych badaczy i pozwalała na pomiary bezwzględnych stężeń rodników generowanych przez promieniowanie [30, 31, 32].

(3) Wyznaczenie wielkości składowej widmowej RIS przez procedurę numerycznego rozkładu widma na składowe modelowe: BG, RIS oraz, dla szkła eksponowanego na światło – sygnału LIS. Pokazano, że zastosowanie tej metody umożliwia oddzielenie składowej dozymetrycznej (RIS) od pozostałych komponentów widma EPR (BG oraz LIS), jednakże metoda ta wymaga znajomości widm modelowych [20, 30].

Tylko w przypadku, gdy analizowane próbki charakteryzują się podobnym widmem tła (np. pochodzą z tej samej partii produkcyjnej) i wykazują podobną historię ekspozycji na światło, zastosowanie metody amplitudowej do analizy wyników może mieć zbliżoną dokładność do analizy metodą numerycznego rozkładu widma (Rys. 6).

Dane literaturowe dotyczące granicy wykrywalności dawki (D_L) w różnych typach szkła oraz zastosowanych metod analizy zebrano w Tabeli 4, np. dla szkła mineralnego (MG) oraz szkła GG – od $D_L \approx 1$ Gy, dla szkła ochronnego $D_L \approx 2$ Gy (matrix method), dla szkła zegarkowego wartość ta wynosiła od ok. 1 Gy do 5 Gy (metoda amplitudowa). Ostatnie nasze badania (Artykuł 4) wykazały dawkę wykrywalną dla szkła zegarkowego na poziomie 0,05 Gy. Zestawienie to może być przydatne ze względu na możliwość oceny czułości oraz zastosowania odpowiedniej procedury analitycznej dla danego rodzaju szkła. Jednakże informacje te należy traktować jako przybliżoną ocenę czułości procedur

dozymetrycznych zastosowanych przez poszczególnych autorów z powodu różnej interpretacji terminu „granica wykrywalności (*ang. detection limit,* D_L)" przez różnych badaczy. Wu i in. [12] zdefiniowali to pojęcie, jako „dawkę poniżej której sygnał dozymetryczny jest zbyt niski, aby można było go odróżnić od sygnału tła", a Longo i in. [13] jako „wartość dawki, która wytwarza w napromieniowanych próbkach sygnał ESR równy średniej wartości sygnału dawki zerowej w próbkach nienapromieniowanych plus trzy odchylenia standardowe". Najdokładniejsza definicja tego terminu określona została przez Fattibene i in. [10] jako „dawka minimalna, którą można wykryć z określonym prawdopodobieństwem". Jednoznaczne zdefiniowanie tego terminu w przyszłych analizach jest istotne, gdyż charakteryzuje ważną cechę metody dozymetrycznej decydującą o jej praktycznej stosowalności.

W kolejnej części artykułu zwrócono uwagę na stabilność sygnału indukowanego radiacyjnie (RIS). Niestabilność długoterminowa RIS w szkle jest wymieniana przez niektórych autorów jako wada tego materiału jako dozymetru. Jednakże pomimo zanikania tego sygnału, RIS był wykrywany w szkłach po wielu miesiącach od napromieniowania [14, 19, 33]. W niektórych przypadkach zmniejszająca się intensywność sygnału indukowanego radiacyjnie nie tylko wpływa na amplitudę sygnału, ale również na kształt widma (Rys. 9a i 9b). Zestawiono także opublikowane dotąd informacje dotyczące kinetyki zaniku sygnału dozymetrycznego wyrażonej przez współczynnik zaniku (*ang. decay factor,* DF) (Rys. 10, Tab. 5). DF zdefiniowano, jako część początkowego RIS zmierzonego po określonej liczbie dni po napromieniowaniu. Pokazano, że dla szkieł ekranów telefonów komórkowych w czasie pierwszych 6-8 dni po napromieniowaniu występuje intensywny zanik sygnału, po czym spadek RIS wyraźnie zwalnia i jest mniejszy niż 25% w ciągu następnych 26 dni.

W końcowej części artykułu przedstawiono analizę danych literaturowych dotyczących wpływu preparatyki próbek (efekt czyszczenia i kruszenia szkła) oraz czynników fizycznych, takich jak temperatura oraz światło, na wielkość i kształt sygnału EPR. Etanol stosowany do oczyszczania próbek szkła nie jest czynnikiem wpływającym na ich sygnał EPR. Dla ziaren szkła o rozmiarach większych niż $315\ \mu m$ nie zaobserwowano dodatkowych składowych w ich sygnałach EPR [14, 19, 22, 23], natomiast dla próbek szkła w postaci drobnego proszku ($< 315\ \mu m$) zauważono dodatkowe sygnały EPR. Wpływ temperatury na sygnały EPR w szkle omówiono z dwóch perspektyw: ze względu na (1) wpływ podwyższenia temperatury otoczenia na kinetykę zaniku RIS (czyli na pogorszenie dokładności dozymetrii) oraz (2) celowe poddanie próbek wygrzewaniu,

które może być pomocne w rekonstrukcji sygnału tła specyficznego dla danej próbki poprzez „wymazanie" z napromieniowanej próbki sygnału radiacyjnego. Zwrócono uwagę na konieczność weryfikacji tego, jak wzrost temperatury wpływa na sygnał EPR dla różnych rodzajów szkła. Engin i in. [25] zaobserwowali całkowity zanik sygnału po 15-minutowym wyżarzaniu szkła okiennego w temperaturze $200℃$ (Rys. 12a), natomiast dla temperatur $60℃ - 150℃$, zanik wynosił od ok. $30\% - 90\%$ (Rys. 12b). Trompier i in. [14] uzyskali dwojakie efekty wyżarzania szkła ekranu LCD (Rys. 13). Dla jednego typu szkła po wygrzaniu w temperaturze $200℃$ zaobserwowano zmniejszenie intensywności sygnału EPR do poziomu niższego niż przed napromieniowaniem, bez zmiany jego kształtu (Rys. 13a), natomiast w innych próbkach (zarówno napromieniowanej i nienapromieniowanej) wyżarzanie spowodowało indukcję dodatkowej linii w widmie EPR, którą można przypisać termicznemu generowaniu dodatkowych centrów paramagnetycznych (Rys. 13b). Z kolei Liu i in. [34] w swoich badaniach pokazali, że przechowywanie próbek w niskich temperaturach $(-18℃)$ przyczynia się do spowolnienia zaniku RIS w porównaniu do tempa zaniku RIS podczas przechowywania próbek w temperaturze pokojowej.

Kończąca omawiany artykuł analiza doniesień literaturowych oraz prac własnych (Artykuł 2) dotyczących wpływu światła na sygnały EPR w szkłach prowadzi do wniosku, że niekontrolowana ekspozycja próbek szkła na światło ultrafioletowe może negatywnie wpływać na dokładność dozymetrii EPR – zarówno poprzez potencjalny wpływ UV na sygnały tła (Rys. 14), jak również na sygnały indukowane radiacyjnie (Rys. 15, 16). Obserwowalność wpływu światła oraz rodzaj tego efektu zależą od rodzaju badanego szkła. Ze względu na ogromną różnorodność występujących materiałów, ocena tego efektu wymaga indywidualnego podejścia.

Przedstawiona analiza wyników badań różnych autorów potwierdza przydatność szkła, w szczególności pochodzącego z przedmiotów powszechnego użytku, do dozymetrii promieniowania jonizującego. Zwrócono uwagę na kluczowe czynniki mogące ograniczać to zastosowanie: różnorodność sygnału tła w różnych szkłach oraz wpływ światła UV na sygnały EPR. Jednocześnie podkreślono, że wprowadzenie odpowiedniej korekty uwzgledniającej zanik sygnału RIS w czasie oraz uwzględnienie potencjalnej ekspozycji szkła na światło UV pozwolą na uzyskanie wyników dozymetrii EPR o dokładności umożliwiającej jej zastosowanie w wypadkach radiacyjnych, np. do triażu osób napromieniowanych na poziomie dawki 1-2 Gy.

Artykuł 4. Porównanie trzech metod retrospektywnej dozymetrii EPR w szkle zegarkowym.

Marciniak A**,** Juniewicz M, Ciesielski B, Prawdzik-Dampc A, Karczewski J. *Comparison of three methods of EPR retrospective dosimetry in watch glass*. Frontiers in Public Health. 2022, 10.

Celem omawianej pracy było porównanie wyników trzech metod: metody kalibracyjnej (CM), metody dawki dodanej (ADM) oraz metody dawki dodanej i wygrzewania (AD&HM) zastosowanych do retrospektywnego pomiaru dawki na podstawie sygnałów EPR w szkle zegarkowym pozyskanym i zbadanym w ramach międzynarodowego projektu dozymetrii porównawczej RENEB ILC 2021 [11].

W badaniach wykorzystano dwie grupy próbek: 6 próbek kalibracyjnych napromieniowanych promieniowaniem rentgenowskim przy napięciu 240 kV dawkami: 0,0 Gy, 0,5 Gy, 1,0 Gy, 2,0 Gy, 3,0 Gy i 6,0 Gy oraz 3 próbki o nieznanych początkowo dawkach, ujawnionych przez organizatorów projektu RENEB dopiero po zgłoszeniu swoich wyników przez uczestników projektu; dawki te wynosiły 0,0 Gy, 1,2 Gy oraz 3,5 Gy. Wszystkie podane dawki to wartości kermy w powietrzu.

W artykule zaproponowano sposób dokonania wyboru odpowiedniej metody rekonstrukcji dawki w zależności od dostępnego materiału badawczego oraz posiadanych informacji na temat jego modelowych widm EPR (Rys. 2). Wykazano liniową zależność sygnału indukowanego radiacyjnie (RIS) od dawki w zakresie 0 Gy – 6 Gy (Rys. 4).

Jako pierwszą omówiono metodę wymagającą kalibracji (CM) sygnału RIS względem dawki przy wykorzystaniu oddzielnych próbek tego samego rodzaju szkła. Pomiary próbek kalibracyjnych wykonano sześciokrotnie w przedziale czasowym między 8 a 126 dniem po napromieniowaniu. Pozwoliło to na określenie kinetyki zaniku sygnału radiacyjnego, uwzględnionej przy obliczaniu dawki w próbkach o nieznanej ekspozycji na podstawie ich pomiarów po napromieniowaniu po czasie innym, niż dla próbek kalibracyjnych. Próbki o nieznanych dawkach zostały zmierzone w 7 i 11 dniu po napromieniowaniu, a obliczone dawki (uśrednione z obu tych pomiarów) wynosiły kolejno: 0,05 Gy, 1,03 Gy oraz 3,16 Gy (Tab. 1).

Metoda ADM jest schematycznie przedstawiona na Rys. 1. Opiera się na koniecznej znajomości sygnału tła (BG) badanego szkła (co stanowi ograniczenie zastosowania tej metody, podobnie jak metody CM) oraz na wykorzystaniu próbki badanej do kalibracji sygnału dozymetrycznego poprzez jej dodatkowe napromieniowanie znaną dawką

kalibracyjną. Kluczowym elementem rekonstrukcji dawki tą metodą było uwzględnienie w obliczeniach kinetyki zaniku sygnału, gdyż pomiary wykonywano w różnym czasie po napromieniowaniu – między 8 a 407 dniem od pierwotnego napromieniowania próbek. W artykule przedstawiono wyprowadzenie wzoru na obliczenie dawki nieznanej, uwzględniającego zanik sygnału w różnych etapach rozciągniętej w czasie procedury: między pierwotnym napromieniowaniem a pierwszym pomiarem EPR, drugim napromieniowaniem dodaną dawką kalibracyjną oraz kolejnym pomiarem EPR. W przedstawionym badaniu dodana dawka kalibracyjna wynosiła $(6{,}0 \pm 0{,}1)$ Gy w wodzie, co odpowiadało $(5{,}17 \pm 0{,}10)$ Gy dawki pochłoniętej w szkle. Nieznaną dawkę przeliczono na kermę w powietrzu (K_{air}) w celu porównania jej z dawkami rzeczywistymi, które organizatorzy projektu podali w tych jednostkach. Wyniki rekonstrukcji dawek tą metodą przedstawiono w Tab. 1, w kolumnie 4.

Ostatnią z metod przedstawionych w omawianym artykule jest metoda AD&HM. Różni się ona od metody ADM tym, że w procedurze dekompozycji widm zastosowano widmo modelowe BG uzyskane przez pomiar EPR wygrzewanych (w temperaturze 200℃ lub 250℃ w czasie 4-45 min) próbek szkła, uprzednio napromieniowanych. Wygrzewanie powodowało zanik sygnału RIS pozwalając na odzyskanie sygnału natywnego BG badanej próbki. Przed wykorzystaniem tej metody do rekonstrukcji dawki sprawdzono, że wygrzewanie w wysokich temperaturach nie wpływa na intensywność i kształt widma nienapromieniowanych próbek szkła zegarkowego (Rys. 5a, 5b). Jest to odmienną obserwacją w stosunku do wyników uzyskanych dla szkieł ekranów telefonów komórkowych [14, 24]. Wykazano, że dla szkła zegarkowego 45 min. wygrzewanie w temperaturze 200℃ zmniejsza intensywność sygnału RIS o ponad 90%, natomiast zaledwie 4 min. wygrzewanie napromieniowanej próbki WG w temperaturze 250℃ spowodowało niemal całkowitą eliminację sygnału RIS (Rys. 6b).

Uzyskano zbliżoną dokładność pomiaru trzema analizowanymi metodami, wynoszącą około 0,3 Gy (Tab. 1), co jest wystarczającą dokładnością dla ich wykorzystania np. do triażu osób napromieniowanych w wypadkach radiacyjnych.

Wyniki metody AD&HM przedstawione w tej pracy stanowią podstawę do zastosowania tej metody w rzeczywistym wypadku radiacyjnym, gdy nie jest dostępny sygnał tła (BG) badanej próbki (tj. gdy do dyspozycji badaczy jest tylko próbka napromieniowana). Jednakże zastosowanie tej metody dla innych rodzajów szkieł, niż zbadane szkło zegarkowe, wymagałoby sprawdzenia stabilności sygnału tła w wysokich temperaturach.

PODSUMOWANIE I WNIOSKI

Badania przeprowadzone w ramach niniejszej pracy doktorskiej potwierdzają, że promieniowanie jonizujące indukuje w badanych szkłach zmiany strukturalne (centra paramagnetyczne), których trwałość umożliwia wiarygodny pomiar ich sygnałów EPR nawet po wielu miesiącach od napromieniowania i pozwala na ich wykorzystanie do retrospektywnej oceny dawki pochłoniętej w szkłach. Wykazano, że sygnał dozymetryczny badanych szkieł zależy liniowo od dawki w zakresie 0-20 Gy i utrzymuje się co najmniej 18 miesięcy po napromieniowaniu. Dużą zaletą tych szkieł jest również ich rozpowszechnienie w najbliższym otoczeniu człowieka, dostępność, łatwość preparatyki próbek i pomiarów EPR. Sygnały EPR obserwowane w napromieniowanych szkłach, poza dawką promieniowania, są zależne od czynników takich jak: skład chemiczny i sposób produkcji, wpływające na różnorodność sygnału tła w różnych typach szkieł oraz ekspozycja szkieł na światło ultrafioletowe. W przebadanych szkłach określono minimalną dawkę wykrywalną na poziomie 0,05-2 Gy, wystarczającym dla triażu osób poszkodowanych w wypadkach radiacyjnych.

W pracy tej zrealizowano pierwsze dedykowane badanie wpływu światła naturalnego oraz sztucznego na dozymetrię EPR w szkłach. Wykazano zmiany sygnału dozymetrycznego RIS we wszystkich rodzajach zbadanych szkieł, które zostały poddane ekspozycji na światło zawierające składową UV. W związku z tym zaproponowano metodę ilościowej korekty sygnału RIS dla tych szkieł, których składowe RIS i LIS charakteryzują się odmiennym kształtem widma EPR. Umożliwia to ilościowe powiązanie stopnia zaniku RIS z wielkością narastającego wskutek ekspozycji na światło sygnału LIS. Brak uwzględnienia tego czynnika może skutkować dużymi błędami w określeniu pochłoniętej dawki w szkle.

Zwrócono również uwagę na trudności związane ze zróżnicowaniem sygnału tła w szkłach różnego rodzaju; znajomość tego sygnału jest kluczowa dla dokładnego wyznaczenia sygnału dozymetrycznego. Dlatego opracowano i zweryfikowano doświadczalnie metodę dawki dodanej i wygrzewania (AD&HM) dla szkła zegarkowego, która pozwoliła na odzyskanie sygnału tła poprzez wygrzewanie próbki badanej w wysokiej temperaturze. Uzyskana dokładność rekonstrukcji dawki tą metodą, wynosząca około 0,3 Gy, była zbliżona do wyników uzyskanych powszechnie stosowanymi metodami (CM oraz ADM). Jednak w przeciwieństwie do nich, do określenia sygnału tła i kalibracji w tej metodzie nie było konieczne użycie innej,

nienapromieniowanej próbki. Odzwierciedlało to prawdopodobne warunki pomiaru w rzeczywistym wypadku radiacyjnym.

Wyniki niniejszej pracy doktorskiej potwierdzają możliwość zastosowania dozymetrii EPR w szkle do wstępnego triażu osób napromieniowanych w wypadkach radiacyjnych, co stanowi potwierdzenie hipotezy roboczej.

SUMMARY IN ENGLISH

INTRODUCTION

Currently, it is common to use radioactive sources in many areas of human activity, for example in industry, medicine - both in diagnosis and therapy, scientific research and measurement techniques. In Poland, in the years 2001-2015, there was an almost threefold increase in the number of entities that use ionizing radiation in various forms of their activity. Despite of many precautions, there are cases of irradiation of people with uncontrolled doses that are not indifferent to their health and life [1]. The use of radioactive materials may also occur during warfare or possible terrorist attacks.

As defined by the International Atomic Energy Agency (IAEA), a radiation accident is "an occurrence, that has led to significant consequences for people, the environment or the facility". An example of a serious “radiation accident" was damage to the reactor core and release of large amounts of radiation in the Chernobyl disaster in 1986 or the Fukushima nuclear power plant accident in 2011 [2]. The International Nuclear and Radiological Event Scale (INES), used in over 60 countries, classifies radiation emergencies into seven levels: levels 1–3 are called “incidents” and levels 4–7 are called “accidents”. The INES scale takes into account the radiation dose to people and to environment in the vicinity of the site, the dissemination of radioactive materials contained in the installation and events, where preventive measures have not worked. For example, the Chernobyl reactor explosion was rated a level 7 major accident. In addition, a significant radiation accident occurs when the radiation exposure of the injured person meets at least one of the following criteria:

(1) the whole body dose is equal to or exceeds 0.25 Gy,
(2) the dose to the skin is equal to or exceeds 6 Gy,
(3) the dose absorbed (from an external source) by other tissues or organs is equal to or exceeds 0.75 Gy [3].

The main consequence of a radiation accident is the damage caused to people present at the accident site and in its vicinity. The complex of clinical symptoms that occur after irradiation of the whole body or a significant part of the body (over 60%) with doses above 1 Gy is described as Acute Radiation Syndrome (ARS) [4].

Mass radiation exposure of the population not having a personal dosimeter at the time of the accident requires segregation (triage) of the victims in order to implement

appropriate medical procedures. The European consensus on medical management in the case of mass exposure to radiation was reached in 2005 by signing the METREPOL protocol (Medical Treatment Protocols for Radiation Accident) [5]. According to this protocol, during the first 48 hours victims of an accident should be subject to an emergency triage system, in which they are assessed both on the basis of clinical symptoms and other criteria allowing an assessment of the absorbed dose. Exposure of the whole body, or a significant part of it, to a dose of 4-5 Gy is potentially lethal to half of the irradiated people. Specialist medical care can significantly increase the likelihood of survival for those, who have received doses of 3–7 Gy to the whole body [2]. In addition, knowledge of the absorbed dose is of particular importance when assessing the risk of late complications and stochastic effects.

In the assessment of individual doses, even many months after exposure, retrospective dosimetry is used to support the diagnosis or the choice of treatment. This term refers to the methods of determining the absorbed dose after a radiation event in situations, where the assessment of doses for exposed persons is necessary or required and conventional dosimeters were not available or were insufficient [6].

Retrospective dosimetry methods can be divided into 2 groups:

(1) physical - based on physical methods, in particular on Electron Paramagnetic Resonance (EPR) spectroscopy, luminescent techniques – thermoluminescence (TL) and optically stimulated luminescence (OSL), and

(2) biological - such as, for example, cytogenetic methods for the assessment of chromosomal changes in peripheral blood lymphocytes (formation of dicentric chromosomes, translocations, micronuclei).

Physical methods use both biological tissues (tooth enamel, bones, nails) and artificial materials found in everyday objects (mobile phones, electronic devices, watches, glasses) to measure radiation-induced changes in these materials. EPR spectroscopy is one of sensitive methods for detecting these changes. It allows for identification and quantitative characterization of paramagnetic centers (e.g. free radicals), induced by ionizing radiation in the tested substances, by measurements of their EPR signals [7, 8]. For practical application of EPR spectroscopy in post-accident dosimetry, it is essential to select the materials, which can act as a detector-dosimeter and to determine accuracy of this method. Sensitivity of such a material to radiation is characterized by the minimum detectable dose (*Detection Limit*, D_L) for a specific dosimetry method. For the glasses constituting the research material in this doctoral

dissertation, the D_L parameter was about 0.05-2.00 Gy, which is sufficient for a triage of people affected by radiation accidents before the necessary medical actions. This justifies the research undertaken by many researchers on EPR dosimetry in glasses from watches or from screens of mobile phones (and other portable electronic devices), including the Gorilla Glass (GG), which in recent years has been commonly used for touch screens.

EPR dosimetry in glasses so far has been the subject of several international comparative dosimetry projects (*Inter-laboratory Comparisons*, ILC), in which the research group from the Department of Physics and Biophysics, Medical University of Gdańsk participated in 2012 and 2021 [9, 10].

Mobile phones are probably one of the most ubiquitous personal devices - at the beginning of 2023, the total number of their users in the world was about 5.4 billion [11] – which corresponds to nearly 70% of the entire world population. In addition, mobile phones are often held close to the body, which is an added advantage facilitating a reliable reconstruction of doses absorbed by their users based on the doses absorbed by their phone screens.

Glass is an inorganic, amorphous, transparent ceramic material. It shows potential as a material useful for EPR dosimetry due to its ubiquity in the human environment, resistance to water and many chemicals, low electric conductivity and low dielectric losses, which enables quick EPR measurements without special, laborious sample preparation. Its properties depend on the production method and chemical composition. In addition, unlike biological samples, glass samples are usually available in sufficient, optimal quantities to enable sensitive measurements of EPR signals.

The EPR spectra of irradiated glass samples include the following signals:

(1) BG (*background signal*) – native background signal of non-irradiated sample, usually complex, wide and stable (at room temperature) signal having spectroscopic splitting factor g≈2.0 for watch glass (WG) [12, 13, 14, 15, 16] and Gorilla Glass [17]. In mineral (MG) and tempered glass (TG) from mobile phones, broad lines were observed in the range of g=1.98-2.01 [18, 19, 20]. The shape of the BG spectrum is specific for different types of glass and the origin of this signal can be diversified and has not yet been fully explained. Griscom [21] attributed EPR signals in non-irradiated glass to the presence of transition group ions, ferromagnetic deposits, photoinduced centers and mechanically induced defects. Also Bassinet et al. [22] and Trompier et al. [23] suggested that the

background signal is generated during the manufacturing process by impurities in the glass. McKeever et al. [24] found that the exposure of glass to ultraviolet light may be one of the contributing factors for the background spectrum.

(2) LIS (*light-induced signal*) – a signal caused by the exposure of the phone/watch to sunlight containing a UV component, or to light from lamps (e.g. used in the production of telephones [24] or from UV lamps used in solariums, beauty salons, etc.).

(3) RIS (*radiation-induced signal*) – signal induced by ionizing radiation; the paramagnetic centers of the dosimetric signal are mainly attributed to the missing oxygen bond between silicon atoms (E' centers), non-bridged oxygen hole centers (NBOHC) and peroxy radicals [21]. No effect of dose rate on EPR spectra induced by ionizing radiation up to 1.63 kGy/h was found [25].

A serious challenge for EPR dosimetry is partial or complete overlapping of the background with the signals induced by ionizing radiation. In our works described in this doctoral dissertation, the method of numerical decomposition of the spectra into their model components: BG, RIS and LIS – for glass exposed to light, was used. It has been shown, that this method enables separation of the dosimetric component (RIS) from the other two components (BG and LIS) and determination of its magnitude. A limitation of this method in real radiation accidents is the need to know the model spectra of these three components. Therefore, an attempt was made (Article 4) to develop a method, that would allow for reconstruction of the absorbed dose without having information about the native background signal of the tested sample. The model RIS signal can be obtained by re-irradiation of the sample with a known dose – which is necessary for calibration of the dosimetric signal vs. the dose. This method here and thereafter is named Added Dose & Heating Method (AD&HM). In this method, the BG model spectrum was obtained by measuring EPR spectra of irradiated watch glass samples after their annealing at 200℃ or 250℃. The annealing caused fading of the RIS signal, allowing to recover the samples' native BG. However, further research is needed to verify the applicability of the AD&HM to other types of glasses and to optimize the annealing conditions for the other glasses. A prospect for further research is also a search for a "screening test" indicating the presence of the effects of UV light in the tested samples (i.e. the presence of the LIS signal). Ignoring these effects can strongly affect the value of the reconstructed dose and their inclusion significantly complicates the procedure and elongates time needed to estimate the dose - which is particularly important in a case of large-scale

measurements. One of the directions of research for the future is also development of resonators, that enable EPR measurements of glass without the need to separate the screen glass (i.e. without damaging the phone). The first attempts of such measuring systems were reported [26].

THE AIMS OF THE DISSERTATION

This research concerned retrospective dosimetry based on the detection and measurement of relative concentrations of stable free radicals generated by ionizing radiation in the glass of mobile phone screens and watch glass using electron paramagnetic resonance (EPR) spectroscopy.

Main goals:

(1) Determination of the stability of EPR signals generated by radiation in glass and determination of the influence of sample preparation (crushing, influence of water) on the background and dosimetric EPR signals in the glass of smartphones' screens.

(2) Characterization of EPR spectra generated by radiation in different types of glasses and verification of a possibility of their use as a potential dosimeter for retrospective determination of doses absorbed during radiation accidents in the dose range up to several dozen Gy.

(3) Evaluation of the effects of exposure to natural and artificial light of non-irradiated and irradiated glass, determination of the impact of these effects on EPR spectra and on reliability of the dosimetry, and analysis of possibility to minimize these effects on the reconstructed dose.

(4) Development of a method, that enables dose reconstruction without having information about the native background signal of the tested sample.

The working hypothesis was to demonstrate the usefulness of EPR dosimetry in glasses for the initial triage of people irradiated in radiation accidents.

MATERIALS AND METHODS

Research material

The studies were performed using five types of glass samples: (1) Gorilla Glass (GG), (2) mineral glass (MG), (3) tempered glass (TG), (4) glass from the iPhone 6S (IP) – obtained from touch screens of mobile phones and (5) watch glass (WG), which was the

research material examined in the international comparative dosimetry project RENEB ILC 2021 [11, 27]. A part of the GG samples used in this study was also used in the international EURADOS Intercomparison 2012 project [10], in which our research group was participating.

Elemental composition of the glasses (Tab. 1) was determined by the Energy Dispersion Spectroscopy (EDS at the Institute of Nanotechnology and Materials Science of the Gdańsk University of Technology, except for Gorilla Glass, whose elemental composition was provided by the organizers of the EURADOS project [28].

Table 1. Elemental composition of glasses.

	SiO_2[%]			**Al_2O_3 [%]**		**Na_2O [%]**		
Gorilla Glass (GG)*	60-80			13-20		not quantified		
	in % (+/- 0.5)							
	Si	**Na**	**Mg**	**Al**	**K**	**P**	**Ca**	**O****
mineral glass (MG)	23.0	2.5	2.0	7.5	8.0	-	-	57.0
tempered glass (TG)	28.0	7.0	2.5	2.5	2.0	-	3.5	54.5
iPhone 6S (IP)	17.5	4.5	1.0	10.5	7.0	4.5	-	55.0
watch glass (WG)	27.5	11.0	2.5	1.0	1.0	-	3.0	54.0

*The elemental composition of GG glass was provided by the organizers of the EURADOS project [28].

**The accuracy is 0.5% for all tested elements, except for oxygen, for which the accuracy is 3.0%.

Sample preparation

Glass samples were obtained from smartphone touch screens by mechanically separating them from the phones. Watch glass, in the form of whole glass discs, was provided by the organizers of the RENEB ILC 2021. The separated glass fragments were crushed into smaller pieces, so as to fit into a sample tube placed in the EPR cavity of the spectrometer. The glass samples were cleaned of residues of glues, paints and other adhesive layers and washed with ethanol.

Samples prepared in this way were stored in the dark between successive EPR measurements, except for periods of intentional, controlled exposure to artificial or natural light, as described in the methodology sections in the articles included in the dissertation.

EPR measurements

EPR measurements were performed using a Bruker EMX 6/1 spectrometer, in the X-band (9.85 GHz). Samples were placed in quartz EPR sample tubes with an internal diameter of 4 mm and measured at room temperature. The measurement of a single sample was repeated at 3 orientations of the sample tube and the spectra were averaged. The following acquisition parameters were applied: microwave power - 22.30 and 32 mW, modulation amplitude - 0.15 and 0.5 mT, sweep width - 10 mT, conversion time - 81.92 ms, time constant - 163.84 ms and number of scans averaged from 5 to 10 for one orientation. Intracavity standard sample Mn^{2+} in MgO powder or the commercially available standard ER 4119HS-2100 Marker Accessory (Bruker BioSPin GmbH, Germany) was measured simultaneously with all samples. The spectra were aligned with respect to the EPR lines of the standard and normalized to their mass and to the mean amplitude of the standards' lines.

Irradiation

The samples were irradiated at the Department and Clinic of Oncology and Radiotherapy of the Medical University of Gdańsk with 6 MV X-rays from medical accelerator Clinac 2300 under electronic equilibrium conditions. Part of the WG samples (Article 4) were irradiated with a Maxishot SPE apparatus (Hamburg, Germany) by 240 kV X-rays of effective energy of 75 keV.

The effect of light

In the work described in Article 2 the effect of exposure of glasses to four light sources was examined - their characteristics are presented in Tab. 2.

Table 2. Characteristics of light sources.

Source of light	**Specification**	**Irradiance**
direct sunlight	The exposures were made around noon on sunny days. The total fluences (in J/m^2) were calculated by multiplying the measured irradiance and duration of the exposure.	$800\ W/m^2$

CLEO Advantage 80W-R lamp (Philips)	Arrangement of two parallel lamps commonly used in solariums, 80 W each.	48 W/m^2
Ultraviolet Radiant Lamp AP-111 (Alle Paznokcie)	The type of lamp used in beauty salons for hybrid varnish curing, with four 9 W bulbs each.	164 W/m^2
Duluxstar fluorescent bulbs (OSRAM)	Arrangement of 6 bulbs of 24 W each.	110 W/m^2

The irradiance of the light sources was measured using an ORION-TH (OPHIR) power meter at the samples placement points. Emission spectra for artificial light sources were measured using a 0.3-m monochromator (SR303i, Andor) equipped with a 600 lines/mm grid and an ICCD detector (DH740, Andor) (Article 2, Fig. 1).

The effect of temperature – heating

Annealing of unirradiated and irradiated samples (Article 4) was performed in a drying oven VWR VENTI-Line with Forced Convection (VL 53, VL 115) at temperature of 200℃ and in a furnace at 250℃.

Quantitative analysis of the spectra

Quantitative analysis of the EPR spectra (alignment to the standard's lines, background subtraction, measurement of amplitudes of spectral lines) and dosimetric calculations were performed using the spectrometer manufacturer's software (Bruker), SlideWrite Plus v.7.7 and Excel from the Microsoft Office 2019 package. Numerical decomposition of the EPR spectra was carried out using the Reglinp procedure in Excel. Descriptive statistics methods were used in the data analysis and the measurement uncertainties presented in the figures as error bars refer to one standard deviation and reflect the combined uncertainty of the sample mass and repeatability of EPR measurements while varying the sample geometry in the spectrometer cavity.

OVERVIEW OF ARTICLES INCLUDED IN THE DISSERTATION

Article 1. Juniewicz M, Ciesielski B, Marciniak A, Prawdzik-Dampc A. *Time evolution of radiation-induced EPR signals in different types of mobile phone screen glasses*. Radiation and Environmental Biophysics. 2019; 58(4): 493-500.

The aim of this work was to assess the usefulness of glass from touch screens of mobile phones in retrospective dosimetry of ionizing radiation. The studies were performed using four different types of glass: Gorilla Glass (GG) – in a part used in Intercomparison 2012 project [10], mineral glass (MG) from the Sony Xperia L phone, tempered glass (TG) commonly used as protection of the phones' screens and screen glass from iPhone 6S (IP).

The effect of crushing (which is necessary procedure in the preparation of samples for EPR measurements) on the EPR signal for MG and TG was performed in two stages: first, larger pieces of glass (about 12×3 mm^2) were measured, and then they were crushed into smaller fragments of 0.3–4 mm and measured again. The obtained results showed no impact of crushing on the intensity and shape of the EPR spectra (Fig. 2 a–c) for both non-irradiated and irradiated samples. Washing of the samples with water had no effect on their EPR signal.

Significant differences between the spectra of various non-irradiated glasses (background signals, BG) are shown in Fig. 3. This inter-sample variability of BG signals may be a significant limitation in use of EPR dosimetry in radiation accidents, when reference samples, in the form of non-irradiated glass of the same type as the tested sample, are not available.

The effect of ionizing radiation on EPR signals for the studied glasses is shown in Fig. 3. Similarity of spectra of irradiated samples of MG, GG and, to some extent, of IP reflects similarity of paramagnetic centers generated in these glasses by ionizing radiation. Based on the shape of the spectra and position of the dominant spectral line with $g<2.00$, E-type paramagnetic centers (electrons) in glasses can be identified, in accordance with literature reports [24, 29]. The component of the spectrum with a lower intensity at $g>2.00$ indicates the presence of H-type paramagnetic centers. The different shape of the RIS spectrum for TG glass, with a single broad line with $g>2.00$, can be assigned to one of the paramagnetic holes, probably to the H2 center.

The calibration curves in the dose range of 0-20 Gy presented in Fig. 4 show a linear dependence of the RIS intensity on the dose. The slope of the regression line for measurements taken 15 days after irradiation was lower, than for data measured 6 days after irradiation (Fig. 4a), suggesting a decay of the dosimetric signal in the GG glass between these measurements. This effect was confirmed for TG glass (Fig. 5b), for which the fastest decrease in RIS was observed during the first 10 days after irradiation. The kinetics of the signal decay was determined for two time ranges: within a month after irradiation for TG glass (Fig. 5b) and during 1.5 years for GG glass (Fig. 5a). After normalization of the data to one point in time (to the 20^{th} day after irradiation), they are presented in the form of a common decay curve (Fig. 5d). It shows that in the first 10 days after irradiation the decrease in the RIS signal in these glasses was about 50% and in the following year it decreased to about 25% of the initial value.

This article shows that the glass of phone screens can be applied for post-accident dosimetry. The mechanical stresses caused by the cutting and crushing of the samples as well as exposure to water do not change EPR signals from the glass. The greatest decrease in the radiation-induced signal was observed within 5-10 days after irradiation, and then the decay process slowed down. Therefore the use of glass as a dosimeter was possible up to 18 months after irradiation. In this article we also underline the potential difficulty in retrospective dosimetry due to the variations in shape of the BG signals in different types of glasses. This feature prevents application of one universal model BG in quantitative analysis of EPR spectra during the dose reconstruction.

Article 2. Juniewicz M, Marciniak A, Ciesielski B, Prawdzik-Dampc A, Sawczak M, Boguś P. *The effect of sunlight and UV lamp exposure on EPR signals in X-ray irradiated touch screens of mobile phones*. Radiation and Environmental Biophysics. 2020; 59(3):539-552.

This work describes the effects of exposure of GG, MG, TG and IP glasses from phone screens to light emitted by two types of ultraviolet lamps (CLEO lamp and cosmetic lamp), to visible light from fluorescent bulbs and direct sunlight – a description of the light sources can be found in the subchapter "Materials and methods". The influence of light on the EPR signals of non-irradiated and irradiated glasses was investigated.

Fig. 2a presents changes in the spectra of non-irradiated MG samples caused by their exposure (5-75 min.) to direct sunlight and to artificial light from the UV lamps. Fig. 2b

shows the EPR spectrum (LIS) induced by light obtained as the difference between two signals: measured in glass not irradiated with ionizing radiation but illuminated by UV light and the background signal (BG).

Two procedures of numerical decomposition of the spectra were used in order to determine the dosimetric signal contained therein: (1) standard procedure marked as B-R - taking into account the presence of the BG signal and the dosimetric RIS component, (2) non-standard procedure marked as B-R-L - additionally taking into account a contribution of the light-induced component (LIS). It has been shown, that numerically extracted BG spectral components from non-irradiated samples (0 Gy) of a given glass type do not change with the increase in the fluence of the cosmetic lamp light (Fig. 2c) when the B-R-L decomposition was used.

Next, the effects of sunlight and UV light on MG (Fig. 3 and 4a), and effects of UV light on GG (Fig. 5a) are presented. The RIS signals in Fig. 3b, 4b and 5b significantly differ in shape from the BG signals and from the LIS. The dependence of the RIS on fluence obtained in the B-R procedure (Fig. 3c, 4c and 5c), clearly shows decay of the RIS even after a short exposure to UV. Qualitatively similar conclusion results from application of the B-R-L procedure (Fig. 3e, 4e and 5c). The dosimetric signal in the UV-exposed GG glass was stable up to about 170 days (Fig. 5d), in contrast to the observed decay in the RIS in samples not exposed to the light, in which monotonic decrease of RIS was observed for at least 600 days (Article 1, Fig. 5a). Re-irradiation of the light-illuminated samples with 10 Gy resulted in reconstruction of their RIS, which shows, that previous exposure to light did not affect their sensitivity to ionizing radiation. In addition, the samples MG_1_10Gy (Fig. 3c) and MG_10Gy (Fig. 4d) were re-irradiated with 10 Gy and exposed to light for 15 minutes. In both cases, a similar decrease in RIS was observed. This shows that both the radiosensitivity and the light-sensitivity of RIS are not affected by exposing the samples to light prior to their irradiation with ionizing radiation.

The application of LIS component in numerical decomposition of spectra generated in MG by sunlight and UV from the CLEO lamp, has little effect on the magnitude of the dosimetric signal (Fig. 3e, 4e). For Gorilla Glass (GG), ignoring the presence of LIS component in the decomposition procedure may result in an overestimation (even by about 90%) of the actual RIS value (Fig. 5c). This can be explained by difference in the shape of the BG and LIS components for the GG glass (Fig. 5b). In spectra of irradiated samples exposed to UV light, RIS is decreasing with increase in LIS. The

maximum of LIS and the minimum of RIS values are observed after about 5-15 minutes of light exposure, which corresponds to a fluence of 700 kJ/m^2 (sunlight) and 20 kJ/m^2 (CLEO lamp) (Fig. 3f, 4f and 5e). As a consequence, the relationships between RIS and LIS (Fig. 3g, 4g and 5g), can be used to introduce a correction allowing to compensate the effect of UV on the RIS. With a known (e.g. experimentally determined for another sample of the same glass) monotonic dependence between RIS and LIS, the corrected signal RIS_{cor}, i.e. the one that would be measured, if the sample was not exposed to light, can be determined on the basis of the following relationship:

$$RIS_{cor} = RIS/LCF$$

(where: LCF is the light correction factor determined based on the relationship between RIS and LIS as shown in Fig. 4g and 5g[1]).

Quantitative analysis of light effects on the dosimetric signal for TG and IP glasses was performed using the B-R procedure. It was observed, that exposure of irradiated TG samples to light from the CLEO lamp (Fig. 6a) and sunlight (Fig. 6b) did not cause significant changes in the shape of the spectra. It was shown, that this glass is less sensitive to light than the other glasses tested in this work - only 30-minute of exposure to light caused about a 50% decay in the RIS. Similarly as for the MG and GG glasses, the RIS was stable over time after exposure of TG to light, and re-irradiation resulted in a renewed increase in the RIS (Fig. 6d).

Exposure to visible light without the UV component (Fig. 7b) did not cause any changes in RIS in the IP glass. Exposure of this glass to UV caused a significant decrease in the RIS, similarly to the MG and GG glasses. The dosimetric signal was stable at least for about 45 days after exposure to UV light (Fig. 7c).

In conclusion, this article demonstrates, that in all types of tested glasses, an exposure to light with a UV component causes a decrease in dosimetric RIS signal obtained using the B-R-L decomposition procedures. Even a few minutes of exposure to sunlight can cause several dozen percent decay of the measured dosimetric signal. The RIS in the protective glass (TG) has been shown to be the least sensitive to light. The omission

[1] There is an error in the article at the bottom of page 547: "Consequently, the corrected magnitudes of the RIS (i.e. which would be measured if the glass was not exposed to light) are 0.62/0.4=1.55 and 0.42/0.5=0.84, respectively.". The value of RIS_{cor} is determined based on the ratio RIS/LCF, and not LIS/LCF, so in this case for the sample used to obtain the relationship RIS vs LIS, we get LCF=0.5 and for RIS_{cor} a value of 0.5 /0.5=1.0 For another sample of GG, analyzed using the same model spectra BG, RIS and LIS, for which different RIS and LIS values would be measured, e.g. RIS=0.7 and LIS=0.42, the value of the correction factor could be read from Fig. 5g as LCF=0.5 and finally we calculate RIS_{cor} =0.7/0.5=1.4.

of LIS component in the numerical decomposition of spectra may cause significant (about 90%) inaccuracy in the reconstruction of the dose. A method of quantitative correction of the dosimetric signal in glasses exposed to both ionizing radiation and UV light, based on the observed dependence between the RIS and LIS spectral components, was proposed. However, this method is applicable provided that both LIS and RIS components are characterized by a different shape of their EPR spectrum.

Article 3. Marciniak A, Ciesielski B, Juniewicz M. *EPR dosimetry in glass – a review.* Radiation and Environmental Biophysics. 2022; 61(2):179-203.

This article is a review of previously published works on EPR signals in glasses. It summarizes information particularly important and helpful in research on retrospective dosimetry within a range of doses typical for radiation accidents.

It underlines the need to develop methods applicable in the event of unexpected irradiation of people or when the need to verify the absorbed dose occurs after a planned irradiation. The advantages of glass as a potential detector material in retrospective dosimetry are presented. The structure and chemical composition of the glasses are described in detail (Tab. 1). Differences in elemental composition of glass and tissues are important for the final assessment of dose absorbed in biological material on the basis of dose measured in another material. The glass/tissue ratios of mass absorption coefficients and stopping powers should be used in approximate dose estimation. These ratios calculated for a wide range of photon and electron energies using elemental compositions given in Tab. 1 and interaction coefficients from NIST Standard Reference Database 124 and 126 (https://www.nist.gov) are presented in Fig. 1.

The article presents basic characteristics of EPR signals observed in glass: native BG signals, light-induced signals and radiation-induced signals. Figure 2 compares the BG spectra of various types of glasses with their spectra after irradiation thus proving the necessity to separate the radiation-induced signals from the remaining spectral components. Table 2 summarizes information concerning paramagnetic centers in various types of glass present in human environment (e.g. laboratory glass, window glass, watch glass and glass from the screens of electronic devices, in particular smartphones) – these centers are responsible for presence of the BG and the RIS. EPR signals in Gorilla Glass (Fig. 4), are presented separately. The GG material is resistant to cracking and scratches, which results in its ubiquitous use as screens of common electronic devices.

The article briefly describes three methods used to quantify the changes in EPR spectra caused by ionizing radiation in glass:

(1) Measurement of deviations of the spectral line from the baseline – so called "peak-to-peak amplitude" method (Fig. 5). The disadvantages of using this popular method when the RIS overlaps with BG or LIS are pointed out.

(2) Determination of the second integral of the EPR spectrum, which reflects the total number of paramagnetic centers forming the EPR signal. This method was used by some researchers and allowed to measure absolute concentrations of radicals generated by radiation [30, 31, 32].

(3) Determination of magnitude of the RIS component by numerical decomposition of the spectrum into the model components: BG, RIS and, for glass exposed to light, LIS. It has been shown, that use of this procedure enables separation of the dosimetric RIS component from the BG and LIS components of the EPR spectrum. However, this method requires knowledge of the model spectra [20, 30].

Only when the analyzed samples have a similar background spectrum (e.g. they come from the same manufactured batch) and have a similar history of light exposure, results obtained with the amplitude method can be of a similar accuracy as those obtained with spectra decomposition (Fig. 6).

Table 4 summarizes published data on dose detection limit D_L in various types of glass together with the used methods of analysis. For example, for MG and GG glass – $D_L \approx$ 1 Gy, for protective glass $D_L \approx 2$ Gy and for watch glass this value ranged from about 1 Gy to 5 Gy. Our latest research (Article 4) showed $D_L = 0.05$ Gy for watch glass. However, this information should be treated as a rough estimate of the sensitivity of dosimetry procedures used by individual authors due to different interpretations of the term "detection limit" by different researchers. Using an unambiguous definition of this term in reports is crucial, as it determines practical applicability of a given method.

The next part of this article describes stability of the radiation-induced signal. A lack of long-term stability of RIS is mentioned by some authors as a disadvantage of glass as a dosimetric material. However, despite the decay, RIS was detected in glasses many months after irradiation [14, 19, 33]. In some glasses the decreasing intensity of the radiation-induced signal not only affects amplitude of the spectrum, but also its shape (Fig. 9a and 9b). Figure 10 and Table 5 summarize the published information on kinetics of the decay of RIS expressed by the decay factor (DF), defined as the fraction of the

initial RIS measured after a given number of days after irradiation. It has been shown, that for glasses from mobile phone screens a fast signal decay occurs during the first 6-8 days after irradiation and then the decrease in RIS significantly slows down and is less than 25% over the next 26 days.

The final part of the article presents an analysis of influence of sample preparation (cleaning and crushing of glass) and physical factors (temperature and light) on magnitude and shape of the EPR signals. Ethanol used commonly to clean the glass samples does not affect the EPR signal. For glass grains larger than 315 μm, no additional components in their EPR signals were observed [14, 19, 22 and 23], while for powder samples (grains <315 μm) additional EPR signals were observed. The effect of temperature on EPR signals was discussed from two perspectives: due to (1) the effect of ambient temperature on the kinetics of RIS decay (i.e. on the deterioration of dosimetry accuracy) and (2) intentional annealing of the samples, which may be helpful in reconstruction of the sample-specific BG signal by "erasing" the RIS from an irradiated sample. The effect of temperature on EPR signals was studied by several authors for different types of glass. Engin et al. [25] observed a complete decay of the signal after a 15-minute annealing of window glass at 200°C (Fig. 12a), while for temperatures within 60°C-150°C, the decay ranged from about 30% to90% (Fig. 12b). Trompier et al. [14] obtained various effects of annealing glass from LCD screens (Fig. 13): for one type of glass a decrease in the intensity of the EPR signal was observed without changing its shape (Fig. 13a), while in other samples (both irradiated and non-irradiated), the annealing caused an induction of additional EPR line, which can be attributed to thermal generation of additional paramagnetic centers (Fig. 13b). Liu et al. [34] showed that a storage of samples at low temperatures (−18 °C) resulted in slower decay of RIS than at room temperature.

Analysis of literature reports and own works (Article 2) concerning the effect of light on EPR signals in glass leads to important conclusion, that uncontrolled exposure of glass samples to UV light may adversely affect the accuracy of EPR dosimetry - both through the potential effect of UV on background signals (Fig. 14), as well as on the radiation-induced signals (Fig. 15, 16). The observability of the effects of light and the way in which light can alter dose reconstruction depend on the type of glass. Due to a huge variety of glass materials, the assessment of this effect in a given glass requires an individual approach.

The presented analysis of results published by many authors confirms usefulness of glass constituents of everyday objects for dosimetry, however with limitations caused

by variety of the background signals in different glasses, decay of the dosimetric signal and effect of UV light on EPR signals. Nevertheless it was emphasized, that the introduction of an appropriate corrections accounting for decay of the RIS and taking into account a potential exposure to UV light allow to use this method for retrospective dosimetry following radiation accidents, e.g. for triage of people irradiated at the dose level of 1-2 Gy.

Article 4. Marciniak A, Juniewicz M, Ciesielski B, Prawdzik-Dampc A, Karczewski J. *Comparison of three methods of EPR retrospective dosimetry in watch glass*. Frontiers in Public Health. 2022, 10.

The purpose of this article was to compare the results of three methods: the calibration method (CM), the added dose method (ADM) and the added dose and heating method (AD&HM) used for retrospective dose measurement based on EPR signals in watch glass obtained and tested as part of international dosimetry project RENEB ILC 2021 [11].
The examined samples were of two types: 6 calibration samples irradiated with 240 kV X-rays with doses: 0.0 Gy, 0.5 Gy, 1.0 Gy, 2.0 Gy, 3.0 Gy and 6.0 Gy and 3 blind samples with doses disclosed by the organizers of the RENEB project only after the participants had reported their results; these doses were 0.0 Gy; 1.2 Gy; 3.5 Gy. All doses given are in terms of kerma in air.
The article proposes selection of the appropriate method of dose reconstruction taking into account availability of the research material and available information regarding its model EPR spectra (Fig. 2). A linear dependence of the RIS on dose in the range of 0-6 Gy was demonstrated (Fig. 4).
The CM method requires calibration of the RIS vs. dose using separate samples of the same type of glass. Calibration samples were measured six times between 8 and 126 days after irradiation. This allowed to determine kinetics of the decay of the dosimetric signal, which was taken into account in calculations of dose in the blinded samples measured at different time intervals after irradiation than the calibration samples. Blinded samples were measured on 7^{th} and 11^{th} day after irradiation, and the reconstructed doses (averaged from both measurements) were: 0.05 Gy, 1.03 Gy, and 3.16 Gy (Tab. 1).
The ADM method is schematically presented in Fig. 1. It is based on necessary knowledge of the BG signal of the tested glass (which is a limitation of this method). The tested sample is used for calibration of the dosimetric signal by additional irradiation of this

sample with a known calibration dose. A crucial element in the dose reconstruction was considering the rate of RIS decay, as the measurements were made at different times after irradiation - between 8 and 407 days after the initial irradiation of the samples. The article presents the derivation of the formula for calculating the unknown dose, taking into account the signal decay in various stages of the time-prolonged procedure: between the initial irradiation and the first EPR measurement, the second irradiation with the added calibration dose and the next EPR measurement. In the presented study, the added calibration dose was (6.0±0.1) Gy in terms of dose absorbed in water, which is equivalent to (5.17±0.10) Gy dose in the glass. The reconstructed doses were converted to kerma in air (K_air) to compare them with the real delivered doses, which were reported in kerma by organizers of the RENEB ILC. The doses reconstructed by this method are presented in Table 1, in column 4.

The AD&HM method differs from the ADM method in that the spectral decomposition procedure uses the BG model spectrum obtained by measurement of glass samples first irradiated and then annealed at 200℃ or 250℃ for 4-45 min. The annealing caused a decay of the RIS component, allowing the measurement of the native BG signal of this test sample. It was checked before, that annealing at high temperatures did not affect EPR spectra of non-irradiated WG samples (Fig. 5a, 5b). This was a different observation than results reported by other authors, who reported changes in background spectra of annealed phone screen glasses [14, 24]. In the irradiated WG 45 min. heating at 200℃ reduced intensity of the RIS by more than 90%, while only 4 minutes of heating at 250℃ resulted in almost complete elimination of the RIS (Fig. 6b).

A similar measurement accuracy of approximately 0.3 Gy was obtained with all three analyzed methods (Tab. 1), which is sufficient for their use for a reliable triage of people irradiated in radiation accidents.

The results of the presented AD&HM method proved applicability of this method in a real radiation accident, when the background signal of tested samples is not available, i.e.when only the irradiated sample is at the disposal of researchers. However, applying this method to other glass types than the tested watch glass requires verification of stability of their BG at high temperatures.

SUMMARY AND CONCLUSIONS

The research described in this doctoral thesis confirms that in the tested glass ionizing radiation induces structural changes in form of paramagnetic centers, stability of which enables reliable measurement of their EPR signals even many months after irradiation and allows their use for retrospective assessment of the dose absorbed in glass. It has been shown, that the dosimetric EPR signal in glasses depends linearly on the dose in the range of 0-20 Gy and persists for at least 18 months after irradiation. An advantage of these glasses for dosimetry is also their ubiquity in humans' environment, availability, ease of sample preparation and EPR measurements. The EPR signals observed in irradiated glasses, apart from the radiation dose, are dependent on factors such as: chemical composition and production method, which are responsible for variation of the background signal (BG) in different types of glass, and the exposure of glasses to ultraviolet light. EPR dosimetry in the examined glasses is characterized by dose detection limit at the level of 0.05-2 Gy, which is sufficient for triage of people exposed in radiation accidents.

In this research, the first dedicated study of the effect of natural and artificial light on EPR dosimetry in glasses was carried out. The changes in the dosimetric RIS signal in glasses exposed to light containing a UV component were demonstrated. In addition, a method of quantitative correction accounting for the UV effects on the RIS was proposed for such glasses, whose RIS and the light-induced LIS components have different shape of their EPR spectrum. This makes it possible to quantitatively relate the light-induced decay of RIS with magnitude of the LIS signal growing due to exposure to light. A neglection of those light effects in dosimetry may result in large errors in determination of the absorbed dose.

It was also noted, that variations of the background signal in different types of glasses introduces an important difficulty in dosimetry, because knowledge of this signal is crucial for accurate determination of the dosimetric signal. Therefore, the Added Dose & Heating Method (AD&HM), which allowed to recover the background signal by annealing samples at high temperature, was developed and experimentally verified for watch glass. The accuracy of dose reconstruction obtained with this method, amounting to about 0.3 Gy, was similar to the results obtained with the commonly used methods CM and ADM. However, unlike them, in the AD&HM it is not necessary to use another non-irradiated sample to determine the background signal and to calibrate RIS vs dose. This

method is of much higher applicability under conditions of a real radiation accident than the other methods.

The results presented in this doctoral dissertation confirm the possibility of using EPR dosimetry in glass for initial triage of irradiated persons in radiation accidents, thus confirming the working hypothesis of this study.

WYKAZ CYTOWANEGO PIŚMIENNICTWA

[1] Wątor W. Radiacja- czy zawsze oznacza alert? https://www.ppoz.pl/czytelnia/ratownictwo-i-ochrona-ludnosci/Radiacja--czy-zawsze-oznacza-alert/idn:1484, dostęp 30.05.2023.

[2] Cerezo L. Radiation accidents and incidents. What do we know about the medical management of acute radiation syndrome? Rep Pract Oncol Radiother. 2011; 16(4):119-22. https://doi.org/10.1016/j.rpor.2011.06.002.

[3] Gabriel Hundeshagen, Stephen M. Milner, 41 - Radiation Injuries and Vesicant Burns, Editor(s): David N. Herndon, Total Burn Care (Fifth Edition), Elsevier, 2018, Pages 414-421.e1, ISBN 9780323476614, https://doi.org/10.1016/B978-0-323-47661-4.00040-X.

[4] Grammaticos P, Giannoula E, Fountos GP. Acute radiation syndrome and chronic radiation syndrome. Hell J Nucl Med. 2013;16(1):56-9.

[5] Fliedner TM, Powles R, Sirohi B, i in. Radiologic and nuclear events: the METREPOL severity of effect grading system. Blood. 2008; 111(12): 5757-5758. DOI: 10.1182/blood-2008-04-150243.

[6] Fattibene P, Trompier F, Bassinet C, i in. Reflections on the future developments of research in retrospective physical dosimetry. Physics Open, 2023; 14, 100132. https://doi.org/10.1016/j.physo.2022.100132.

[7] Punchard NA, Kelly FJ. (Eds.), Free Radicals: A Practical Approach Oxford University Press, Oxford, 1996.

[8] Halliwell B, Gutteridge J. Free radicals in Biology and Medicine, Oxford University Press, Oxford, UK, 352 pp, 2007.

[9] Fattibene P, Trompier F, Wieser A, i in. EPR dosimetry intercomparison using smart phone touch screen glass. Radiat Environ Biophys. 2014; 53(2):311–320. DOI: 10.1007/s00411-014-0533-x.

[10] Port M, Barquinero JF, Endesfelder D, i in. RENEB Inter-Laboratory Comparison 2021: Inter-assay comparison of eight dosimetry assays. Radiat. Res. 2023; 199(6), 535-555. https://doi.org/10.1667/RADE-22-00207.1.

[11] Majchrzyk Ł. Digital, mobile i social media w 2023 roku. https://mobirank.pl/2023/01/26/digital-mobile-i-social-media-w-2023-roku/, dostęp 3 czerwca 2023.

[12] Wu K, Sun CP, Shi YM. Dosimetric properties of watch glass: a potential practical ESR dosemeter for nuclear accidents. Radiat Prot Dosim. 1995; 59:223– 225. DOI: 10.1093/oxfordjournals.rpd.a082654.

[13] Longo A, Basile S, Brai M, i in. ESR response of watch glasses to proton beams. Nucl. Instrum. Methods Phys. Res. B. 2010; 268(17-18), 2712-2718. DOI: 10.1016/j.nimb.2010.05.073.

[14] Trompier F, Della Monaca S, Fattibene P, i in. EPR dosimetry of glass substrate of mobile phone LCDs. Radiat Meas, 2011; 46:827–831. https://doi.org/10.1016/j.radmeas.2011.03.033.

[15] Marrale M, Longo A, D'oca MC, i in. Watch glasses exposed to 6 MV photons and 10 MeV electrons analysed by means of ESR technique: A preliminary study. Radiat. Meas. 2011; 46(9), 822-826. DOI: 10.1016/j.radmeas.2011.05.003.

[16] Aydaş C, Yüce ÜR, Engin B, i in. Polymeris GS. Dosimetric and kinetic characteristics of watch glass sample. Radiat. Meas. 2016; *85*, 78-87. DOI: 10.1016/j.radmeas.2015.12.030.

[17] Trompier F, Burbidge C, Bassinet C, i in. Overview of physical dosimetry methods for triage application integrated in the new European network RENEB. Int J Radiat Biol. 2017; 93(1):65–74. DOI: 10.13140/RG.2.2.20057.26725.

[18] Sholom S, McKeever SWS. Developments for emergency dosimetry using components of mobile Phones. Radiat Meas. 2017; 106:416–422. https://doi.org/10.1016/j.radmeas.2017.06.005.

[19] Juniewicz M, Ciesielski B, Marciniak A, i in. Time evolution of radiation-induced EPR signals in different types of mobile phone screen glasses. Radiat. Environ. Biophys. 2019; 58(4):493-500. DOI: 10.1007/s00411-019-00805-1.

[20] Juniewicz M, Marciniak A, Ciesielski B, i in. The effect of sunlight and UV lamp exposure on EPR signals in X-ray irradiated touch screens of mobile phones. Radiat. Environ. Biophys. 2020; 59(3):539-552. DOI: 10.1007/s00411-020-00858-7.

[21] Griscom DL. Electron spin resonance in glasses. J. Non-Cryst. Solids. 1980; *40*(1-3): 211-272. DOI: 10.1016/0022-3093(80)90105-2.

[22] Bassinet C, Trompier F, Clairand I. Radiation accident dosimetry on glass by TL and EPR spectrometry. Health Phys. 2010; 98(2):400–405. DOI: 10.1097/01.HP.0000346330.72296.51.

[23] Trompier F, Bassinet C, Wieser A, De Angelis C, Viscomi D, Fattibene P. Radiation-induced signals analysed by EPR spectrometry applied to fortuitous dosimetry. Ann Inst Super Sanita. 2009; 45(3):287–296.

[24] McKeever SWS, Sholom S, Chandler JR. A comparative study of EPR and TL signals in Gorilla® glass. Radiat. Prot. Dosim. 2019; 186(1):65-69. DOI: 10.1093/rpd/ncy243.

[25] Engin B, Aydas C, Demirtas H. ESR dosimetric properties of window glass. Nucl. Instrum. Methods Phys. Res. B. 2006; 243(1):149-155. DOI: 10.1016/j.nimb.2005.08.151.

[26] Trompier F, Method for the dosimetry of ionizing radiation by direct EPR measurement on the glass of a screen of an electronic device, International Patent WO (2016), 2016/055315 A1.

[27] Port M, Kulka U, Wojcik A, i in. Reneb inter-laboratory study on biological and physical dosimetry employing eight assays, Radiation Research Society. In: 67th Annual International Meating: Connected by Science (2021).

[28] Trompier F, Institute for Radiological Protection and Nuclear Safety (IRSN), France. Personal communication at International Workshop on Radiation Dosimetry in Glass, Multibiodose/EURADOS, IRSN, Paris (2012).

[29] Sholom S, Wieser A, McKeever SWS. A comparison of diferent spectra deconvolution methods used in EPR dosimetry with Gorilla glasses. Radiat Prot Dosim. 2019; 186(1):54-59. https://doi.org/10.1093/rpd/ ncy260.

[30] Ranjbar AH, Durrani SA, Randle K. Electron spin resonance and thermoluminescence in powder form of clear fused quartz: effects of grinding. Radiat. Meas. 1999; 30: 73-81. DOI: 10.1016/S1350-4487(98)00088-2.

[31] Hassan GM, Sharaf MA, Desouky OS. A new ESR dosimeter based on bioglass material. Radiat. Meas. 2004; 38(3):311-315. DOI: 10.1016/j.radmeas.2004.01.020.

[32] Hassan GM, Sharaf MA. ESR dosimetric properties of some biomineral materials. Appl. Radiat. Isot. 2005; 62(2):375-381. DOI: 10.1016/j.apradiso.2004.08.013.

[33] Bortolin E, De Angelis C, Quattrini MC, i in. Detection of ionizing radiation treatment in glass used for healthcare products. Radiat. Prot. Dosim. 2019; 186(1):78-82. DOI: 10.1093/rpd/ncz014.

[34] Liu YL, Huo MH, Ruan SZ, i in. EPR dosimetric properties of different window glasses. Nucl. Instrum. Meth. B. 2019; 443, 5-14. DOI: 10.1016/j.nimb.2019.01.022.

ARTYKUŁY WCHODZĄCE W SKŁAD ROZPRAWY DOKTORSKIEJ

Radiation and Environmental Biophysics (2019) 58:493–500
https://doi.org/10.1007/s00411-019-00805-1

ORIGINAL ARTICLE

Time evolution of radiation-induced EPR signals in different types of mobile phone screen glasses

Małgorzata Juniewicz[1] · Bartłomiej Ciesielski[1] · Agnieszka Marciniak[1] · Anita Prawdzik-Dampc[2]

Received: 7 February 2019 / Accepted: 19 June 2019 / Published online: 1 July 2019

Abstract

In this study, samples of smart phone touch screen glass sheets and tempered glass screen protectors were examined with respect to their potential application in the dosimetry of ionizing radiation. The glass samples were obtained from various phones with different types of glass. Electron paramagnetic resonance (EPR) spectra of the radiation-induced signals (RIS) are presented and their dose dependence within a dose range of 0–20 Gy. Despite the observed fading with time of the dosimetric components of the signal, the remaining RIS turned out to be strong enough for a reliable dosimetry even 18 month after irradiation. The study also shows that crushing of the glass sheets and water treatment of the samples have no effect on the background and dosimetric EPR signals.

Keywords EPR · Dosimetry · Glass · Retrospective · Mobile phone · Radiation

Introduction

The investigation of electron paramagnetic resonance (EPR) spectra of different materials exposed to ionizing radiation is a subject of research of many laboratories worldwide. The EPR technique can be a valuable tool for retrospective, non-destructive dosimetry in radiation accidents, in particular for mass casualty incidents resulting in the exposure of numerous people to ionizing radiation. In such situations, a quick and simple sampling method followed by a fast identification of the absorbed dose is needed for the triage of the victims and for planning an appropriate medical treatment of those exposed (Trompier et al. 2017). Human tissues, such as tooth enamel and bone, already proved to be useful in ex vivo EPR dosimetry (Trompier et al. 2009b; Fattibene and Callens 2010; Krefft et al. 2014; Kaminska et al. 2016; Kinoshita et al. 2018). However, their applicability is limited due to the obvious difficulty in sample acquisition. Initial studies on EPR dosimetry in nail clippings indicated potential large inaccuracies in reconstructed doses, due to the presence of confounding EPR signals generated mechanically in the samples by cutting, and due to the fading of the dosimetric signal caused by exposure of nails to water (Trompier et al. 2009a; Marciniak et al. 2018) or induction of obscuring EPR signals by light (Sholom et al. 2018; Marciniak et al. 2019). Therefore, artificial materials in the vicinity of exposed individuals as well as personal belongings could provide better dosimetric materials more convenient in usage, provided that they preserve any radiation-induced EPR signals. Various laboratory glassware samples (e.g., from Jena, Rasotherm, Thuring, window glass) exhibit specific EPR signals induced by irradiation, which differ depending on the chemical content of the investigated glass (Gancheva et al. 2006). Kortmis and Maltar Strmecki (2018) studied soda-lime glass samples from six different glass batches and demonstrated the influence of temperature on the fading of RIS components over time.

Bortolin et al. (2019) studied glass samples used for blood test tubes, to reveal illegal omission of radiation sterilization of the blood in glass by means of the thermoluminescence (TL) and EPR techniques. Both techniques allowed detection (up to 1 year after the exposure) of effects induced by high doses of ionizing radiation (10^3 Gy) in the glass at the manufacture stage. Recently, commonly used electronic devices containing glass elements, such as watches, eyeglasses or mobile phones, were investigated by several researchers with regard to their potential suitability as EPR dosimeters (Teixeira et al. 2008; Trompier et al. 2009b, 2010, 2011a, b; Bassinet et al. 2010). Touch screen

✉ Małgorzata Juniewicz
mjuniewicz@gumed.edu.pl

[1] Department of Physics and Biophysics, Medical University of Gdańsk, Dębinki 1, 80-211 Gdańsk, Poland

[2] Department of Oncology and Radiotherapy, Medical University of Gdańsk, Dębinki 7, 80-952 Gdańsk, Poland

glass from mobile phones is a particularly attractive material taking into account its widespread use and non-invasive, easy, and fast sample preparation (Marrale et al. 2012). Trompier et al. (2009b) measured mobile phone screen glass sheets and observed changes in EPR line shape after irradiation, which proved generation of a radiation-induced signal (RIS) in this material. So far, most of the EPR research of irradiated glass from mobile phones has been carried out on Gorilla Glass®. A report of Fattibene et al. (2014) summarized the results of an international intercomparison dosimetry project, in which the parameters of calibration lines and detection limits for irradiated Gorilla Glass® were compared between participating laboratories. Recently, Sholom and McKeever (2017) studied EPR spectra of protective glasses from various manufacturers of mobile phones. Modern smartphones contain different types of screens, which may differ with respect to the properties of their EPR spectra generated by radiation. The variability of the background signals (BGSs) in different glasses was presented in articles of Sholom and McKeever (2017) and Sholom et al. (2018). Moreover, it was shown by McKeever et al. (2018) that the BGS may differ between samples cut from different regions of the same screen. Sholom et al. (2018) presented two methods of dose reconstruction. Particularly, a higher intensity of EPR signals around the edge of the investigated screen was observed, which was assigned to an exposure to UV radiation during manufacturing.

A reliable retrospective dosimetry in real accidents requires also a knowledge regarding the time dependence of the dosimetric signals, as well as the effects of water and mechanical stress caused during preparation of the samples. Therefore, in the present study, results are presented regarding the time evolution of radiation-induced EPR signals by showing the kinetics of their decay during a long period—from a few hours up to 18 months after irradiation. The dose dependence of these signals in different types of glasses used in popular mobile phones is also presented, as well as the effects of water treatment and crushing of the samples on the EPR spectra. These are important practical factors in a potential post-accident dosimetry, when intact phones got irradiated and later their screens were exposed to water (e.g., in a rain or during cleaning) and crushed for EPR measurements.

Materials and methods

The samples were obtained from four types of glass used for touch screens in mobile phones: Gorilla Glass (GG)—some of these samples had also been irradiated during a past intercomparison project (Fattibene et al. 2014) and other came from different batches: mineral glass (MG) from Sony Xperia L, model C2105, tempered glass (TG) used commonly as additional protective cover of the original screen—0.3 mm thickness, ninth level of hardness according to the Mohs' scale, from Samsung S5, and screen glass obtained from iPhone 6S (IP).

After separation of the glass parts from the LCD layers, the samples were washed with ethanol and crushed in a mortar into pieces of grain size of 0.3–4 mm. Some larger pieces were also measured to check the effect of crushing on the background signal (Fig. 1).

EPR measurements were performed with Bruker EMX 6/1 in X band with regular cavity type 4119HS W1/0430 at room temperature, using quartz sample tubes with 3 mm and 5 mm internal diameter. The following spectra acquisition parameters were applied: microwave power 32 mW, modulation amplitude 0.15 mT, sweep width 10 mT, conversion time 81.92 ms, and time constant 163.84 ms. As internal reference sample the marker ER 4119HS-2100 (Bruker BioSpin GmbH) was applied during all measurements, and the spectra were aligned and normalized with respect to the marker's EPR line before further analysis. For every sample, 10 to 20 scans were averaged. The measurements were repeated three times at three different orientations of the sample in the cavity to minimize any potential effect of the samples' anisotropy on the EPR spectra. The spectra were normalized to the mass of the samples which was in the 100–250 mg range. The spectrum of the empty tube was subtracted before further analysis of the spectra.

Irradiations of the samples were performed in the Department of Oncology and Radiotherapy, Medical University of Gdańsk (Poland) with 6 MVp photons from a Clinac 2300 medical accelerator. The crushed samples were irradiated with doses of 0.8, 2.0, 4.0, and 10.0 Gy (Gorilla Glass); 4.0,

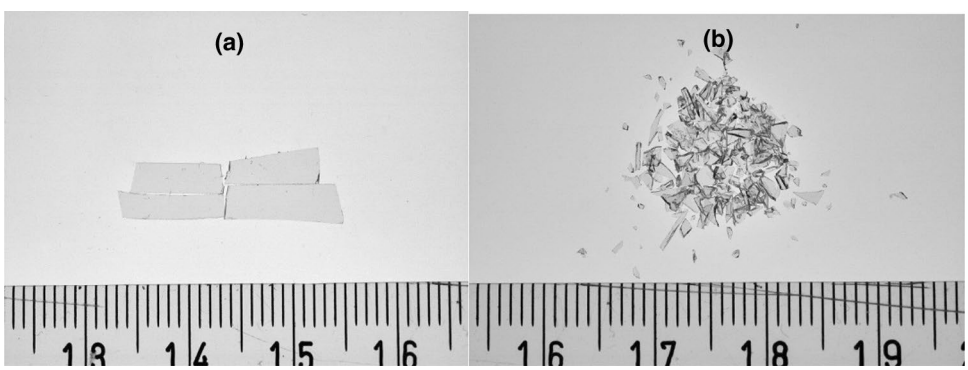

Fig. 1 Microphotography of the mineral glass samples (MG_10 Gy) before (**a**) and after crushing (**b**). Their respective EPR spectra are presented in Fig. 2a

8.0, 10.0, and 20.0 Gy (mineral glass); 2.0, 4.0, and 8.0 Gy (tempered glass); and 10.0 Gy (iPhone 6S).

The measurements of the background signals in the unirradiated samples were made at least 5 days after their crushing. The samples were stored at room temperature (about 24 °C) in the darkness; only the samples from the intercomparison project were kept in normal laboratory light conditions (but not exposed to direct sunlight) before and after irradiation.

For quantitative analysis of the spectral components, the same analytical method which was used by participants of the intercomparison project (Fattibene et al. 2014) was also applied in the present study. More specifically, the spectra of the irradiated samples were numerically separated into two benchmark model spectra: one was the background spectrum (i.e., that measured in the unirradiated sample) and the other was a model RIS spectrum obtained by subtraction of the background spectrum from the spectrum measured in the same sample irradiated with the highest dose (10 or 20 Gy). The same method was also used in Sholom et al. (2018) and McKeever et al. (2018). The magnitudes of the radiation-induced signals presented in the "Results and discussion" refer to the contributions of the model RIS components in the experimental spectra, calculated by numerical decomposition of the spectra. The decomposition was performed using the Reglinp procedure in the MS Excel package. The uncertainties (error bars) presented in the figures below refer to one standard deviation and reflect the repeatability of the EPR measurements (at three orientations of the sample tube in the cavity).

Results and discussion

Effect of crushing and water treatment

The marker line was removed from all spectra presented below, due to subtraction of the empty tube spectrum.

Figure 2a–c shows the effect of crushing of the unirradiated and irradiated samples on the shapes of their EPR spectra. The spectra were first measured in large pieces (about 16×3 mm^2, like those shown in Fig. 1a), and then measured

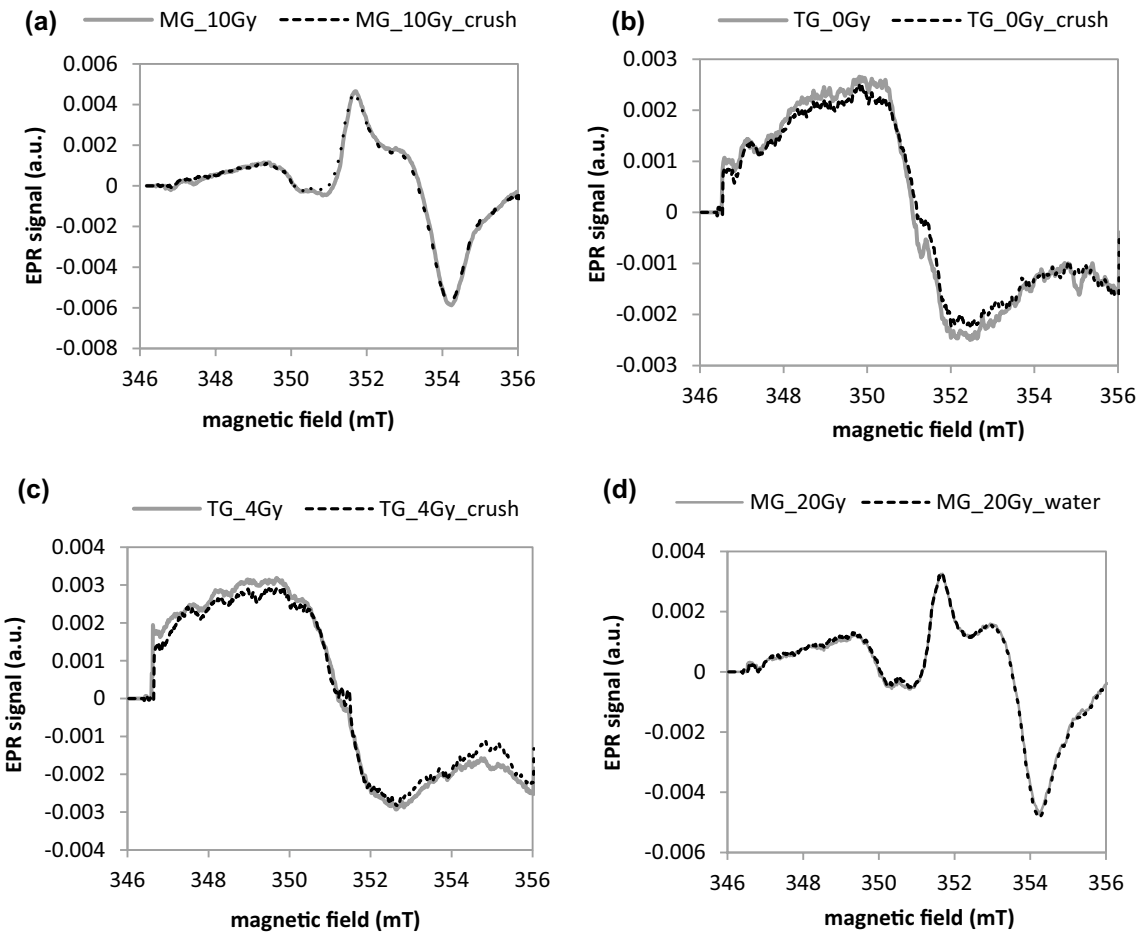

Fig. 2 **a–c** Effect of crushing of unirradiated and irradiated samples on their EPR spectra; gray solid lines—large piece samples; black dotted lines—sub-millimeter grains. **d** Effect of water treatment on EPR spectrum of mineral glass phone screens irradiated to 20 Gy; solid line—before washing; dashed line—after 10 min of washing. *MG* mineral glass, *TG* tempered glass

again about 10 min after crushing the large pieces into sub-millimeter grains (like those shown in Fig. 1b).

Figure 2d shows the effect of immersion of the sample for 10 min into water for the glass sample irradiated to 20 Gy before the treatment.

The spectra presented in Fig. 2 prove that crushing of the glass samples to sub-millimeter grains did not affect their EPR signals—in both unirradiated (MG and TG) and irradiated (TG) samples, even when the samples were measured directly after crushing. This is in accordance with data of Bassinet et al. (2010), who reported a change in shape of the background signal and an increase in its intensity after grinding glass samples to a fine powder with grains below 315 µm, but did not observe any changes when grinding glass samples to larger grains. This mechanically induced increase in intensity of the background spectra in grains smaller than 315 µm decayed in about 10 h after crushing, as was shown by Trompier et al. (2011a). Furthermore, exposure of the irradiated MG sample to water did not induce any changes in its EPR spectrum. These results are important for practical applications of EPR dosimetry, because washing and crushing are necessary, indispensable steps in preparation of samples for EPR measurements. Also, in retrospective dosimetry an unintended exposure of the samples to water cannot be excluded. Therefore, the sensitivity of the EPR signals to water would be a potential, serious confounding factor.

The effect of irradiation

Figure 3 shows the effect of a dose of 10 Gy on the EPR spectra for Gorilla Glass (A), mineral glass (B), tempered glass (C), and iPhone glass (D). The background spectra (0 Gy) of the four examined glass samples presented in Fig. 3 differ significantly. This variability imposes a serious limitation on the practical application of EPR dosimetry in screen glasses in real exposure scenarios when samples of unirradiated glass of the same type are not available.

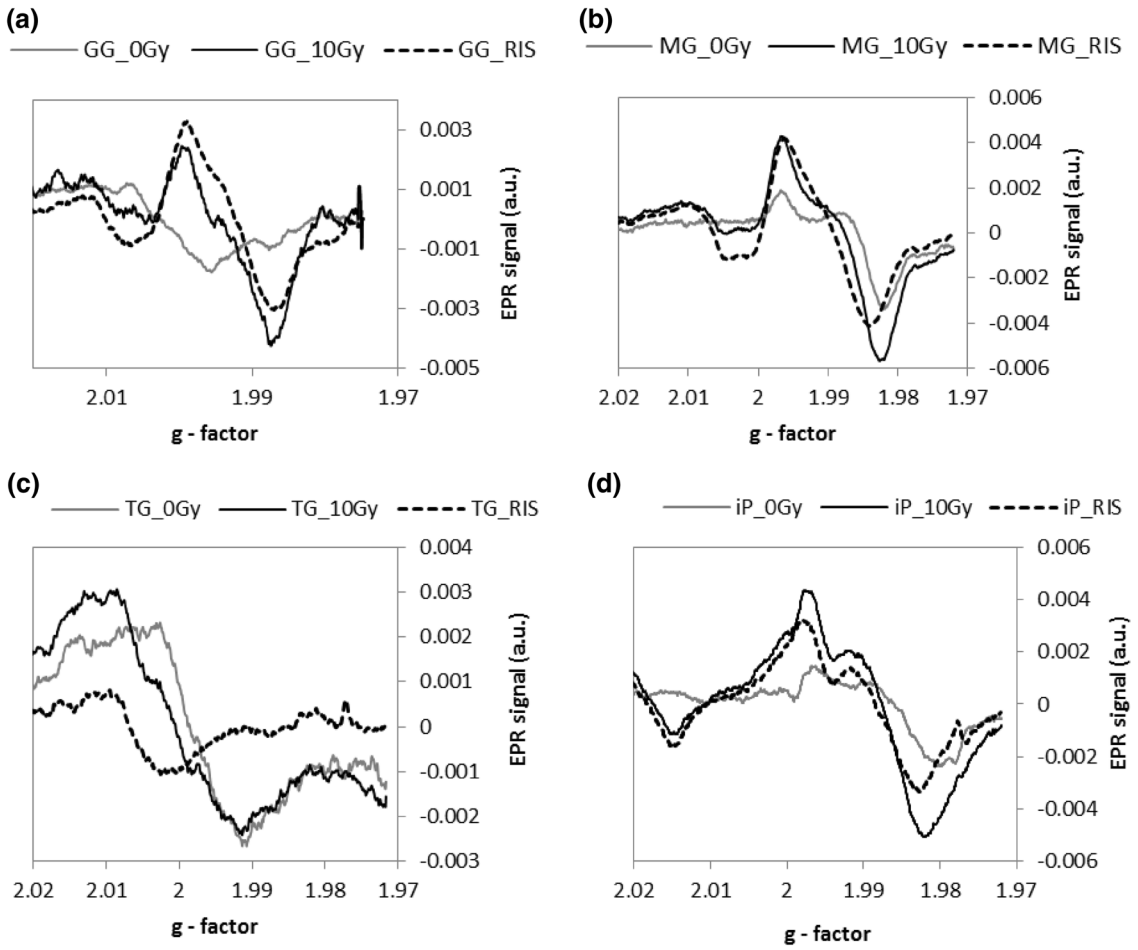

Fig. 3 EPR spectra for unirradiated (gray lines) and irradiated (black solid lines) mobile phone glasses. The characteristic radiation-induced signals (RISs, dashed lines) were obtained by subtraction of the background spectra from the spectrum of irradiated sample. **a** *GG* Gorilla Glass, **b** *MG* mineral glass, **c** *TG* tempered glass, **d** *iP* iPhone glass

Moreover, as shown by McKeever et al. (2018), the intensity of the background signals from different locations of a screen may differ, which creates additional problems in accurate determination of the radiation-induced signal components.

The first EPR spectra for the irradiated samples were measured 6 days after irradiation for GG, 5 days for MG, 5 days for TG, and 10 days for iP. The data obtained suggest similar EPR spectra of paramagnetic centers produced by radiation in the MG, GG and, to a certain extent, IP samples—the shape of the spectra and the g factors of the dominating line (below 2.00) allow to identify the paramagnetic centers as the electron E centers reported by Sholom et al. (2018) and McKeever et al. (2018), accompanied by the presence of a lower intensity component at $g > 2.00$ which can be attributed to the presence of H centers. Also, the magnitude of the RISs is similar, suggesting that the radiation-induced defects may have a similar structure in these materials. In contrast, the RIS spectrum in the TG sample is completely different to that of the other samples, showing only one broad line at a g factor above 2.00, suggesting assignment of this paramagnetic center to one of the hole centers (probably the H2 center), without any spectral lines at $g < 2.00$. The amplitude of the RIS induced in the TG sample by 10 Gy is also significantly smaller in comparison to that of the other three glasses. Nevertheless, on the basis of the calibration line shown in Fig. 4, the precision of dose determination in the TG sample would be similar to that in the other materials—the dependence of the RIS on dose is monotonic with similar uncertainties in parameters of the regression lines (i.e., uncertainties in their slopes and intercepts).

Figure 4 shows the dose dependence of the RISs for Gorilla Glass samples measured 6 days and 15 days after irradiation (Fig. 4a), mineral glass (Fig. 4b) and tempered glass (Fig. 4c) samples measured 5 days after irradiation. The solid lines represent a linear regression of the data. For all samples, within the studied dose ranges, the dose dependence is linear. The dose response curves of Gorilla Glass (Fig. 4a) measured 6 days and 15 days after irradiation slightly differ. The slope of the regression lines for samples measured after 15 days is lower than that for samples measured 6 days after irradiation. This may suggest the decay of the RIS in the time period between these two measurements. Such decay of the RIS in the first 2 weeks after irradiation was demonstrated for the TG samples

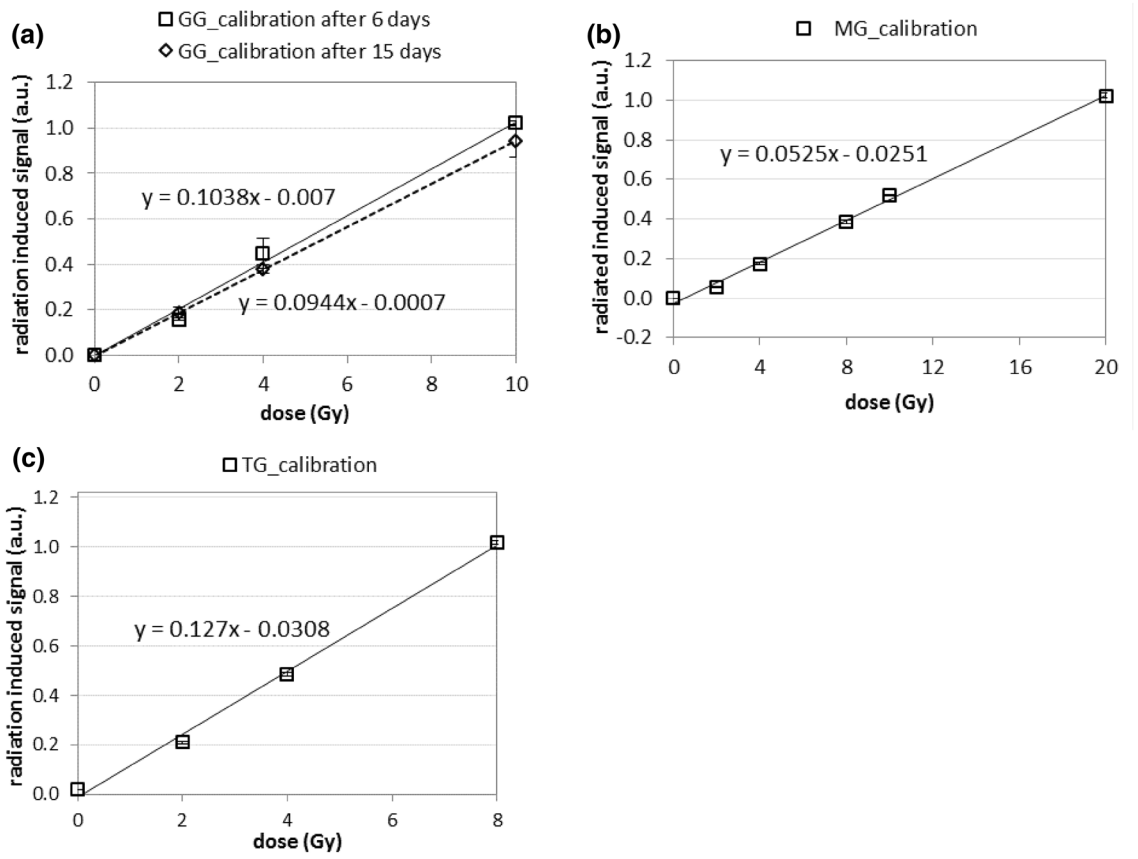

Fig. 4 Dose dependence of radiation-induced signals for different types of the glasses. **a** *GG* Gorilla Glass, **b** *MG* mineral glass, **c** *TG* tempered glass, solid and dashed lines—linear regressions of the data; error bars represent one standard deviation

(Fig. 5b) showing a rapid decay in RIS within the first 10 days after irradiation.

Figure 5 presents variations of the dosimetric signal (the RIS) with time after irradiation for two types of glasses (Gorilla Glass and the tempered glass) irradiated to various doses. The long-term decay of RIS in the GG samples can be roughly approximated by single exponential decay.

$$a0 + a1 \cdot e^{-x/a2}$$

with the decay time $a2$ in the range of 150–230 days (R^2: − 0.98). The fading of RIS in TG can be approximated with a high correlation coefficients $R^2 = 0.99$ by two exponential decay.

$$a0 + a1 \cdot e^{-x/a2} + a3 \cdot e^{-x/a4}$$

with the slow decay constant $a2$ of about 70 days and the fast decay constant $a4$ of about 1 day. The fitted parameters are presented in Table 1.

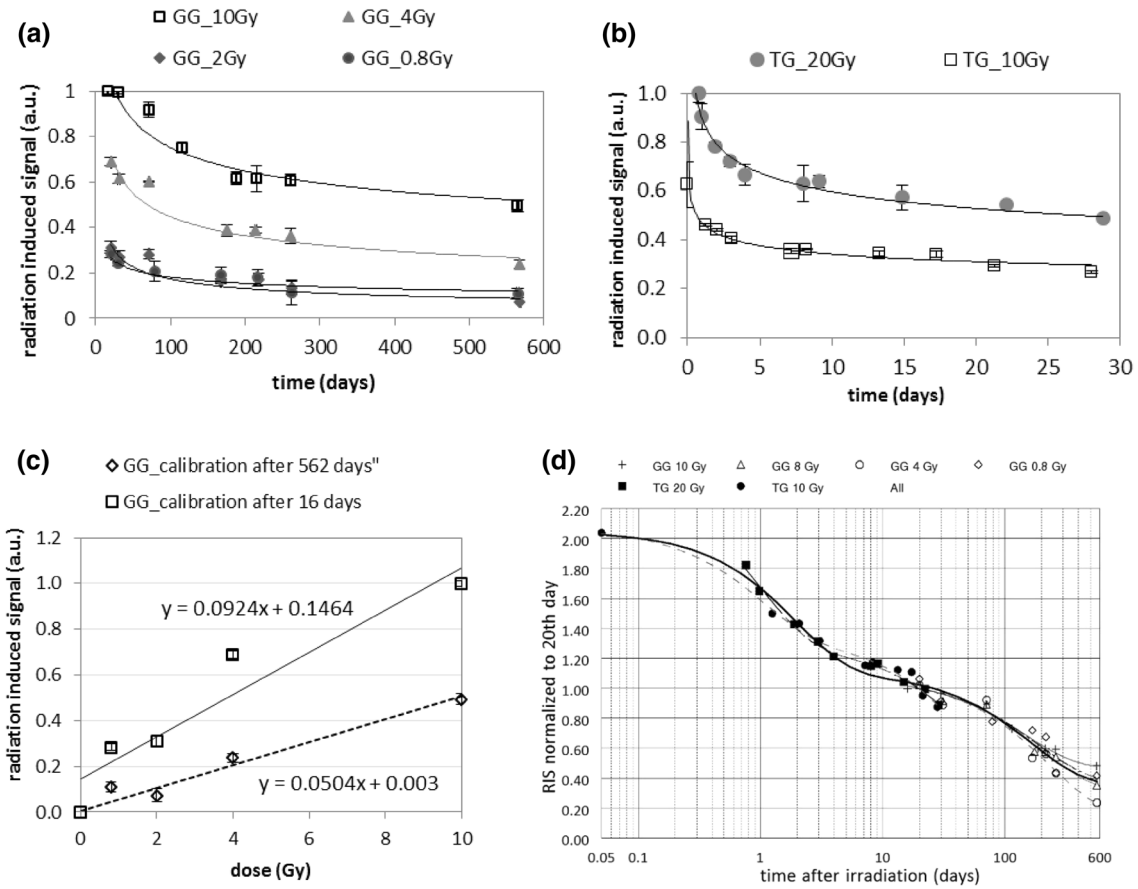

Fig. 5 Changes in magnitude of the dosimetric signal with time for **a** four Gorilla Glass (GG) samples (that were also used by Fattibene et al. 2014); **b** two tempered glass (TG) samples; **c** calibration lines for GG are for data measured on 16th and 562nd day after irradiation; **d** time evolution of the dosimetric signals for TG samples (filled symbols) and GG samples (open symbols) normalized at the 20th day after irradiation; error bars represent one standard deviation

Table 1 Fitted parameters for data in Fig. 5a, b

Fitted parameter	GG 10 Gy	GG 4 Gy	GG 2 Gy	GG 0.8 Gy	TG 20 Gy	TG 10 Gy
a0	0.479	0.210	0.046	0.099	0.034	0.041
a1	0.63	0.51	0.28	0.19	0.67	0.37
a2 (days)	146	197	235	188	76	61
a3	–	–	–	–	0.64	0.23
a4 (days)	–	–	–	–	0.97	1.0
R^2	0.982	0.977	0.960	0.902	0.994	0.988

GG Gorilla Glass, *TG* tempered glass

Figure 5a shows the change in the EPR signals with time for the irradiated GG samples, however, for a longer time scale (from 16 to 560 days after irradiation) than that for the TG samples. Exponential fitting of the data in Fig. 5a, b did not reveal any statistically significant differences in the decay kinetics between the GG and TG samples irradiated with different doses. Due to the difference in time scale for GG and TG (Fig. 5a, b), however, any reliable quantitative comparison of the decay kinetics between GG and TG is not possible. If one assumes that the signal fading observed in the GG and TG samples follows the same kinetics and if one normalizes the data for the GG and TG samples at the 20th day after irradiation (i.e., at a time point included in both sets of data), then the fading of the RIS can be illustrated as shown in Fig. 5d, in which the black solid line represents the fit of the data points for the all samples using the two exponential function mentioned above, with the slow ($a2$) and fast ($a4$) decay constants of about 170 and 1.9 days, respectively. Taking into account the uncertainty of the fit, these values are in rough agreement with the decay constants calculated separately for the GG and TG samples (i.e., about 150–230 days (GG) or 70 days (TG) for the slow decay, and about 1 day for the fast decay (in TG); see Table 1). However, more experimental data are necessary to validate the possibility of approximating the RIS decay in different glasses and for different doses by one joint mathematical function like the one proposed in Fig. 5d. The decrease in RIS amplitudes with time observed in all types of glass examined in the present study clearly demonstrates the need, for retrospective EPR dosimetry, to take into account the kinetics of signal fading. During the first 10 days after irradiation, the absolute loss in the RIS is about the same as during the following year. The decay curve in Fig. 5d allows to estimate roughly that during the whole observation period of almost 19 months the initial RIS (measured about 1 h after irradiation) decreased to about 20% of its initial value.

The effect of the resulting decrease in the slope of the dose calibration with time is illustrated in Fig. 5c, which shows the difference between the calibration lines for the GG samples measured 16 and 562 days after irradiation. Despite the significant decrease in the RIS in the GG samples during this period, the dosimetric EPR signal is still clearly seen, shows an evident, monotonic increase with dose, and thus can be useful for dosimetry in a dose range of several Gy, even delayed in time by many months after irradiation. The fast initial decay of the RIS is a strong contraindication for dosimetry in samples irradiated less than 5 days before measurement. For samples measured later than 5–10 days after irradiation, the signal calibration curve should be corrected for long-term decay, for example, using an approximation like the one given in Fig. 5d.

Conclusion

In the present study, glass samples from different types of mobile phone screens were investigated. The results obtained show that glass screens from mobile phones can provide a good detector material in accident dosimetry. The EPR signals (background and the radiation-induced) are resistant to water and mechanical stress (crushing, cutting). Despite the observed decay of the RIS, dosimetry using mobile phone glasses is possible even 18 months after irradiation, due to the decay process which becomes much slower after about 5–10 days as compared to the initial fast decay. However, a serious limitation in accuracy of glass used for retrospective EPR dosimetry arises due to the variability in background signals between different glass samples. Solving this problem requires additional research focused on (1) the nature of this variability and (2) methods to separate the radiation-induced spectral EPR components from background, in EPR spectra of irradiated samples.

Compliance with ethical standards

Conflict of interest The authors declare that they have no conflict of interests.

References

Bassinet C, Trompier F, Clairand I (2010) Radiation accident dosimetrry on glass by Tl and EPR spectrometry. Health Phys 98(2):400–405

Bortolin E, De Angelis C, Quattrini MC, Barlascini O, Fattibene P (2019) Detection of ionizing radiation treatment in glass used for healthcare products. Radiat Prot Dosim. https://doi.org/10.1093/rpd/ncz014

Fattibene P, Callens F (2010) EPR dosimetry with tooth enamel: a review. Appl Radiat Isot 68(11):2033–2116

Fattibene P, Trompier F, Wieser A, Brai M, Ciesielski B, De Angelis C, Della Monaca S, Garcia T, Gustafsson H, Hole EO, Juniewicz M, Krefft K, Longo A, Leveque P, Lund E, Marrale M, Michalec B, Mierzwińska G, Rao JL, Romanyukha A, Tuner H (2014) EPR dosimetry intercomparison using smart phone touch screen glass. Radiat Environ Biophys 53(2):311–320

Gancheva V, Yordanov ND, Karakirova Y (2006) EPR investigation of the gamma radiation response of different types of glasses. Spectrochim Acta A 63(4):875–878

Kaminska J, Ciesielski B, Drogoszewska B, Emerich K, Krefft K, Juniewicz M (2016) Verification of radiotherapy doses by EPR dosimetry in patients' teeth. Radiat Meas 92:86–92

Kinoshita A, Baffa O, Mascarenhas S (2018) Electron spin resonance (ESR) dose measurement in bone of Hiroshima A-bomb victim. PLOS One. https://doi.org/10.1371/journal.pone.0192444

Kortmis MV, Maltar-Strmecki N (2018) ESR response of soda-lime glasses irradiated with gamma radiation in the 0.5–20.0 Gy range. Radiat Eff Defect Solids 173(11–12):978–985

Krefft K, Drogoszewska B, Kaminska J, Juniewicz M, Wołąkiewicz G, Jakacka I, Ciesielski B (2014) Application of EPR dosimetry in bone for ex vivo measurements of doses in radiotherapy patients. Radiat Prot Dosim 162(1–2):38–42

Marciniak A, Ciesielski B, Czajkowski P, Krefft K, Boguś P, Prawdzik-Dampc A, Lipniewicz J (2018) EPR dosimetry in nail samples irradiated in vivo during total body irradiation procedures. Radiat Meas 116:24–34

Marciniak A, Ciesielski B, Juniewicz M, Prawdzik-Dampc A, Sawczak M (2019) The effect of sunlight and UV lamp on EPR signal in nails. Radiat Environ Biophys 58(2):287–293

Marrale M, Longo A, Brai V, Tomarchio E (2012) ESR response of watch glasses to neutron irradiation. Nuclear Instrum Methods Phys Res 292:30–33

McKeever SWS, Sholom S, Chandler JR (2018) A comparative study of EPR and TL signals in Gorilla® glass. Radiat Prot Dosim. https://doi.org/10.1093/rpd/ncy243

Sholom S, McKeever SWS (2017) Developments for emergency dosimetry using components of mobile Phones. Radiat Meas 106:416–422

Sholom S, Wieser A, McKeever SWS (2018) A comparison of different spectra deconvolution methods used in EPR dosimetry with Gorilla glasses. Radiat Prot Dosim. https://doi.org/10.1093/rpd/ncy260

Teixeira MI, Da Costa ZM, Da Costa CR, Pontuschka WM, Caldas LVE (2008) Study of the gamma radiation response of watch glasses. Radiat Meas 43(2–6):480–482

Trompier F, Romanyukha A, Kornak L, Calas C, LeBlanc B, Mitchell C, Swartz H, Clairand I (2009a) Electron paramagnetic resonance radiation dosimetry in fingernails. Radiat Meas 44:6–10

Trompier F, Bassinet C, Wieser A, De Angelis C, Viscomi D, Fattibene P (2009b) Radiation-induced signals analysed by EPR spectrometry applied to fortuitous dosimetry. Ann Inst Super Sanita 45(3):287–296

Trompier F, Bassinet C, Clairand I (2010) Radiation accident dosimetry on plastics by EPR spectrometry. Health Phys 98(2):388–394

Trompier F, Della Monaca S, Fattibene P, Clairand I (2011a) EPR dosimetry of glass substrate of mobile phone LCDs. Radiat Meas 46:827–831

Trompier F, Bassinet C, Della Monaca S, Romanyukha A, Reyes R, Clairand I (2011b) Overview of physical and biophysical techniques for accident dosimetry. Radiat Prot Dosim 144(1–4):571–574

Trompier F, Burbidge C, Bassinet C, Baumann M, Bortolin E, De Angelis C, Eakins J, Della SM, Fattibene P, Quattrini MC, Tanner R, Wieser A, Woda C (2017) Overview of physical dosimetry methods for triage application integrated in the new European network RENEB. Int J Radiat Biol 93(1):65–74

Radiation and Environmental Biophysics (2020) 59:539–552
https://doi.org/10.1007/s00411-020-00858-7

ORIGINAL ARTICLE

The effect of sunlight and UV lamp exposure on EPR signals in X-ray irradiated touch screens of mobile phones

Małgorzata Juniewicz[1] · Agnieszka Marciniak[1] · Bartłomiej Ciesielski[1] · Anita Prawdzik-Dampc[2] · Mirosław Sawczak[3] · Piotr Boguś[1]

Received: 17 February 2020 / Accepted: 11 June 2020 / Published online: 20 June 2020

Abstract

Electron paramagnetic resonance (EPR) signals generated by ionizing radiation in touch-screen glasses have been reported as useful for personal dosimetry in people accidently exposed to ionizing radiation. This article describes the effect of light exposure on EPR spectra of various glasses obtained from mobile phones. This effect can lead to significant inaccuracy of the radiation doses reconstructed by EPR. The EPR signals from samples unexposed and exposed to X-rays and/or to natural and artificial light were numerically separated into three model spectra: those due to background (BG), radiation-induced signal (RIS), and light-induced signal (LIS). Although prolonged exposures of mobile phones to UV light are rather implausible, the article indicates errors underestimating the actual radiation doses in dose reconstruction in glasses exposed to UV light even for low fluences equivalent to several minutes of sunshine, if one neglects the effects of light in applied dosimetric procedures. About 5 min of exposure to sunlight or to light from common UV lamps reduced the intensity of the dosimetric spectral components by 20–60% as compared to non-illuminated samples. This effect strongly limits the achievable accuracy of retrospective dosimetry using EPR in glasses from mobile phones, unless their exposure to light containing a UV component can be excluded or the light-induced reduction in intensity of the RIS can be quantitatively estimated. A method for determination of a correction factor accounting for the perturbing light effects is proposed on basis of the determined relation between the dosimetric signal and intensity of the light-induced signal.

Keywords EPR · ESR · Glass · Mobile phone · Radiation · Retrospective dosimetry

Introduction

Electron paramagnetic resonance (EPR) signals have been observed in different types of commercial glasses (window glass, windscreen glass, watch glass, glass used for cathode ray tubes, and glass kitchenware) after their exposure to ionising radiation (Engin et al. 2006; Teixeira et al. 2008). The EPR signals generated by doses of a few grays are stable enough to be measured even months after irradiation (Bassinet et al. 2010; Trompier et al. 2011; Juniewicz et al. 2019; Bortolin et al. 2019). Therefore, these materials may be used as potential fortuitous individual dosimeters in radiation accidents. Currently one of the most abundant use of glass worldwide is that for screens of electronic devices, in particular mobile phones. Statistics show that in 2019, the total number of mobile phone users in the world is about 4.7 billion. Screens of mobile phones are especially attractive as radiation detectors not only because of their widespread distribution, but also due to advantages such as chemical inertness, rigidity, insolubility and the fact that a mobile phone is usually kept close to the body, which facilitates estimation of the radiation dose absorbed by its owner. The dosimetric use of screen glasses was already proposed in several reports and articles (e.g., Trompier et al. 2009, Ainsbury et al. 2011).

One of important requirements for reliable retrospective EPR dosimetry is resistance of the dosimeter to other, non-radiation factors, which might affect accurate determination

✉ Małgorzata Juniewicz
mjuniewicz@gumed.edu.pl

[1] Department of Physics and Biophysics, Medical University of Gdańsk, Dębinki 1, 80-211 Gdańsk, Poland

[2] Department of Oncology and Radiotherapy, Medical University of Gdańsk, Smoluchowskiego 17, 80-214 Gdańsk, Poland

[3] Heat Transfer Department, The Szewalski Institute of Fluid-Flow Machinery Polish Academy of Sciences, Generała Józefa Fiszera 14, 80-231 Gdańsk, Poland

of the intensity of the dosimetric EPR signals, causing errors in dose reconstruction. One of such potential factors is light, both natural and artificial, which is permanently present in human's environment and has a potential for generation of free radicals. Engin et al. (2006) studied the light sensitivity of window glass samples—unirradiated and irradiated with γ-rays using a 60 W white room fluorescent lamp (up to 8 months) and exposed to daylight (up to 1 year period). No changes in EPR signal were observed in comparison to samples kept in dark for the both types of samples—irradiated and not irradiated. However, in contrast to window glass, the effect of light on EPR spectra was noticed in screen glasses. During an interlaboratory comparison study of retrospective dosimetry using smart phone touch screen glass carried on in 2013, the participants were recommended to expose the irradiated samples to daylight for at least 5 days, to speed up the fading of any unstable EPR signal components (Fattibene et al. 2014). The organizers referred to preliminary findings of the MULTIBIODOSE 2013 report where the light-sensitive component of the EPR spectrum was mentioned. However, the origin of this component and the mechanism and kinetics of its decay after illumination as well as its effect on dosimetry were not described in details.

The results published by McKeever et al. (2019) suggest that the strong background, in both EPR and thermoluminescence (TL) signals observed in some types of mobile phone screens, is caused by their exposure to UV light during production processes. The authors measured a higher intensity of EPR and TL signals along the edge as compared to that in the center of a screen from a Samsung S3 mobile phone, possibly from curing the adhesive between the glass layers by exposure to UV light. Sholom et al. (2019) presented spectra of seven types of paramagnetic centers observed in Gorilla Glass samples—two hole centers (H1 and H2) and five electron centers (E1–E5). Two of them—E2 and E5—were sensitive only to light exposure, while the centers E3 and E4 showed sensitivity to both gamma radiation and light, fading in 6 days after exposure. Sensitivity to light was also proven for other materials used in EPR dosimetry like alanine, where visible light causes fading of radiation-induced radicals, a change in the shape of the spectra, and a decrease in magnitude of the dosimetric signal (Ciesielski et al. 2004, 2008). Also in human nails, generation of a strong EPR signal, similar to the radiation-induced signal, by the UV component of light was recently reported by Marciniak et al. (2019).

In this study, we present effects of exposure of irradiated and un-irradiated mobile phone screen glass to artificial visible light (from fluorescent bulbs), to artificial light including a UV component (from UV lamps used in solaria and cosmetic saloons), and to natural sunlight, on EPR signals of the samples. Consequences of these effects on EPR dosimetry are discussed.

Materials and methods

Samples

The samples, each about 90–180 mg in total mass, were obtained from different types of glasses taken from touch screens of mobile phones: Gorilla Glass (marked GG), the type which was also used in the intercomparison study reported by Fattibene et al. 2014; screen glass from iPhone 6S (marked iP_6S); mineral glass from Sony Xperia L, model C2105 (marked MG); and protective screen, a tempered glass (marked TG) used commonly as additional protective cover of the original screen with a thickness of 0.3 mm thickness, and a ninth level of hardness according to the Mohs' scale. In the periods between the acquisition and crushing of the glass and all subsequent procedures (EPR measurements, irradiations, illuminations), the samples were stored in closed Eppendorf tubes in darkness at room temperature at about 24 °C. After separating the glass screen from LCD layers and after separating the TG plates from the adhesive plastic foil, the samples were washed with ethanol and crushed in a mortar into pieces of approximate shape of elongated triangles or quadrangles with a width of 1–3 mm and a length ranging from 4–22 mm.

EPR measurements and spectrometer settings

The EPR measurements were performed at room temperature using a Bruker EMX—6/1 spectrometer (Bruker BioSpin) in X-band (9.85 GHz) with a cylindrical cavity of type 4119HS W1/0430. The samples were measured in a quartz EPR tube of 4 mm inner diameter positioned in the central region of the EPR cavity. The cavity was equipped with an internal standard (ER 4119HS-2100 Marker Accessory, Bruker BioSpin GmbH). The EPR acquisition parameters are presented in Table 1. Quantitative analysis of the spectra (alignment and normalization of their amplitudes to the standard's lines, subtractions of the empty tube spectrum, averaging) was carried out using Microsoft Office Excel 2010.

Table 1 Parameters of EPR spectra acquisition

Settings	
Modulation frequency	100 kHz
Modulation amplitude	1.5 G
Microwave power	22.30 mW
Time constant	163.84 ms
Sweep time	83.89 s
Number of scans	10

Numerical fitting/decomposition of the experimental spectra was performed using the Reglinp procedure in Excel with two sets of model spectra: a set denoted as B-R consisting of BG (native background spectrum) and RIS spectra used for all examined types of samples, and a second set consisting of BG, RIS, and LIS (light-induced signal) spectra denoted as B-R-L and used only for the MG and GG glass. The spectra were fitted using g values ranging from $g = 2.014$ to $g = 1.978$ (for TG, MG and iPhone glass) and from $g = 2.017$ to $g = 1.981$ (for the GG samples). The analysis with the B-R set of benchmark spectra is equivalent to ignoring the effects of light, while using the B-R-L set takes into account the light effects in determination of the dosimetric signal. The model BG, RIS, and LIS components were always determined experimentally (separately for each type of the glass samples): the BG was measured in the four types of glass samples neither exposed to ionising radiation nor to light, the model RIS spectra were obtained by subtraction of the spectrum of irradiated (with 10 or 20 Gy), but non-illuminated samples and their BG spectra, while the model LIS spectra were obtained by subtracting spectra of the illuminated, un-irradiated samples and their BG spectra. All those model spectra were determined separately for different types of the glass. The B-R-L decomposition procedure was performed to study the light effects on the BG, RIS, and LIS spectral components in more detail. The results obtained with the B-R procedure, which simulates disregarding in the dosimetric procedures the effects of potential light exposures during normal usage of the phones, allowed to assess how this may affect the numerical values of the reconstructed doses.

To minimize any potential effect of the samples' anisotropy on the EPR spectra, the measurements were repeated at three orientations of the sample in the cavity, and the resulting three EPR spectra were normalized to the EPR standard's line, averaged, and normalized to the sample mass. Repeatability of EPR amplitudes at the different orientations of the samples in the cavity was about 7%, uncertainties of the mean amplitudes (standard deviations) were about 4%, uncertainties of the BG, RIS, and LIS spectral components determined by numerical decompositions of the spectra were within 5% of their respective maximum values in each of the figure presented below figures; these uncertainties were not marked in the figures to maintain clarity of the presented data.

Irradiations

For determination of the dose–response of the EPR signals, the samples were irradiated by 6 MVp photons at the Department of Oncology and Radiotherapy, Medical University of Gdańsk, Poland, using Clinac 600 C/D. The delivered doses were 2 Gy, 4 Gy, 10 Gy and 20 Gy (in terms of absorbed dose to water) involving a dose uncertainty of 2%.

Illuminations

Three types of light lamps as well as direct sunlight were used for light exposures of the samples. The irradiances of the light sources were measured at the samples positions with an ORION-TH power meter (OPHIR). The artificial light sources were:

1) A lamp made of two parallel CLEO advantage 80 W-R bulbs (Philips) with a power of 80 W each. The total irradiance was 48 W/m^2.
2) An UV lamp commonly used in cosmetic nail salons for hybrid nail polishing (Ultraviolet Radiant Lamp AP-111, Alle Paznokcie) with four bulbs, 9 W each. The irradiance at the sample position was 164 W/m^2.
3) A lamp made of six fluorescent bulbs Duluxstar (OSRAM), 24 W each. The irradiance was 110 W/m^2.

The exposures of the samples to sunlight were done by placing them on a white paper attached to a window sill outside the building at about noon. The irradiance measured during the exposure was about 800 W/m^2. The total energy exposures (in J/m^2) were calculated by multiplication of the measured irradiances and the duration of the exposures. The first EPR measurements of the illuminated samples were performed almost immediately (within 0.2 h) after the light exposures and were repeated in the very same samples for several months, as described in the "Results" section.

Figure 1 shows the light emission spectra for the artificial sources used in this study and UV–VIS spectra for MG and TG. The UV components (below 400 nm) covered about 63% and 72% of the total light intensity, in the cosmetic and Philips CLEO, respectively.

UV–VIS measurements of glass absorbance

The glass absorbance was measured for layers of TG (Fig. 1b) and for MG with a UV–VIS spectrometer (Lambda 35, Perkin Elmer) in the wavelength range of 200–500 nm. The dependence of the absorbance on the wavelength for the MG and TG is plotted in Fig. 1c.

The data presented in Fig. 1 show that the cosmetic lamp emitted UV light with maximum intensity in the 350–370 nm range, the CLEO lamp in the 350 nm, while the light from the Duluxstar bulbs had only a negligible UV component. The absorbance curves in Fig. 1b demonstrate that neither samples of MG nor TG (with foil) absorb the light emitted by these lamps. Consequently, the protective tempered glass used in this study and/or the adhesive foil do not provide any protection against the radiation-induced

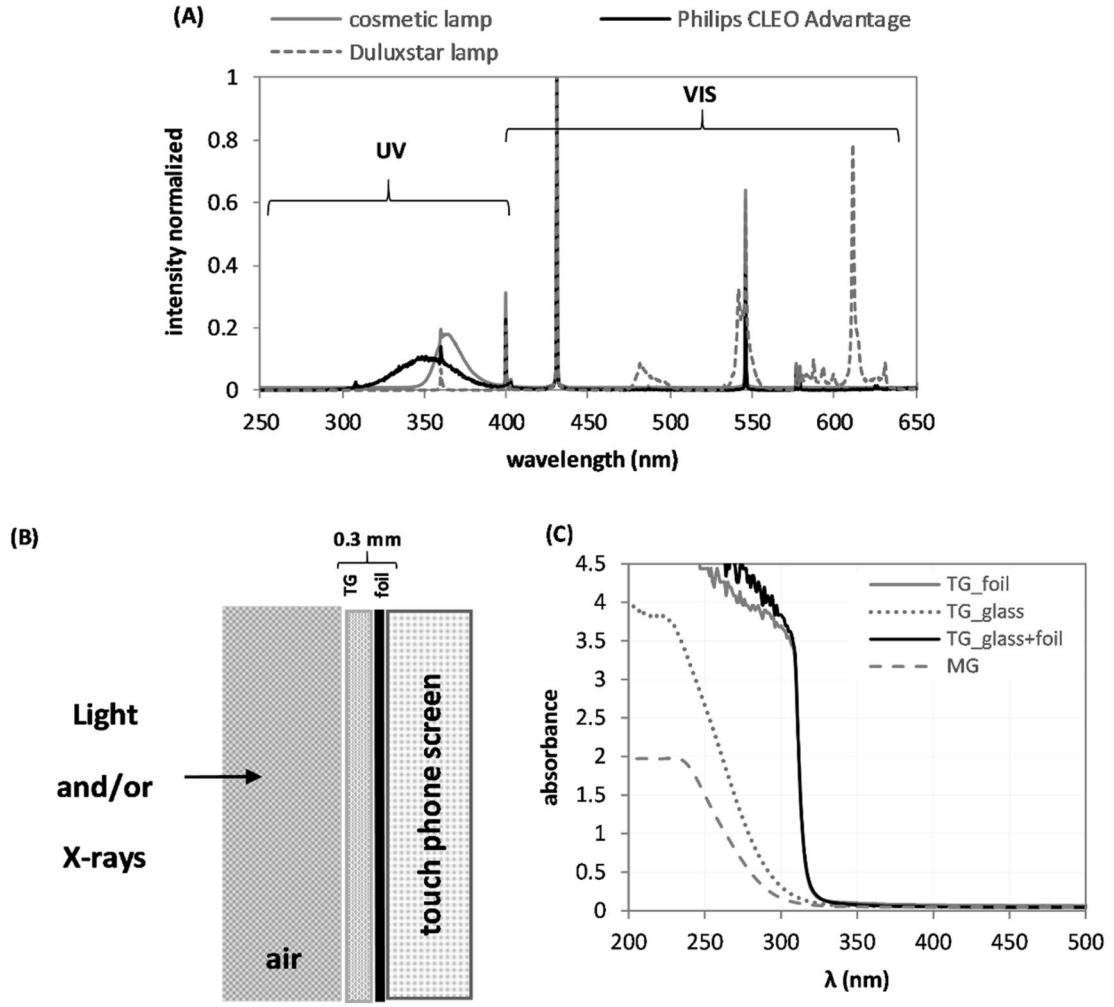

Fig. 1 **a** Emission spectra of the Philips CLEO advantage lamp, a cosmetic UV lamp and Duluxstar fluorescent lamp. **b** Schematic representation of the screen layers with the protective layer of tempered glass (TG) and adhesive layer of the plastic foil. **c** The UV–VIS spectra for two types of glass: mineral glass (MG) and TG

effects that might be caused in the screen glass by light with a wavelength of more than 320 nm.

Results

The effect of illumination of the un-irradiated MG samples with three types of light including a UV component is presented in Fig. 2. Figure 2a shows changes in the shape of the EPR spectra caused by 5 min of exposure to sunlight, 75 min of exposure to the CLEO lamp, and 30 min of exposure to the cosmetic lamp. The fluences used in these three light exposures were within 216–295 kJ/m^2. Figure 2b presents the EPR spectra of LIS generated by the three light sources for the MG_0Gy samples. Figure 2c compares the light fluence dependences of the respective BG spectral components in the un-irradiated glasses illuminated with the cosmetic lamp, as determined applying the two decomposition procedures: the B-R-L (i.e., including LIS) and the B-R (without LIS, i.e., ignoring the exposure of the samples to light).

The effects of sunlight on the MG_1 sample irradiated with 10 Gy X-rays are presented in Fig. 3. Figure 3a shows changes in EPR spectra of the MG sample due to its irradiation with 10 Gy and subsequent illumination by sunlight with 216 kJ/m^2. Figure 3b presents the three spectra contributing to the overall EPR signal: BG, RIS and LIS, measured as described in the "Materials and methods" section. Figure 3c shows the light effects in X-ray-irradiated MG samples, expressed as dependences of their calculated RIS components (using the B-R decomposition) on the sunlight fluence. Before the illuminations, the samples MG_4Gy, MG_1, and MG_2 were irradiated with X-rays to doses of 4 Gy, 10 Gy and 10 Gy, respectively. The scale on the vertical axis shows contributions of the benchmark dosimetric

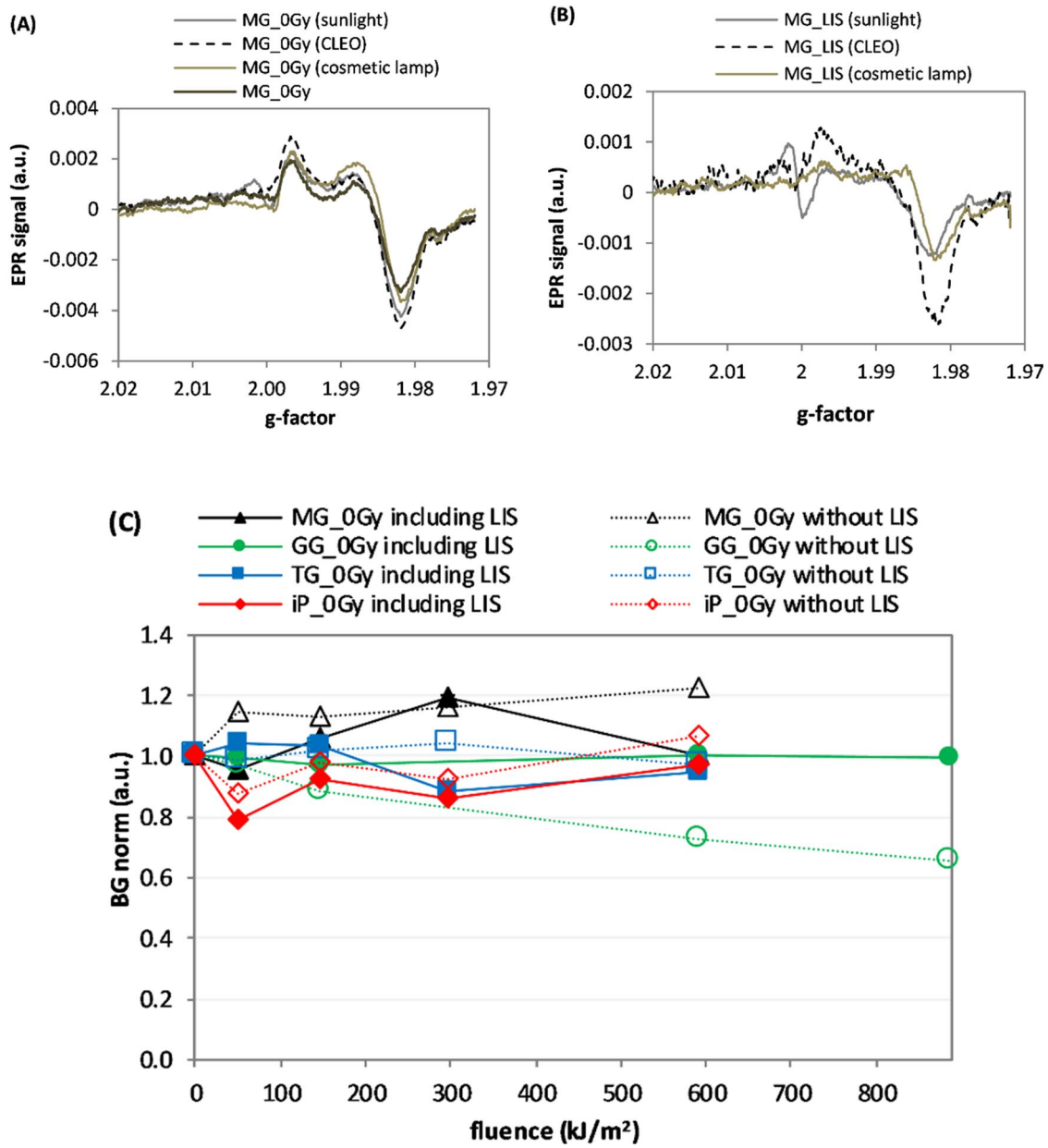

Fig. 2 **a** EPR spectra of four mineral glass (MG) samples—one non-illuminated [i.e., the background (BG) signal] and three illuminated with light from three sources including a UV component: direct sunlight, CLEO lamp, and cosmetic lamp with fluences in the range 216–295 kJ/m^2. **b** light-induced signal (LIS) components in EPR spectra of three un-irradiated MG samples. **c** Comparison of the light effect (for the cosmetic lamp) on the BG components in the samples, determined with the B-R-L and B-R decompositions. Measurement uncertainties are not marked in the figures for the sake of clarity in presentation (for details see text)

RIS component (obtained from the MG sample irradiated to 20 Gy) to the measured spectra. The evolution of the RIS with time after illumination is shown in Fig. 3d. The arrows marked by '+10 Gy' point at rapid increases of the RIS signals in those samples after their additional exposure to 10 Gy of X-rays. The drop in the RIS intensity in the MG_1 sample after an additional illumination by sunlight for 15 min is indicated by the arrow marked by '+15 min sunlight'. The dependences of the RIS and LIS spectral components on sunlight fluence are presented in panels E and F of Fig. 3, respectively, while Fig. 3g presents the corresponding relation between these two spectral features (RIS vs. LIS).

Figure 4 presents similar data as Fig. 3 but for the MG samples illuminated by the CLEO lamp. Figure 4a shows the spectral changes for the MG sample irradiated with

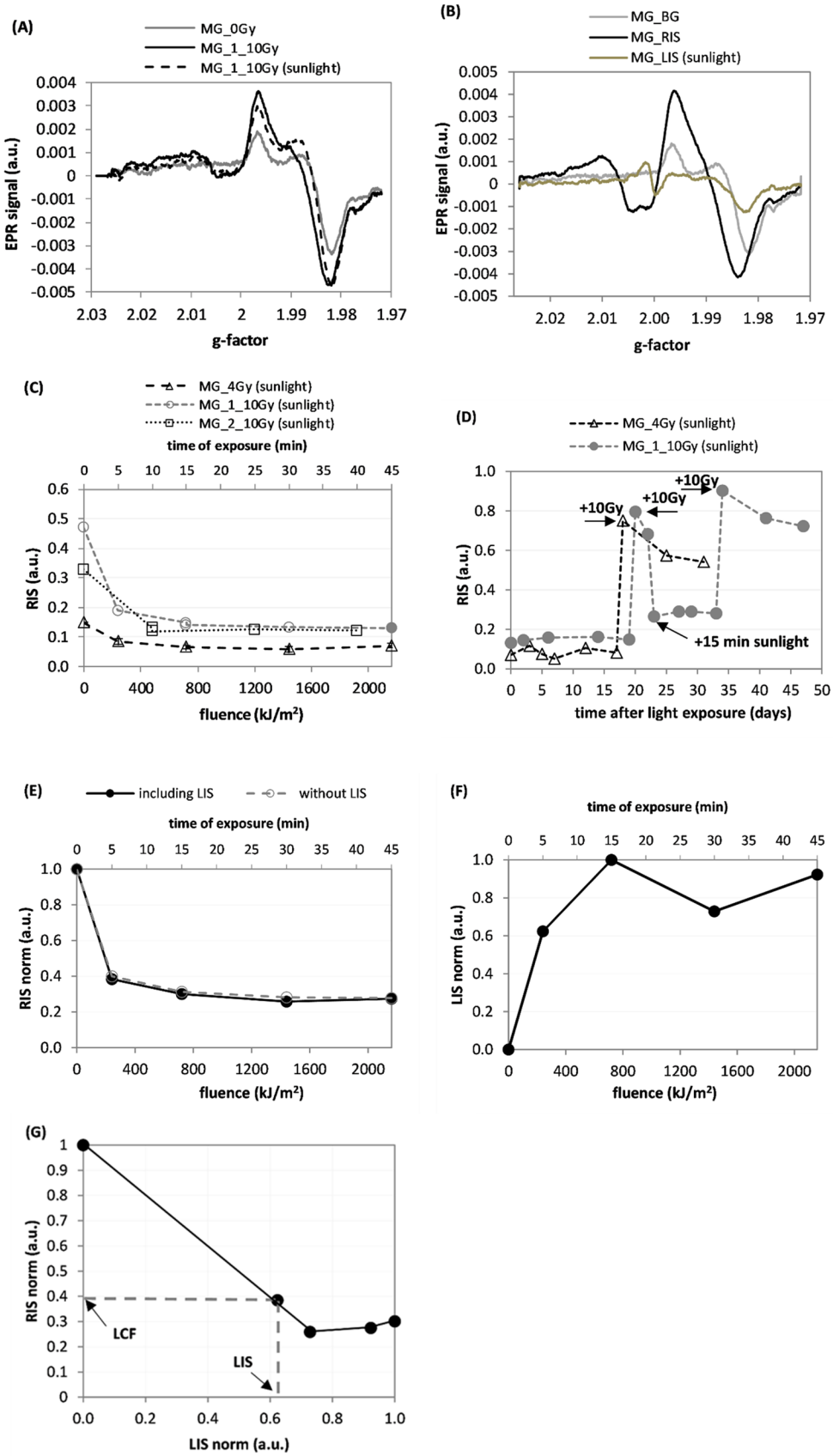
(A)
MG_0Gy
MG_1_10Gy
MG_1_10Gy (sunlight)
EPR signal (a.u.)
g-factor
(B)
MG_BG
MG_RIS
MG_LIS (sunlight)
EPR signal (a.u.)
g-factor
(C)
MG_4Gy (sunlight)
MG_1_10Gy (sunlight)
MG_2_10Gy (sunlight)
time of exposure (min)
RIS (a.u.)
fluence (kJ/m²)
(D)
MG_4Gy (sunlight)
MG_1_10Gy (sunlight)
+10Gy
+10Gy
+10Gy
+15 min sunlight
RIS (a.u.)
time after light exposure (days)
(E)
including LIS
without LIS
time of exposure (min)
RIS norm (a.u.)
fluence (kJ/m²)
(F)
time of exposure (min)
LIS norm (a.u.)
fluence (kJ/m²)
(G)
LCF
LIS
RIS norm (a.u.)
LIS norm (a.u.)

◂**Fig. 3** **a** EPR spectra for sample MG_1 after its irradiation to 10 Gy X-rays followed by 45 min exposure to direct sunlight. **b** Three components of EPR spectra for the sample MG_1: background (BG), 20 Gy radiation-induced signal (RIS) and light-induced signal (LIS). **c** Effect of sunlight exposures on magnitude of the RIS component for three MG samples (B-R decomposition). **d** Time evolution of RIS signals for the two samples presented in the (**c**): the MG_4Gy sample was irradiated with an additional dose of 10 Gy on the 17th day after illumination; The sample MG_1 was irradiated with an additional dose of 10 Gy on the 20th day after illumination, and then exposed to 15 min of sunlight on the 22nd day followed by an additional irradiation with a dose of 10 Gy on the 34th day after illumination. These re-irradiations and re-illuminations are marked by arrows. **e** Comparison of RIS vs. light fluence dependences determined by the B-R-L (solid line) or the B-R (disregarding the LIS) decomposition procedure. **f** Effect of sunlight on the LIS component. **g** Dependence of the RIS vs the LIS for sunlight. The dashed lines and the arrows indicate the light correction factor (LCF) determined on basis of the measured LIS component (for details see text). Measurement uncertainties are not marked in the figures for the sake of clarity in presentation (for details see text)

10 Gy X-rays and then, after 7 days of storage, measured and exposed to the CLEO lamp. Figure 4b shows the three spectra contributing to the overall EPR signal: BG, 20 Gy RIS, and LIS generated by the CLEO lamp. The data presented in Fig. 4c show the light-induced decrease in RIS (calculated using the B-R decomposition) for three MG samples irradiated to 2, 10, and 20 Gy prior to their exposure to the CLEO lamp. Follow-up of the data from Fig. 4c i.e., the time evolution of the RIS in these samples, is presented in Fig. 4d. The sample MG_10Gy was irradiated once more to 10 Gy on the 173rd day after illumination. On the 181th day, this sample was re-illuminated for 15 min with sunlight. Variations of the RIS and LIS vs light fluence are presented in panels (E) and (F) of Fig. 4, respectively, while panel (G) shows the corresponding relation between the RIS and LIS spectral components.

Figure 5a presents changes in the EPR spectra of the GG sample irradiated with 10 Gy X-rays and 23 days later measured, then illuminated with the CLEO UV lamp with a light fluence of 130 kJ/m^2 and measured again. The light-induced changes in the RIS component determined by both B-R and B-R-L procedures are shown in Fig. 5c. The time evolution of these RIS components is plotted in Fig. 5d; the arrow marked by '+10 Gy' shows the increase in magnitude of the RIS components after additional exposure to 10 Gy. Panel (E) illustrates the dependence of the LIS on the light fluence, while panel (F) shows variations of the LIS with time after illumination for the irradiated and un-irradiated GG samples. The decrease in LIS for the 10 Gy sample observed after the 166th day after illumination (Fig. 5f) is probably an artefact resulting from the decomposition procedure: probably a small part of the LIS component was erroneously assigned by the numerical fitting procedure to the spectrally roughly similar RIS component, which strongly increased due to the second irradiation with a dose of 10 Gy on the 166th day.

The light-induced spectral changes in the TG and iP_6S samples did not indicate generation of any specific LIS. In these samples, the light effects were manifested by fading of their RIS components. Therefore, the quantitative analysis for these samples could only be performed using the B-R decomposition procedure.

Figure 6a and b shows EPR spectra of the TG samples irradiated with a dose of 10 Gy and either illuminated 13 days later by the CLEO UV lamp (light fluence: 173 kJ/m^2) or 10 days later with direct sunlight (light fluence: 2160 kJ/m^2). The respective decreases in magnitude of the RIS reconstructed by decomposition of the spectra into their BG and RIS components are presented in Fig. 6c, while the evolution in time of these RIS components is shown in Fig. 6d. The arrow marked by '+10 Gy' for the TG_2_10Gy sample indicates generation of the RIS after exposure of this sample to an additional dose of 10 Gy X-rays.

The effect of irradiation of the iPhone 6S glass samples with a dose of 10 Gy, followed by illumination with the CLEO UV lamp at a light fluence of 173 kJ/m^2, is presented in Fig. 7a, while the effect of visible light from the Duluxstar bulbs is shown in Fig. 7b. These figure panels compare the effect of exposure to different artificial light sources (Duluxstar bulbs vs CLEO lamp) on RIS (determined by the B-R decomposition), in samples from the same type of mobile phone. In Fig. 7b, the greatest light fluences shown (for the CLEO UV lamp at about 75 kJ/m^2, for the Duluxstar bulbs at about 225 kJ/m^2) correspond to illumination times of 60 min. Figure 7c demonstrates the effect of time after the illumination on the RIS component.

Discussion

Figure 2a demonstrates the changes in the shape of the EPR spectra of un-irradiated mineral glass (MG) caused by exposure to direct sunlight, the CLEO lamp and the cosmetic lamp. The EPR spectra of the illuminated samples, as well the extracted LIS spectra presented in Fig. 2b suggest generation of spectral components by the light for $g < 2.00$ with a shape similar to that of the native background, and also indicate the presence of an additional paramagnetic center with EPR line at about $g = 2.00$, which was most prominent in the sample exposed to sunlight. Intensities of the BG spectral components in un-irradiated samples did not vary with increase of light fluence from the cosmetic lamp (Fig. 2c), which is particularly evident for the B-R-L decomposition of the spectra.

Analysis of the spectra in Figs. 3a and particularly in 3B shows shapes of the RIS component that are different to those of the BG and LIS components. The initial data points

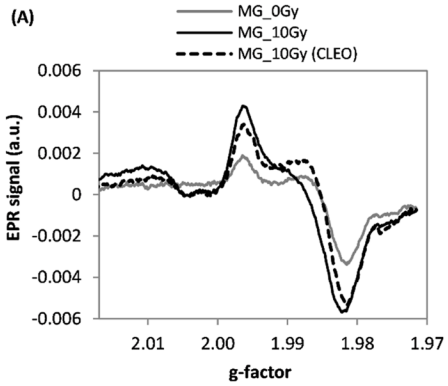
(A)
MG_0Gy
MG_10Gy
MG_10Gy (CLEO)
EPR signal (a.u.)
g-factor

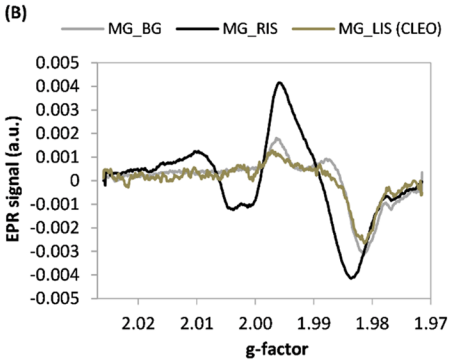
(B)
MG_BG
MG_RIS
MG_LIS (CLEO)
EPR signal (a.u.)
g-factor

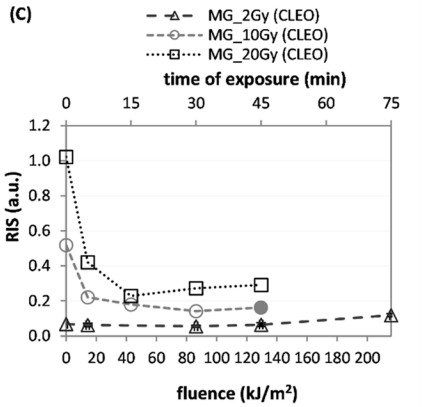
(C)
MG_2Gy (CLEO)
MG_10Gy (CLEO)
MG_20Gy (CLEO)
time of exposure (min)
RIS (a.u.)
fluence (kJ/m²)

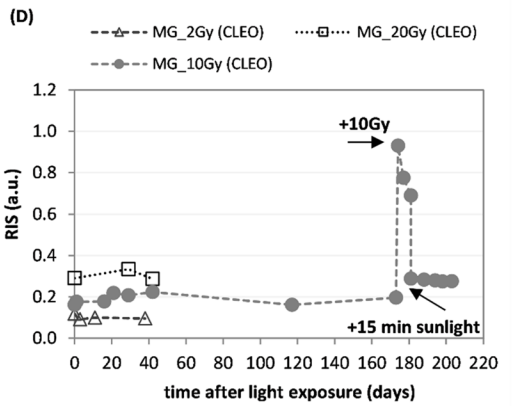
(D)
MG_2Gy (CLEO)
MG_20Gy (CLEO)
MG_10Gy (CLEO)
+10Gy
+15 min sunlight
RIS (a.u.)
time after light exposure (days)

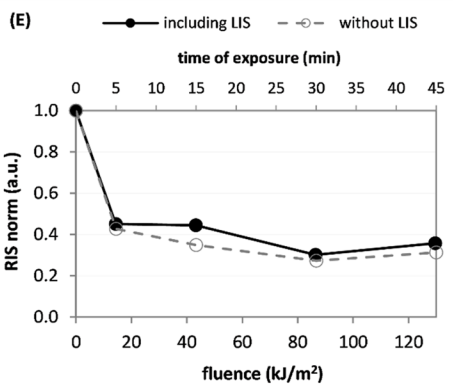
(E)
including LIS
without LIS
time of exposure (min)
RIS norm (a.u.)
fluence (kJ/m²)

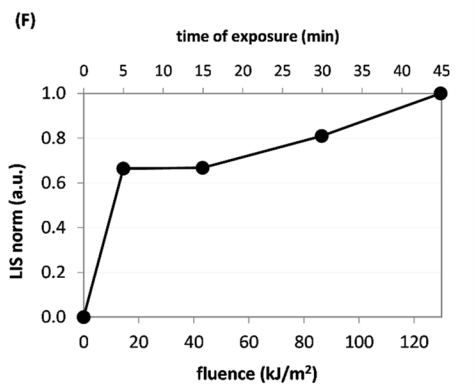
(F)
time of exposure (min)
LIS norm (a.u.)
fluence (kJ/m²)

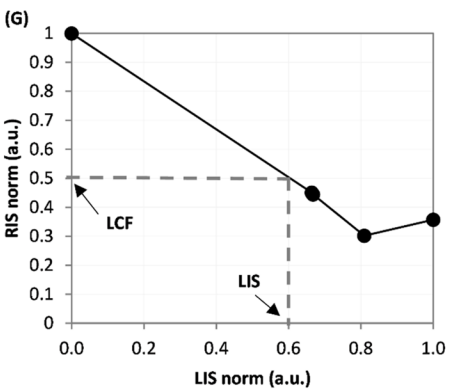
(G)
RIS norm (a.u.)
LCF
LIS
LIS norm (a.u.)

◂**Fig. 4** **a** Change of EPR spectra for the MG sample after irradiation to 10 Gy X-rays and then after exposure to the CLEO lamp for 45 min (130 kJ/m^2). **b** Three components of EPR spectra for the sample MG_10Gy: background signal (BG), 20 Gy radiation-induced signal (RIS) and light-induced signal (LIS). **c** Changes in RIS components (B-R decomposition) after exposure of various doses of X-rays (to 2 Gy, 10 Gy, and 20 Gy) and exposure to light from the CLEO lamp. **d** Time evolution of the RIS for the samples presented in (**c**). The MG_10Gy sample was irradiated at the 173rd day with an additional dose of 10 Gy, and at the 181st day, it was exposed to sunlight for 15 min. **e** Comparison of the radiation-induced (RIS) signal vs. fluence as determined by the B-R-L (solid line) or the B-R (disregarding the LIS) decomposition procedure (dashed line). **f** Dependence of the LIS spectral component in the MG_10Gy sample on fluence of light from the CLEO lamp. **g** Dependence of the RIS on the LIS for the CLEO UV lamp. The dashed lines and the arrows indicate the light correction factor (LCF) determined on the basis of the measured LIS component (for details see text). Measurement uncertainties are not marked in the figures for the sake of clarity in presentation (for details see text)

in Fig. 3c (for a light fluence of 0 kJ/m^2), on the lines showing sunlight-induced decrease in RIS (open squares and circles in Fig. 3c), were measured at different times after X-ray irradiations of those samples. These times were 9 days after irradiation for MG_1 and about 3 months after irradiation for MG_2. The model RIS spectrum used in this analysis was measured in a sample that was exposed to a dose of 20 Gy immediately after irradiation. Different decay of the RIS in these samples explains why the circle and square symbols at 0 kJ/m^2 light fluence are not at the 0.5 value (which would be expected for samples irradiated with 10 Gy, if no RIS decay occurred). The step-like increases in RIS presented in Figs. 3d and 4d measured after re-irradiation of the samples with an additional dose of 10 Gy, are similar in their magnitudes (about 0.68). This suggests that the radiation sensitivity of these samples (i.e., RIS per unit dose) was not affected by previous light exposures. Also, the decreases in RIS after additional 15 min of exposure to sunlight of the MG_1_10G sample (Fig. 3d) and exposure by the CLEO lamp of the MG_10Gy sample (Fig. 4d) are similar in their magnitudes (about 0.42). This indicates, that the sensitivity of the RIS to light was not affected by previous light exposures of these samples. The light–response curves for RIS and LIS presented in Figs. 3e, f and 4e, f reach a roughly constant minimum value (for RIS) or maximum value (for LIS) after about 5–15 min of light exposure (which corresponded to fluences of about 700 kJ/m^2 and 20 kJ/m^2 for sunlight and the CLEO lamp, respectively). The BG and LIS spectra in Figs. 3b and 4b are similar in shape and both are very different from the corresponding RIS (particularly in the spectral region close to $g = 1.985$). This can explain why disregarding the LIS in the numerical decomposition of the EPR spectra of the X-irradiated and then illuminated samples have only minimal influence on the magnitudes of the calculated RIS contributions (Figs. 3e and 4e). Additionally, the contribution from the real LIS in the numerical decomposition of the EPR spectra is accounted for by the BG component, with only a little effect on the reconstructed magnitude of the RIS component.

As can be noticed in Fig. 5a, exposure to X-rays and light causes evident changes in the shape of the EPR lines in the GG samples; the three spectra contributing to the EPR spectrum of the irradiated and illuminated sample, i.e., the BG, RIS, and LIS are very different (Fig. 5b). The light-induced changes in the dosimetric component (RIS) in the GG sample differ significantly when the RIS is determined including or disregarding the presence of LIS in the decomposition procedures (Fig. 5c). This suggests that ignoring the LIS in the decomposition procedures can result in a significant bias on the magnitude of the reconstructed RIS and can cause an overestimation of the actual RIS (i.e., as compared to the situation when the RIS is calculated including the LIS in decomposition procedure) by about 90% for high light fluences. The step-like increase in RIS measured after re-irradiation of the sample with additional 10 Gy (Fig. 5d), is approximately the same as that after the first 10 Gy dose, thus proving, similarly as in the case of the MG and TG samples, that light illuminations prior to X-ray exposure do not affect sensitivity of the GG samples to X-rays. The light–response curve for RIS calculated with the B-R-L decomposition (Fig. 5c) reaches a plateau in the fading after about 5 min of light exposure, whereas the LIS still increases up to about 30–40 min of exposure (Fig. 5e). The magnitude of LIS (Fig. 5f), after a 10–20% drop within the first 1–2 weeks after illumination, was stable over the next 4 weeks (in the un-irradiated sample) and over 6 months (in the sample irradiated with a dose of 10 Gy). The RIS as a function of LIS for the MG and GG samples (Figs. 3g, 4g, and 5g) are of important for practical applications. Namely, they show that the RIS is decreasing with increasing LIS. This relationship may be used to correct the RIS measured in samples exposed to light, thus allowing to minimize the bias in reconstructed radiation doses caused by exposures of the glasses to light. Determination of the LIS component (marked on the abscissa of the RIS vs LIS plots) gives a value for the light correction factor (LCF)—read at the ordinate axis)—as shown in Figs. 3g, 4g, and 5g. The corrected dosimetric signal $RIS_{cor} = RIS/LCF$ can be used for dose reconstruction using an ordinary dose–response curve determined for RIS in a sample not exposed to light. For example, in a MG sample exposed to sunlight with a LIS of 0.62 the LCF is about 0.4 (Fig. 3g), while in a GG sample with a LIS of 0.42 the LCF is about 0.5 (Fig. 5g). Consequently, the corrected magnitudes of the RIS (i.e. which would be measured if the glass was not exposed to light) are $0.62/0.4 = 1.55$ and $0.42/0.5 = 0.84$, respectively. At lower light fluences resulting in a lower intensity of the

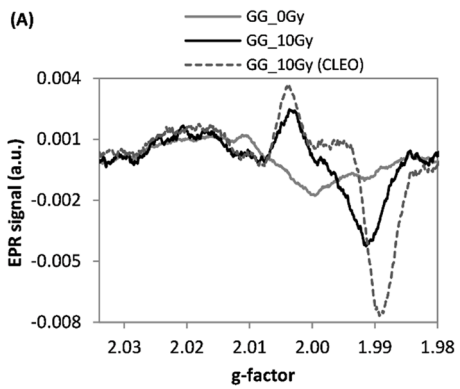
(A)
GG_0Gy
GG_10Gy
GG_10Gy (CLEO)
EPR signal (a.u.)
g-factor

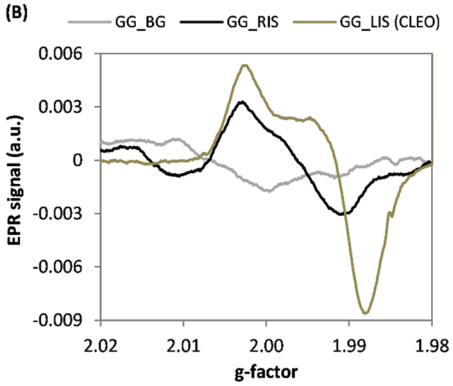
(B)
GG_BG
GG_RIS
GG_LIS (CLEO)
EPR signal (a.u.)
g-factor

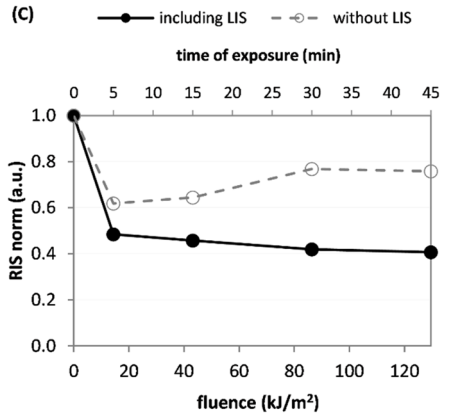
(C)
including LIS
without LIS
time of exposure (min)
RIS norm (a.u.)
fluence (kJ/m²)

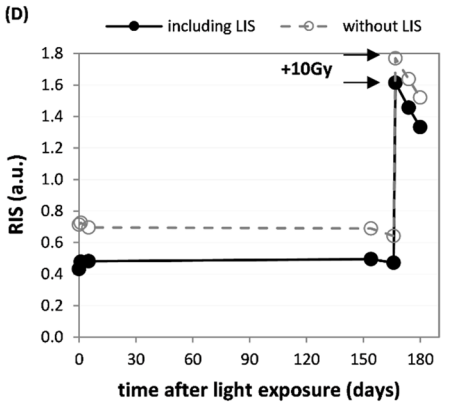
(D)
including LIS
without LIS
+10Gy
RIS (a.u.)
time after light exposure (days)

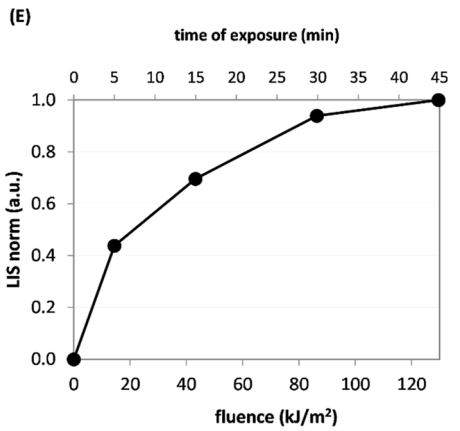
(E)
time of exposure (min)
LIS norm (a.u.)
fluence (kJ/m²)

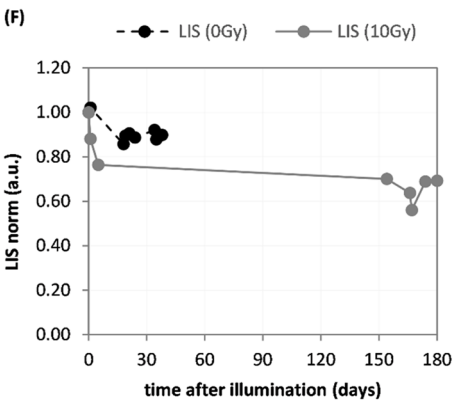
(F)
LIS (0Gy)
LIS (10Gy)
LIS norm (a.u.)
time after illumination (days)

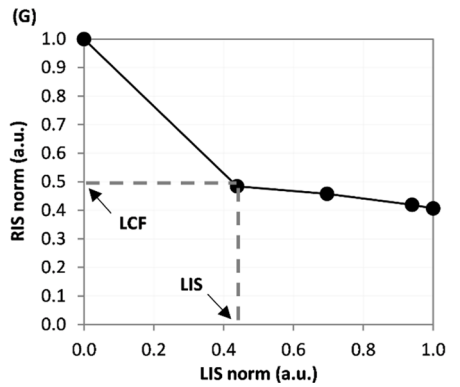
(G)
RIS norm (a.u.)
LCF
LIS
LIS norm (a.u.)

◂**Fig. 5** **a** EPR spectra demonstrating the effect of irradiation of the Gorilla Glass (GG) sample with a dose of 10 Gy X-rays, and the effect of a subsequent 45 min illumination with the CLEO UV lamp. **b** Three components of EPR spectra for the GG sample: background signal (BG), radiation-induced signal (RIS), and light-induced signal (LIS). **c** Dependence of the RIS (for the B-R and B-R-L decompositions) on the light fluence from the CLEO UV lamp. **d** Time evolution of the RIS (for the B-R and B-R-L decompositions); on the 166th day, after illumination, this sample was re-irradiated with a dose of 10 Gy. **e** Effect of illumination by the CLEO lamp on the LIS spectral component. **f** Time evolution of the LIS signals in two GG samples: un-irradiated and irradiated with a dose of 10 Gy. **g** Dependence of the RIS on the LIS for the CLEO UV lamp. The dashed lines and the arrows indicate the light correction factor (LCF) determined on the basis of measured LIS component (for details see text). Measurement uncertainties are not marked in the figures for the sake of clarity in presentation (for details see text)

LIS spectra, accurate determination of the corresponding LCF requires more data points than measured in the present study, to resolve the trend of the RIS vs. LIS dependence in more detail. The trends used in the present study were obtained only by a rough approximation connecting the two, first left-side points in Figs. 3g, 4g, and 5g, by straight lines. Future studies should also examine how the dependence of RIS on LIS also depends on the time periods between irradiation, illumination, and EPR measurements. This is demonstrated by Fig. 5f showing a decay of the LIS in the first several days after illumination. Further studies are planned for verification and optimization of the proposed correction method and its application in retrospective dosimetry using GG and MG glasses.

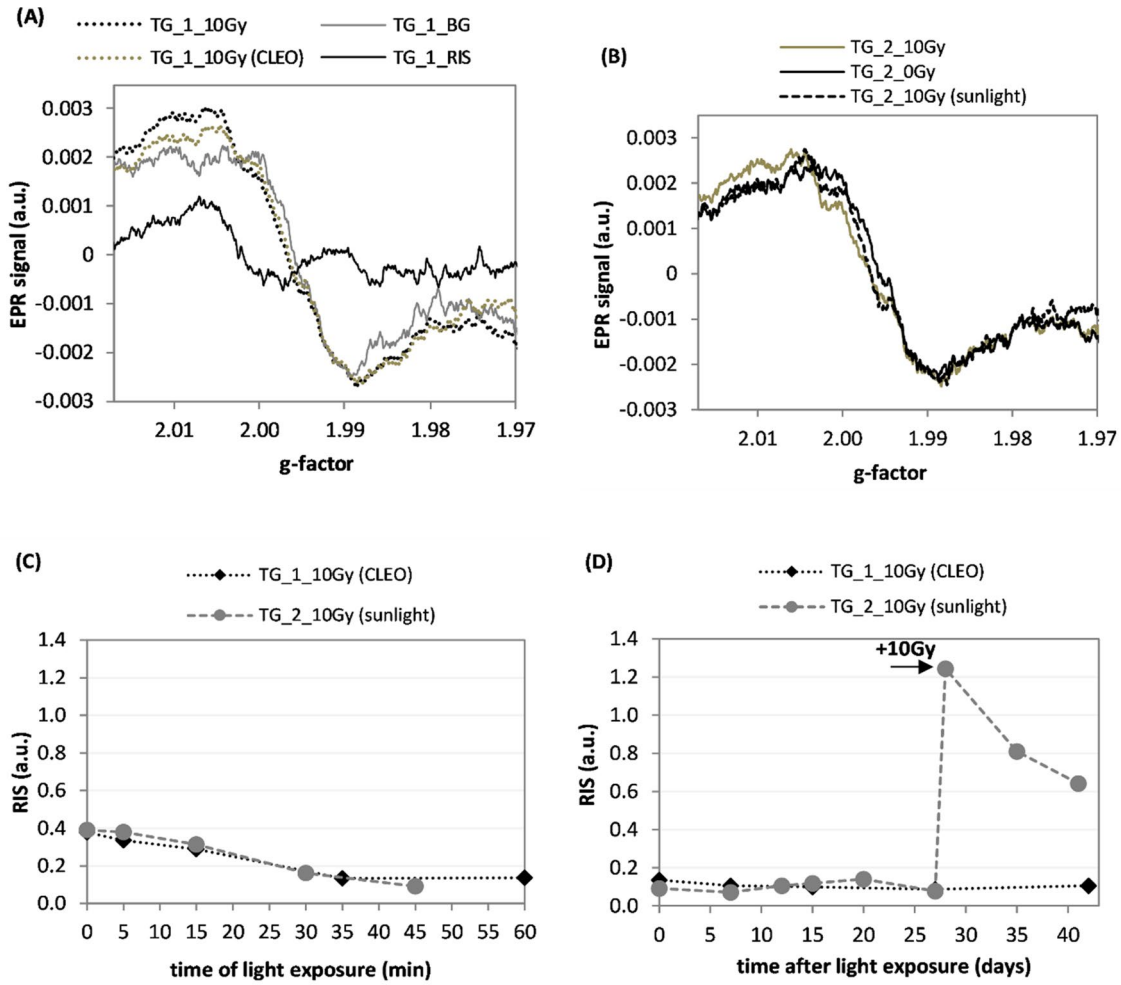

Fig. 6 **a** EPR spectra of the TG_1_BG sample—the background signal (0 Gy), 10 Gy radiation-induced signal (TG1_RIS) and the effect of a dose of 10 Gy X-rays and a subsequent 60 min illumination with the CLEO UV lamp [see last data point in p(**c**)]. **b** EPR spectra of the TG_2 sample irradiated with a dose of 10 Gy and then illuminated with direct sunlight. **c** Effect of illumination of the samples TG_1_10Gy and TG_2_10Gy by the CLEO lamp and to sunlight on RIS. **d** Time evolution of the RIS in samples TG_1_10Gy and TG_2_10Gy; the TG_2 sample was re-irradiated with 10 Gy on the 28th day after illumination. Measurement uncertainties are not marked in the figures for the sake of clarity in presentation (for details see text)

Exposures of the X-ray-irradiated TG samples by the CLEO lamp (Fig. 6a) or to sunlight (Fig. 6b) did not induce any significant changes in the shape of their EPR spectra, only a reduction in their intensities. The numerical analysis (i.e., decomposition of the spectra into their corresponding BG and RIS components) proved that illumination of the TG samples caused an about threefold decrease in magnitude of their RIS components (Fig. 6c). The residual RIS in the illuminated TG samples was stable at least for the next four weeks (Fig. 6d). The re-irradiation of the TG_2_10Gy sample with a dose of 10 Gy on the 28th day after illumination caused increase in magnitude of its RIS followed by a decrease of the signal to about 50% in 13 days (Fig. 6d). This result is consistent with those in a previous study (Juniewicz et al. 2019), in which the authors observed a quantitatively similar rate of decay of the RIS components in TG samples. Comparison of the sensitivity to light of the studied samples showed that even a few minutes of exposure of the MG, GG, and iPhone 6S samples to light including a UV component caused a 20–60% decrease of the RIS component (Figs. 3e, 4e, 5c and 7b). It is noted that for the TG glass, this fading was significantly slower than that for the other samples, i.e., an about 50% decay occurred only after 30 min of exposure to light (Fig. 6c).

The RIS signal generated in the iPhone samples was similar to the BG signal, despite the spectral regions at g values of about 1.980–1.985 and 2.02 (Fig. 7a)—these spectral differences apparently were sufficient for the Reglinp procedure to differentiate between the RIS and BG spectral components.

Visible light without a UV component did not cause any evident decrease in the RIS in the illuminated iP1_6S_10Gy sample (Fig. 7b). A lack of any effect of visible light on the EPR signal was also reported by Marciniak et al. (2019) for nails clippings—in their study, the light without any UV component had no effect on the nails' EPR signal, in contrast

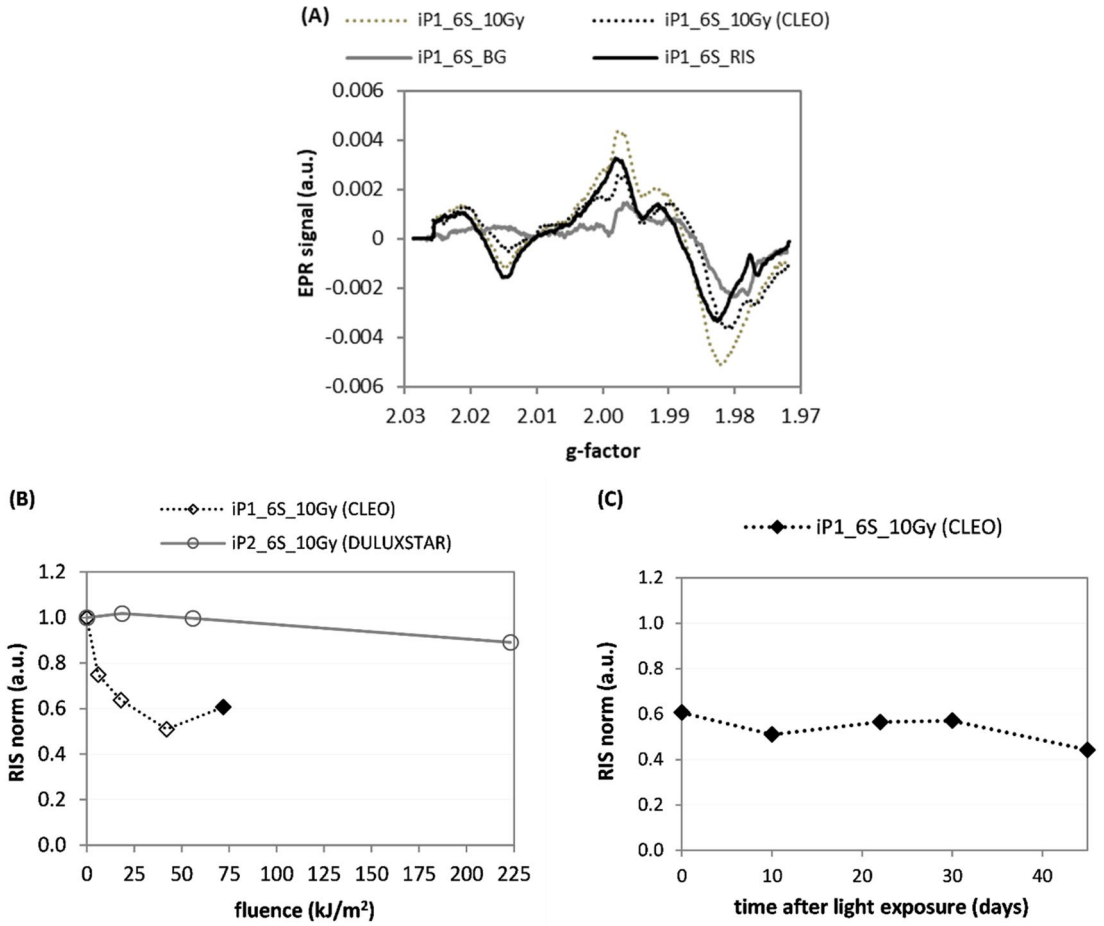

Fig. 7 **a** EPR spectra of the iPhone 6S sample—their background signal (BG), 10 Gy RIS and the spectra after exposure to X-rays to a dose of 10 Gy dose, and after illumination by the CLEO UV lamp (for data point marked in **b** by the filled diamond). **b** Effect of light exposure by the CLEO lamp and Duluxstar bulbs on the RIS in irradiated iP_6S. **c** Time evolution of the RIS component in the sample exposed to light from the CLEO lamp (follow-up of the last, black diamond point in (**b**). Measurement uncertainties are not marked in the figures for the sake of clarity in presentation (for details see text)

to light including a UV component. For the iP1_6S_10Gy sample, the RIS stabilized after the initial light-induced decay and maintained its magnitude about 45 days at about 50% of its value measured shortly after illumination (Fig. 7c).

Conclusions

The present study showed that in all four types of examined glasses, exposures to light including a UV component (from the CLEO lamp, from a cosmetic lamp, and sunlight) caused significant fading of the dosimetric signal (RIS), which was determined by decomposition of EPR spectra into two separate spectra: background and radiation-induced components. In MG and GG screen glasses, only 5 min of exposure to UV lamps or sunlight was enough to cause a 40–60% reduction of the RIS, while in iP_6S glass this caused an about 20% reduction. The tempered glass (TG) from protective screens was less sensitive to light showing an about 50% reduction in RIS after exposure of about 30 min to the light. Although prolonged exposures of mobile phones to UV are rather implausible, the present results indicated that there is a possibility of underestimating the actual radiation doses in dose reconstruction efforts, in glasses exposed to UV light, if one neglects the discussed effects of light in applied dosimetric procedures. Decomposition procedures performed for the MG and GG samples, taking into account a light-induced reference spectrum (LIS), also showed the light-induced decay of RIS, which in the MG sample was the same for the two procedures. For the GG samples, taking into account the reference LIS spectrum that can be considered as a more appropriate (realistic) and more accurate analytical approach, revealed a much stronger decay in RIS. It is concluded that the light sensitivity of the dosimetric signal can result in a significant bias in retrospectively determined doses. It is emphasized, however, that the present study offers a possibility of quantitative corrections accounting for these effects, based on applying the observed relationship between the LIS and RIS spectral components. This is important, because it has some practical implications in that it improves the accuracy of EPR dosimetry using mobile phone glasses, often being exposed to light in regular everyday use. It is emphasized, however, that this correction can be applied only for glasses, in which light generates LIS that is spectrally different from other EPR signals.

Acknowledgements This study was funded by Gdański Uniwersytet Medyczny (Grant number Internal Grant ST70).

Compliance with ethical standards

Conflict of interest The authors declare that they have no conflict of interests.

References

Ainsbury EA, Bakhanova E, Barquinero JF, Brai M, Chumak V, Correcher V, Darroudi F, Fattibene P, Gruel G, Guclu I, Horn S, Jaworska A, Kulka U, Lindholm C, Lloyd D, Longo A, Marrale M, Monteiro Gil O, Oestreicher U, Pajic J, Rakic B, Romm H, Trompier F, Veronese I, Voisin P, Vral A, Whitehouse CA, Wieser A, Woda C, Wojcik A, Rothkamm K (2011) Review of retrospective dosimetry techniques for external ionizing radiation exposures. Radiat Prot Dosim 147(4):573–592

Bassinet C, Trompier F, Clairand I (2010) Radiation accident dosimetrry on glass by Tl and EPR spectrometry. Health Phys 98(2):400–405

Bortolin E, De Angelis C, Quattrini MC, Barlascini O, Fattibene P (2019) Detection of ionizing radiation treatment in glass used for healthcare products. Radiat Prot Dosim. https://doi.org/10.1093/rpd/ncz014

Ciesielski B, Schultka K, Penkowski M, Sagstuen E (2004) EPR study of light illumination effects on radicals in gamma-irradiated L-alanine. Spectrochim Acta Part A 60:1327–1333

Ciesielski B, Tyszkowska M, Grudniewska A, Penkowski M, Schultka K, Peimel-Stuglik Z (2008) The effect of dose on light-sensitivity of radicals in alanine EPR dosimeters. Spectrochim Acta Part A Mol Biomol Spectrosc 69(5):1405–1416

Engin B, Aydas C, Demirtas H (2006) ESR dosimetric properties of window glass. Nucl Inst Methods Phys Res B243(1):149–155

Fattibene P, Trompier F, Wieser A, Brai M, Ciesielski B, De Angelis C, Della Monaca S, Garcia T, Gustafsson H, Hole EO, Juniewicz M, Kreft K, Longo A, Leveque P, Lund E, Marrale M, Michalec B, Mierzwińska G, Rao JL, Romanyukha A, Tuner H (2014) EPR dosimetry intercomparison using smart phone touch screen glass. Radiat Environ Biophys 53(2):311–320

Juniewicz M, Ciesielski B, Marciniak A, Prawdzik-Dampc A (2019) Time evolution of radiation-induced EPR signals in different types of mobile phone screen glasses. Radiat Environ Biophys 58:493–500

Marciniak A, Ciesielski B, Juniewicz M, Prawdzik-Dampc A, Sawczak M (2019) The effect of sunlight and UV lamps on EPR signal in nails. Radiat Environ Biophys 58(2):287–293

McKeever SWS, Sholom S, Chandler JR (2019) A comparative study of EPR and TL signals in Gorilla® glass. Radiat Prot Dosim 186:65–69

Sholom S, Wieser A, McKeever SWS (2019) A comparison of different spectra deconvolution methods used in EPR dosimetry with Gorilla glasses. Radiat Prot Dosim 186(1):54–59

Teixeira MI, Da Costa ZM, Da Costa CR, Pontuschka WM, Caldas LVE (2008) Study of the gamma radiation response of watch glasses. Radiat Meas 43(2–6):480–482

Trompier F, Bassinet C, Wieser A, De Angelis C, Viscomi D, Fattibene P (2009) Radiation-induced signals analysed by EPR spectrometry applied to fortuitous dosimetry. Ann Ist Super Sanità 45(3):287–296

Trompier F, Della Monaca S, Fattibene P, Clairand I (2011) EPR dosimetry of glass substrate of mobile phone LCDs. Radiat Meas 46:827–831

Radiation and Environmental Biophysics (2022) 61:179–203
https://doi.org/10.1007/s00411-022-00970-w

REVIEW

EPR dosimetry in glass: a review

Agnieszka Marciniak[1] · Bartłomiej Ciesielski[1] · Małgorzata Juniewicz[1]

Received: 23 July 2021 / Accepted: 26 February 2022 / Published online: 20 March 2022

Abstract
Electron Paramagnetic Resonance (EPR) spectroscopy enables detection of paramagnetic centers generated in solids by ionising radiation. In the last years, the ubiquity of glass in personal utility items increased significance of fortuities retrospective dosimetry based on EPR in glass parts of mobile phones and watches. Despite of fading of the signals and their susceptibility to light, it enables dosimetry at medical triage level of 1–2 Gy. In this article information relevant for assessment of applicability and planning of the EPR dosimetry is presented—particularly at dose levels typical for radiation accidents. Reported data on fading of the radiation-induced spectral components are presented and compared. Effects of light on background spectra and on the dosimetric signals are also presented. It is concluded that when properly accounting for the fading and for the obscuring effects of light, the EPR dosimetry in glasses from mobile phones and watches can be used in dose assessment after radiation accidents.

Keywords EPR · Dosimetry · Ionizing radiation · ESR · Glass · Dose

Introduction

Widespread use of radiation sources in human environment is inevitably accompanied by a growing risk of negative effects after exposure to ionising radiation of people and also of other biological and artificial objects (Ruano-Ravina and Wakeford 2020). Such an exposure can be caused by radiation accidents (e.g. in radiotherapy or in nuclear industry), terrorists attacks with use of radiation sources (e.g. "dirty" bombs) or nuclear explosions. Adverse effects of radiation also occur in some materials during their normal, planned usage under radiation exposure (construction elements in technics, sterilization of products, long-term storage of radioactive materials or radioactive waste etc.). Determination of the involved absorbed doses is a crucial issue for radiation protection or medical treatment of exposed people, is useful in detection of irradiated food, in verification of sterilization procedures, or in monitoring aging and radiation-caused detrimental effects in construction materials. In general, various dosimetry methods should cover a broad range of doses—practically from a few mGy (in radiation protection, medical imaging, research) to tens of kGy (in sterilization). Various dosimetric methods are being used in this dose range using various instruments: from classical ionization chambers, scintillation probes, semiconductor detectors and radiochromic films through thermoluminescence (TL), spectrophotometry or electron paramagnetic resonance (EPR), to biological methods using cytogenetic techniques.

Application of a proper method in a properly pre-planned measurement enables to achieve satisfactory accuracy. However, in many cases people, who do not wear personal dosimeters, can be involved in accidental radiation exposures. Therefore, there is a need for development of methods of reconstructive dosimetry applicable in situations when the irradiation was unexpected (in radiation accidents) or when a need to determine the dose became evident after the irradiation. In such cases, the determination of doses cannot be done with any preinstalled detectors and has to be based either on theoretical simulation of the radiation field or on measurements of long-lived and dose-dependent effects in the irradiated materials. Those effects may include formation of any defect centers and/or free radicals due to an inherent property of ionising radiation, which is the ability to brake molecular bonds, resulting in generation of species with unpaired electrons, which are detectable by EPR spectroscopy. Such long-lived radicals or paramagnetic centers are generated in many solids, including substances

✉ Bartłomiej Ciesielski
bciesiel@gumed.edu.pl

[1] Department of Physics and Biophysics, Medical University of Gdańsk, Dębinki 1, 80-211 Gdańsk, Poland

both inside (in hard tissues) and outside the human body (in victim's personal belongings or in other neighboring objects). The main problem in application of this method in radiation protection or medicine is its sensitivity in the relatively low-dose range, from tens of mGy up to about 100 Gy, relevant to radiobiological and medical effects of the radiation. The whole-body lethal effective dose is about 3.5–5 sieverts (Lopez et al. 2011, https://www.nrc.gov, access December 2021), but local doses absorbed by victims of radiation accidents can be much higher—dozens of Gy, as determined e.g. by EPR dosimetry in accidents reported by Desrosiers (1991), Schauer et al. (1996), Kinoshita et al. (2002), Trompier et al. (2007). As an indirect determination of doses delivered to victims of radiation accidents, also measurements of even higher doses absorbed in materials in the neighboring environment can by useful for reconstruction of the radiation field and, finally, for determination of doses to the victims. This justifies consideration of methods of retrospective dosimetry with detection limits even higher than those required in a direct dosimetry in irradiated persons.

In the situation of a large number of casualties, a triage of suspected victims with respect to the magnitude of absorbed doses is crucial. The effectiveness of emergency actions is dependent on identification of individuals who were exposed enough to require a treatment, those who were not exposed at a level that should be treated, and those with too high dose to benefit from any treatment and require palliative care (Flood et al. 2007). The dose-based triage criteria are still being discussed, but 1.5 Gy for whole-body exposure is generally recognized as a threshold dose, above which immediate medical assistance in hospitals is necessary (Alexander et al. 2007). Rea et al. (2010) suggested the following triage categories: "<0.75 Gy for unaffected, 0.75–2 Gy for minimal care, 2–3 Gy for variable care, 3–6 Gy for urgent care, 6–10 Gy for immediate care, and >10 Gy for expectant care". Beinke et al. (2021) considered a 2 Gy limit as whole-body single dose requiring hospitalization. This justifies the dose of about 1–2 Gy as necessary minimum detection level of methods of reconstruction of the dose absorbed by victims. Moreover, it is recommended that the triage should be processed within 48 h after exposure (Cerezo 2011). In case of partial body exposures, several times higher local doses can be considered as non-lethal, depending on the exposed body region and its size, and their assessment can be helpful in undertaking decisions regarding the optimal treatment. But even in the case of whole-body exposure, dose distribution in the victim's body is usually heterogeneous and then only physical dosimetry can determine the local dose in a specified region (Ainsbury et al. 2011). A comprehensive summary of biodosimetry and physical dosimetry techniques in dose assessment in individuals following acute exposure to ionsing radiation is described in ICRU Report 94 (2019). The importance of such studies and their implementation is reflected by the foundation of the European Network of Biological and Physical-Retrospective Dosimetry (RENEB—Realizing the European Network in Biodosimetry) (Kulka et al. 2017; Trompier et al. 2017). EPR dosimetry in glass has been included in a recent RENEB project (Port et al. 2021) as one of the physical dosimetry methods verified in international intercomparisons with participance of researchers from many countries.

EPR dosimetry using hard tissues like enamel, bone or nails has sufficient sensitivity to be applicable in the 0–100 Gy dose range: with detection limits from tens of mGy in enamel (Fattibene et al. 2011; Ciesielski et al. 2011), to a few Gy in bone (Trompier et al. 2009; Krefft et al. 2014). Measurements in Q-band allow for the reduction of sample size to 2–4 mg (Romanyukha et al. 2007). Nevertheless, due to the invasiveness of obtaining samples from teeth and bones, EPR dosimetry in nails would be an attractive alternative. However, more studies are still needed to overcome inaccuracies related to background signals (native, mechanically induced or induced by UV light) and to susceptibility of the dosimetric EPR signal in nails to water (Marciniak et al. 2018 and 2019)—the term "background signal" here and thereafter refers to the EPR spectrum present without any radiation-induced component, "native" refers to the signal caused by intrinsic paramagnetic centers, which were not induced by any recognized, environmental physical factors like mechanical stress, light, etc.

Glass shows a potential as a suitable material for accidental EPR dosimetry due to its ubiquity in the human environment, resistance to water and many chemicals, low conductivity, and low dielectric losses, which facilitates prompt EPR measurements without special treatment of the samples. In addition, in contrary to biologicals samples used in retrospective EPR dosimetry (enamel, bone, nails), glass samples usually are available in a sufficient and optimal amount to be used for sensitive measurements. Potentially, the most useful glass for personal dosimetry is glass in displays of mobile phones and other electronic portable devices. Mobile phones probably represent the most ubiquitous personal item in a large part of the world—in 2020, the total number of mobile phone users in the world was about 4.8 billion (https://www.statista.com, access December 2021)—larger than half of the Earth's population. This justifies studies undertaken by many researchers on characterization of EPR dosimetry in those glasses, including Gorilla Glass (GG), which has been widely used in manufacturing of touchscreens in recent years. Mobile phones are often kept close to the body, which is an additional advantage facilitating reconstruction of the dose absorbed by their users on the basis of the dose absorbed by glass of their phones' screens.

In this article information related to the application of EPR in various glasses in dosimetry is summarized. While

there is a rich literature on studies of EPR signals in irradiated glasses, the present review is restricted mainly to those reports which, in our opinion, are most relevant in the low-dose range, retrospective accidental dosimetry. Nevertheless, for completeness of this review, some data reported for glass irradiated to much higher doses are also included, for example regarding studies on the structure of the paramagnetic centers or on the fading of the radiation-induced EPR signals.

Structure and composition of glasses

Glass is an inorganic amorphous, transparent, ceramic material. Its properties depend on the melting method and chemical composition. The properties of glass (e.g. brilliance, thermal resistance, transparency, infrared absorption, color) change with various ingredients like lead, boron, barium, cerium and others, usually added in the form of oxides.

Elemental composition of glasses (Table 1) differs from that of soft tissues, which typically include 99% of hydrogen, carbon, nitrogen, and oxygen. Due to the presence of elements with a higher atomic number not present in tissues, absorption of ionising photons by glass at energies below 100 keV is remarkably stronger than in tissues. This is generally a disadvantage in dosimetry focused on radiation doses absorbed by biological objects, because accurate dose conversion between different materials require a detailed knowledge of the radiation field involved. For an approximate dose assessment, ratios of mass absorption coefficients and stopping powers of tissue and glass must be applied for such a conversion. Those ratios are presented in Fig. 1. For example, the energy absorbed in GG from photons with energies below 80 keV is more than three times larger and that from electrons below 1 MeV is about 20% lower than in a soft tissue, as can be estimated by the respective ratios of mass absorption coefficients and stopping powers. Detailed analyses of the conversion of dose from glass displays in mobile phones to kerma (kerma—kinetic energy released in matter) in air, taking into account irradiation geometry, show that the dose in mobile phone screens can exceed doses in

Table 1 Examples of reported elemental compositions of some glasses. Compositions are given in terms of percentage by mass

	Elemental compositions (%)							References
	SiO_2	Al_2O_3	Na_2O	CaO	MgO	PbO	B_2O_3	
Soda lime glass	70–75	–	12–16	10–15	–	–	–	Hasanuzzaman et al. (2016)
Borosilicate glass	70–80	2–8	4–8	–	–	–	7–13	Hasanuzzaman et al. (2016)
Lead glass	55–65	–	or K_2O 13–15	–	–	18–38	–	Hasanuzzaman et al. (2016)
Watch glass	72.5	1.6	12.7	5	6	–	–	Marrale et al. (2012)
Turkish window glass	73.65	2.6	11.67	5.89	1.91	–	–	Engin et al. (2006)
Soda alumino silicate glass (Gorilla Glass)	60–80	13–20	Not quantified	–	–	–	–	Trompier (2012)

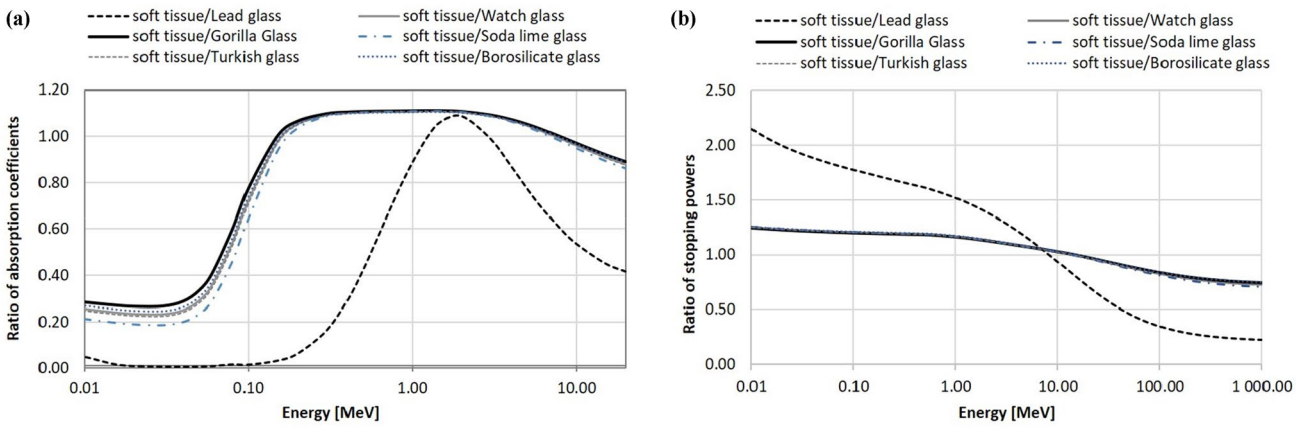

Fig. 1 Ratios of mass absorption coefficients (**a**) and stopping powers (**b**) of some glasses and the soft tissue. Calculated on the basis of the elemental composition from Table 1 and interaction coefficients from NIST Standard Reference Database 124 and 126 (https://www.nist.gov)

body organs by a factor of about 5 at low photon energies of 40–50 keV, as reported by Discher et al. (2014, 2015).

EPR signals in mineral glass

EPR signals observed in various glasses can be assigned to three main categories: native signals, signals induced by light (both components often called background signal), and signals induced by ionising radiation.

Background EPR signals

In EPR dosimetry all spectral components, which were not generated by the ionising radiation, represent a background signal (BG), which has to be accounted for by analytical procedures aiming at determination of the radiation-induced signal (RIS—the dosimetric signal). The amplitude of the native or light-induced signals (i.e. vertical distance between the maximum and the minimum deflections from the baseline, often called peak-to-peak amplitude) can be similar in magnitude or even larger, than the amplitude of the RIS generated by ionising radiation in a dose range typical for radiation accidents, i.e. from a fraction of Gy up to several dozens of Gy. Therefore, the presence of background signals in un-irradiated detectors is an important and widespread confounding factor in EPR dosimetry. The main challenge in dosimetric procedures is separation of the RIS component from the other spectral components, not related to the absorbed ionising radiation, namely: (1) the inherent native signal from the bulk of the sample, assigned to intrinsic centers: paramagnetic defects and impurities caused by manufacturing processes (2) signals induced mechanically e.g. by crushing, or by light (LIS—light-induced signal) in already fully formed glass material—these disturbing signals can be minimized by avoiding crushing glass samples to a fine powder before EPR measurements and by avoiding exposures of samples to light (if possible).

Typically, un-irradiated samples show a complex, broad and stable (at room temperature) signal with $g \approx 2.0$ (Fig. 2), as was reported by many authors: for watch glass (Wu et al. 1995; Longo et al. 2010; Trompier et al. 2011a; Marrale et al. 2011; Aydaş et al. 2016), window glass (Gancheva et al. 2006), LCD glass (Bassinet et al. 2010), and Gorilla Glass (Trompier et al. 2017). In mineral glass and tempered (protective) glass from mobile phones broad lines in the $g = 1.98–2.01$ range were observed (Sholom and McKeever 2017; Juniewicz et al. 2019, 2020).

Those background signals are partially or completely superimposed on the signals induced by ionising radiation. Native signals are spread out over a spectral range of several mT in X-band EPR spectra (or from $g \approx 1.97$ to $g \approx 2.02$, approximately). At high doses of hundreds of Gy the RIS is clearly distinguishable from BG, but at lower doses, the peak-to-peak BG amplitude can be similar to the RIS amplitude from about 5–20 Gy dose (Fig. 2a, b, d, f). In a study of lime-soda glass by Kortmis and Maltar-Strmecki (2018), the 6 Gy RIS was even hard to differentiate visually from the BG spectrum (Fig. 2b).

The origin of the background signal in glasses is various and so far has not been completely resolved. Griscom (1980) attributed EPR signals in non-irradiated glass to the presence of transition-group ions, ferromagnetic precipitates, photo-induced centers, and mechanically induced defects. Also, Bassinet et al. (2010) and Trompier et al. (2009) suggested that the background signal is likely generated during the manufacturing process by impurities in the glass. McKeever et al. (2019) found that an exposure of glass to ultraviolet (UV) light is one of the factors inducing the background. This observation concurs with Juniewicz et al. (2020), who proved generation of EPR signal even by a short (a few minutes) exposure of screens of mobile phones to sunlight.

Another EPR line in non-irradiated glasses is observed at $g \approx 4.27$. This signal is assigned to the presence of Fe^{3+} ions substituting silicon (Teixeira et al. 2005; Muralidhara et al. 2010). Its intensity can be modified by high doses of ionising radiation (Teixeira et al. 2005) due to the $Fe^{2+} \rightarrow Fe^{3+}$ reaction. This signal was not considered as useful for dosimetry purposes and its dependence on doses of several tens of Gy has not yet been reported.

Radiation-induced signals (RIS)

Paramagnetic centers induced by ionising radiation are mainly attributed to a missing oxygen bond between silicon atoms (E' centers), non-bridging oxygen hole centers (NBOHC), and peroxy radicals (Griscom 1980), illustrated in Fig. 3. Engin et al. (2006) reported lack of dose rate effects on shape and magnitude of radiation-induced EPR spectra up to 1.63 kGy/h.

Basic EPR characteristics of centers in various types of glass, which can be found in human-made items, are presented in Table 2.

EPR signals in gorilla glass

Gorilla® Glass (GG) developed by Corning Inc. is made from a special, chemically strengthened glass with high resistance to cracking and scratches, which makes it very suitable for touch-screens in modern mobile phones, tablets or smart-watches. Due to its ubiquity in electronic devices of everyday use, this type of glass has been more thoroughly investigated recently by researchers with respect to its potential application in accidental EPR dosimetry. Several EPR signals were experimentally identified and successfully simulated (Fig. 4). These

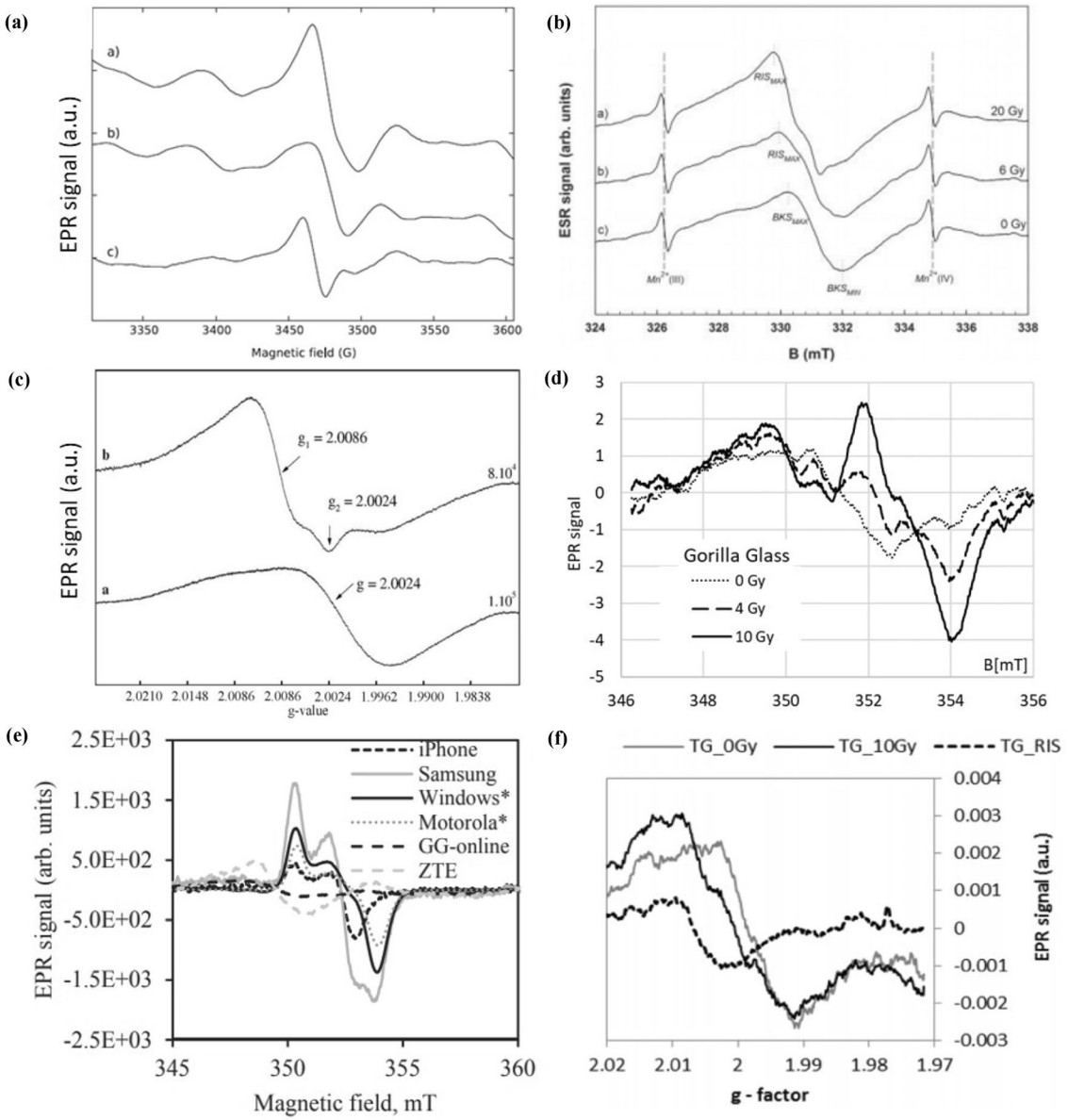

Fig. 2 Comparison of background EPR spectra (from un-irradiated samples) with spectra from samples irradiated by various doses. **a** watch glass, BG—middle spectrum, 20 Gy—upper spectrum, their difference—lower spectrum, taken with permission from Marrale et al. (2011), **b** soda-lime window glass, background (BKS), 6 Gy and 20 Gy, reproduced from Kortmis and Maltar-Strmecki (2018), **c** soda-lime window glass, BG—lower spectrum a, 500 Gy—upper spectrum b, adapted from Gancheva et al. (2006), **d** Gorilla Glass, 4 Gy and 10 Gy, **e** variations in shape and intensity of BG in protective glasses from various mobile phones taken with permission from Sholom and McKeever (2017)—spectra of samples from Windows and Motorola phones were multiplied by a factor 0.1, **f** tempered glass, BG—grey spectrum, 10 Gy—black solid spectrum, their difference plotted by dashed line (reproduced with permission from Juniewicz et al. (2019))

signals can be used as benchmark spectra in numerical decompositions of experimental signals—thus allowing for extraction of the dosimetric, radiation-sensitive signal components (Wieser et al. 2015; Sholom et al. 2019). This is particularly important when dealing with weak and overlapping signals that cannot be reliably determined quantitatively by measurement of their peak-to-peak amplitudes. Basic characteristics of those centers are presented in Table 3.

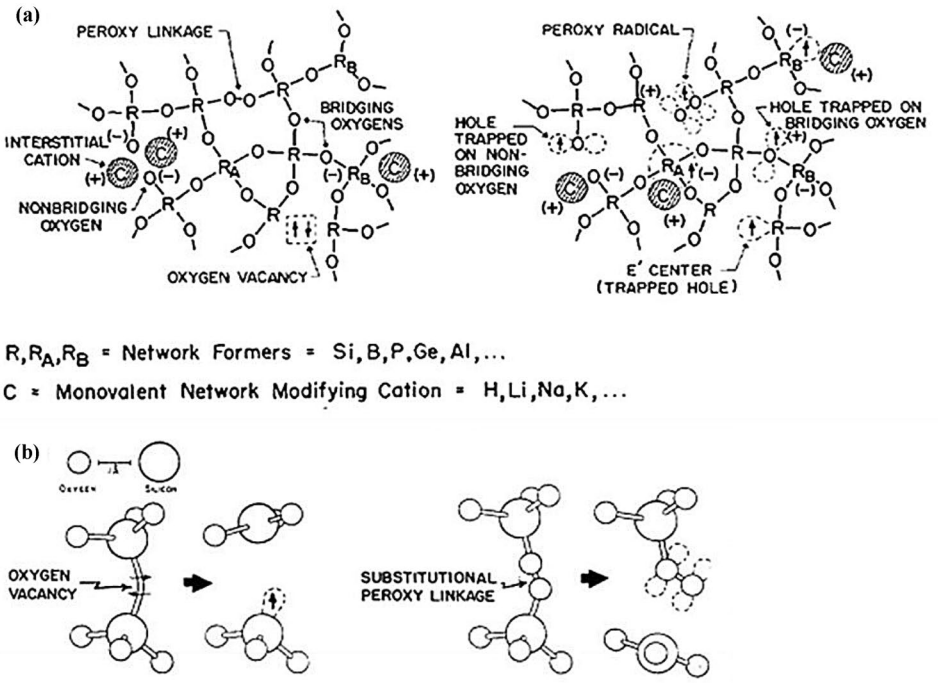

Fig. 3 **a** Schematic illustration of changes in the original molecular structure of glass (left) caused by irradiation, which generates in the structures *E′* centers holes and peroxy radicals (right); **b** *E′* center (left) generated by radiation at the site of oxygen vacancy. The oxygen atom in defect-free structure is located between two silicon atoms (at right). The peroxy radical (right) is generated by breaking O–Si bond. Reproduced with permission, from Griscom (1980)

Determination of the radiation-induced signal and its dependence on dose

The dose dependence of the RIS is crucial for the applicability of a given material in dosimetry. The majority of early reports on EPR in glasses was focused on signals induced by very high doses—in the range of kGy or MGy (Griscom et al. 1976; Boizot et al. 1998; Wieser and Regulla 1990). These studies were useful in identification of structures of the radiation-induced paramagnetic centers, but their applicability in practical dosimetry is limited only to dosimetry in industrial applications like, for example, in food preservation, studies of defects in materials exposed to high doses, or sterilization of medical equipment. In contrast, dosimetry in humans following radiation accidents requires measurements of much smaller doses. As already mentioned above, the generally accepted decision dose in triage of victims in large casualty accidents is within 1–2 Gy (Rea et al. 2010). Taking into account long-term health consequences of post-irradiation reactions, severity of medical symptoms and effectiveness of medical treatment, the range of doses which should be covered by emergency dosimetry is roughly from hundreds of mGy up to about 10^2 Gy.

Table 4 presents published information on detection limits and ranges of monotonic dependence of the EPR signal on radiation dose in various glasses that present sufficient radio-sensitivity to be useful in accidental dosimetry. The dose range in parenthesis given in the second column represents the range of linearity with dose, if reported.

Reconstruction of dose is based on quantitative determination of the radiation-induced changes in the measured EPR spectra. These changes are determined quantitatively by:

(1) difference in deviations of the spectral line from the baseline measured at two g values (or two magnetic field values) within a spectrum range affected by the RIS (i.e. the peak-to-peak amplitude). In the range of a linear dependence on dose, this amplitude (ΔA) of a signal from a sample irradiated with dose D can be represented by Eq. (1):

$$\Delta A = \Delta BG + \Delta L + \Delta RIS \cdot D, \quad (1)$$

where the "Δ" symbols mean the differences in the signal magnitudes: ΔBG—in the native background, ΔL—in other signal components like those caused by light-induced centers and/or electronic bias (drift) of baseline, and ΔRIS—in the radiation-induced signal per unit dose, as shown in Fig. 5,

(2) second integral of the EPR spectrum (or its part attributed to the RIS), reflecting total number of paramagnetic centers contributing to the EPR line; its dependence on dose can be described by an equation similar to Eq. (1),

(3) magnitude of spectral components obtained by numerical decomposition of the spectra (fitting of the experimental spectra by a set of model reference spectra, characteristic to the paramagnetic centers contributing

Table 2 Characteristics of paramagnetic centers in mineral glass used in production of various commercial items

Type of glass	Application	Structure of the center	Spectral characteristics of radiation-induced (^{R}) and background (^{BG}) centers	Instrumental parameters	Type of instrument	References
Borosilicate glasses B_2O_3–$3SiO_2$	Cladding in optical fibers	Boron–oxygen hole centers (BOHC)	$g_1 = 2.003^{R}$, $g_2 = 2.012^{R}$, $g_3 = 2.036^{R}$	Field modulations = 0.5 G or 0.2 G; microwave power = 30 mW	X band (9 GHz) or K band (35 GHz), Varian E-9 spectrometer	Griscom et al. (1976)
Sodium borosilicate, sodium aluminoborosilicate, sodium and calcium aluminoborosilicate	Glasses used in nuclear waste disposal	Boron–oxygen hole centers (BOHC)	$g_1 = 2.0029^{R}$, $g_2 = 2.0115^{R}$, $g_3 = 2.0500^{R}$; ($A_1 = 12.3$ G, $A_2 = 14.4$ G, $A_3 = 11.7$ G)	Modulation amplitude = 1 G; microwave power = 1 mW	X band (9.420 GHz), ESP300E Brucker spectrometer	Boizot et al. (1998)
		Electron center E'	$g = 2.0011^{R}$			
		Peroxy radical (Oxy defect)	$g_1 = 2.0024^{R}$, $g_2 = 2.0110^{R}$, $g_3 = 2.0439^{R}$			
		Hole centers near alkaline ions HC_1	$g_1 = 2.0023^{R}$, $g_2 = 2.0088^{R}$, $g_3 = 2.0213^{R}$			
Silicate glasses Suprasil and Heralux	Labware, UV optics, electronics	E' center	$g_{\parallel} = 2.0018^{R}$, $g_{\perp} = 2.0005$–2.0006^{R}	Modulation amplitude = 250 μT (25 mG); microwave power = 25 μW	ESR spectrometer (Bruker ESP 300), X band	Wieser and Regulla (1990)
Crystalline quartz powder	Lack of information	E' center	$g_1 = 2.0019$R, $g_2 = 2.0006$R, $g_3 = 2.0005$R			
Alkali silicate phosphate glasses of SiO_2–Na_2O–CaO–P_2O_5	Bioglass	Fe^{3+} impurities	$g \cong 4.3^{BG}$	Lack of information	X-band (9.4 GHz)	Padlyak (2000), Hassan et al. (2004)
		Oxygen hole center (OHC)	$g \cong 2.0130^{R}$			
Yb-doped phosphate glasses	Bioglass, vitrification of nuclear waste, optics	Peroxy radicals I	$g_1 = 2.0045^{R}$, $g_2 = 2.0100^{R}$, $g_3 = 2.0441^{R}$	Lack of information	Bruker X-band (9.8 GHz) and Q-band (34.0 GHz) EMX and EMX + spectrometers	Pukhkaya et al. (2014)
		Peroxy radicals II	$g_1 = 2.0015^{R}$, $g_2 = 2.0159^{R}$, $g_3 = 2.0261^{R}$			
		r-POHC with l-POHC defects (Phosphorus Oxygen Hole Centers)	Lack of information			
		S center	$g = 2.00389^{R}$			

Table 2 (continued)

Type of glass	Application	Structure of the center	Spectral characteristics of radiation-induced (^{R}) and background (^{BG}) centers	Instrumental parameters	Type of instrument	References
Soda-lime aluminosilicate glasses	Lack of information	Silicon OHC	$g \approx 2.00–2.01^{R}$	Modulation amplitude = 3 G; microwave power = 0.01 mW	X-band (9.81 GHz) EMX Bruker spectrometer	Le Gac et al. (2017)
		Aluminum OHC	broad signal: $g_1 = 2.0023^{R}$, $g_2 = 2.0182^{R}$, $g_3 = 2.0353^{R}$			
		Trapped-electron center	$g_1 = 1.937^{R}$, $g_2 = g_3 = 1.973^{R}$			
		E′ center	$g = 1.9992^{R}$			
Soda-lime hardened	Windscreen	Hole centers	$g = 2.0024^{BG}$; $g_1 = 2.0088^{R}$, $g_2 = 2.0024^{R}$	Modulation amplitude = 1.0 mT; microwave power = 50 mW	Bruker ER 200D SRC spectrometer X-band, cavity (ER 4102ST)	Gancheva et al. (2006)
Soda-lime	Window	Hole centers	$g = 2.0024^{BG}$, $g_1 = 2.0086^{R}$, $g_2 = 2.0024^{R}$	Modulation amplitude = 0.8 mT; microwave power = 16 mW		
Soda lime with 3–4% Al_2O_3 (soda-lime type of low aluminum oxide content)	"Thuring" laboratory glass	Hole centers	$g = 2.0024^{BG}$; $g_1 = 2.0088^{R}$, $g_2 = 2.0024^{R}$	Modulation amplitude = 1.0 mT; microwave power = 50 mW		
Alkali-borosilicate glass	"Rasotherm" laboratory glass	Hole interacting with a neighboring ^{11}B nucleus	Broad signal ($g = 2.045$)^{R} and quintet: $g_{\|} = 2.013^{R}$, $g_{\perp} = 2.003^{R}$	Modulation amplitude = 0.6 mT; microwave power = 40 mW		
Alkali-borosilicate glass	"Jena" laboratory glass	Lack of information	$g = 2.0024^{BG}$ $g = 2.0086^{R}$, $g = 2.0024^{R}$, $g = 2.045^{R}$	Modulation amplitude = 1.0 mT; microwave power = 50 mW		
Silico-sodo-calcic glass	Turkish commercial window glass	Nonbridging oxygen hole center (OHC)	$g = 2.0128^{R}$ ($\Delta H_{pp} = 1.48$ mT)	Modulation amplitude = 0.7 mT; microwave power = 80 mW	Bruker EMX spectrometer, X band, TE102 cavity	Engin et al. (2006)
Lack of information	Transparent and colored window glass, float manufacturing process	Fe^{3+} ions in the substitution-nal silicon, pairs of exchange coupled Fe^{3+} ions	$g \approx 2.01^{BG,R}$	Modulation amplitude = 0.1 mT; microwave power = 20 mW	Bruker EMX spectrometer (cavity ER4102 ST), X band (9.75 GHz)	Teixeira et al. (2005)

Table 2 (continued)

Type of glass	Application	Structure of the center	Spectral characteristics of radiation-induced (^{R}) and background (^{BG}) centers	Instrumental parameters	Type of instrument	References
Lack of information	Window glass	Nonbridging oxygen hole center	Background signals (BKG) at $g = 2.000 \pm 0.001$ $g = 2.0038 \pm 0.0016^{R}$ Irradiated transparent window glasses ($g = 2.005$, $\Delta H_{pp} = 34$ G) Frosted glass and CoLal t glass ($g = 2.002$, $\Delta H_{pp} = 34$ G)	Modulation amplitude = 5 G; microwave power = 25 mW	Bruker EPR (A300, Germany), X-band (9.8 GHz)	Liu et al. (2019)
Lack of information	Watch Glass	Lack of information	$g = 2.0027^{BG}$, $g = 2.0082^{R}$ ($\Delta H_{pp} = 1.1$ mT)	Modulation amplitude = 0.3 mT; microwave power = 2 mW	Bruker-ESP300 spectrometer X band, TE104 double cavity	Wu et al. (1995)
Lack of information	Watch glass	Non-bridging oxygen hole center	$g \approx 2$ (peak-to-peak line width of 1.52 mT)	Modulation amplitudes between 0.1 and 1.5 mT; microwave power between 0.04 and 159 mW	Bruker ECS106 spectrometer,TE102 rectangular cavity (9.7 GHz)	Longo et al. (2010)
Lack of information	Watch glass	Oxygen hole center (OHC)	$g = 2.0122$ ($\Delta H_{pp} = 1.52$ mT)	Modulation amplitude = 0.1 mT; microwave power = 2 mW	Bruker e-scan spectrometer, Pyrex tubes of 4.0 mm inner diameter, microwave frequency 9.8 GHz	Aydaş et al. (2016)
Mineral glass, Type I	Wristwatches and display windows of mobile phones	Lack of information	Complex signal $g = 2.002^{BG}$, $g = 2.01^{R}$	Modulation amplitude = 3 G; microwave power = 2 mW	Bruker, EMX X-band spectrometer, SHQ cavity	Bassinet et al. (2010)
Mineral glass, Type II		Lack of information	$g = 2.01^{R}$			
Soda-lime glass, classified into three types (I–III) on the basis of EPR signal in un-irradiated glass	Display LCD windows of mobile phones	Lack of information	Complex, broad signal with g = 2.0024 ^{BG}; Complex signal of three types at g≈2.0 ^{R}	Modulation amplitude = 0.3 mT; microwave power = 2 mW	X-band spectrometer, SHQ cavity	Trompier et al. (2011a)

Table 2 (continued)

Type of glass	Application	Structure of the center	Spectral characteristics of radiation-induced (^{R}) and background (^{BG}) centers	Instrumental parameters	Type of instrument	References
Wet silico-sodo-calcic glass	LCD displays of mobile phone; similar EPR radio-induced signals than window glass or watch glass	Non-bonding oxygen hole centre (high OH^- content)	Lack of information	Lack of information	X-band EPR spectrometer	Trompier et al. (2011b
Dry silico-sodo-calcic glass	LCD displays of mobile phone	Peroxy radical (low OH^- content)	Lack of information			
Borosilicate glass	LCD displays of mobile phone	Lack of information	Lack of information			
Classified into five types I–V on the basis of EPR signal in un-irradiated glass	mobile phones screens (LCD (types I–III, V) and touch screens (I, IV)	Lack of information	Complex, broad signals at $g \approx 2.0^{BG}$ Complex, broad signals in types 1-IV at $g \approx 2.0^{R}$	Lack of information	X-band spectrometer	Trompier et al. (2012)
Lack of information	Mineral eyeglasses (CR-39)	Lack of information	$g \approx 2.0$	Modulation amplitude = 0.05–33, 0.7 mT; microwave power = 0.1–10 mW	Bruker e-scan X-band spectrometer	Karaaslan and Engin (2021)

The table includes only centers with EPR signals that can be relevant to dosimetry (with $g \approx 2.0$)

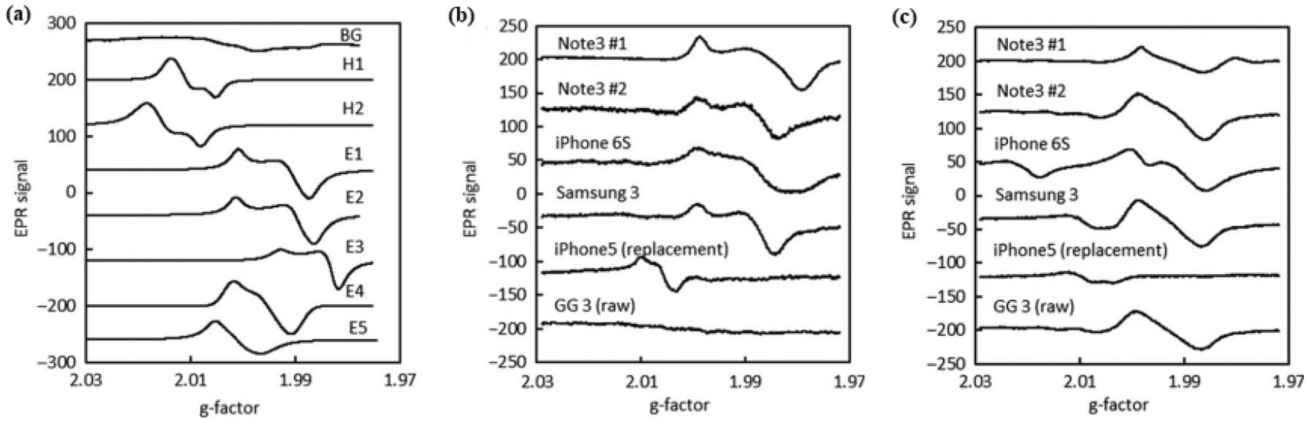

Fig. 4 **a** Simulated spectra of paramagnetic centers in GG. **b** Experimental BG spectra, **c** experimental dosimetric signals (RIS) in GG glass from various mobile phones (reproduced with permission from Sholom et al. 2019).

to the overall signal of the sample). In its simplest version, this can be presented by Eq. (2):

$$S(g) = a \cdot BG_r(g) + D \cdot RIS_r(g) + c \cdot B(g) + k, \quad (2)$$

where $S(g)$ is the measured magnitude of an EPR line as a function of *g-factor* (or magnetic field), $BG_r(g)$ is the reference native background spectrum, $RIS_r(g)$ stands for the reference radiation-induced spectrum per one Gy, $B(g)$ stands for a function approximating any discovered or potential variations in the baseline (for example, a linear function for electronic drift, as shown in Fig. 5), and k is a constant (upward or downward shift of the spectrum). The a, D, c and k are unknown parameters to be determined by the fitting procedure. In particular, a describes the contribution of the background and D (the dose) describes the contribution of the model RIS_r in the samples' spectra to the measured signal.

Fitting can be done in two ways. In the first version, named "matrix method", the radiation-induced spectral component is extracted numerically using the reference spectra determined experimentally, i.e., using the model BG (i.e. the native background signal) and the model RIS spectrum (Sholom et al. 2019). When the examined samples could have been exposed to light, then an additional light-induced component (the model LIS spectrum) should be included in this procedure (Juniewicz et al. 2020). The RIS and LIS model spectra can be determined as differential signals between the native BG and the spectrum of the irradiated (for the RIS) or light-illuminated (for the LIS) samples of the same glass. In the second version, named "universal method", the reference spectra are simulated theoretically on the basis of known spectral parameters (g factors, hyperfine splittings, etc.) for paramagnetic centers present in the samples: for those naturally abundant (from lattice defects, inclusions) and those generated by ionising radiation and light (Wieser et al. 2015; Sholom et al. 2019).

The extraction of the RIS is a crucial and common problem in EPR dosimetry in all materials; the methods used for a quantitative determination of the RIS are described in more details in many articles on EPR dosimetry in enamel (ISO 2020; Fattibene and Callens 2010; Ivannikov et al. 2010).

In many reports on EPR at high doses (at kGy and higher doses) the meaning of "intensity" of the measured EPR signal is not defined. However, the high amplitude of signals induced by such high doses, strongly overwhelming any background signals, allows to assume that their "intensities" were simply amplitudes of the most evident peaks in the spectral regions affected by radiation—mostly the peak-to-peak amplitudes. Such method for a quantitative determination of RIS was also applied for lower doses (of several Gy) when the dosimetric component was still clearly detectable in the spectra (e.g. Marrale et al. 2011; Longo et al. 2010). Only a few authors used the area under the EPR signal line, which is equivalent to the second integral of the EPR signal (Ranjbar et al. 1999) and which allows for measurements of absolute concentrations of the radicals produced by the radiation (Hassan et al. 2004; Hassan and Sharaf 2005). The simplest method, i.e. the amplitude method, was used so far by most of the researchers for determination of the RIS intensity (or overall EPR intensity in irradiated glass). In future studies on dosimetric applications of EPR at low doses, when the RIS strongly overlaps with unwanted native and light-induced signals, the use of the amplitude method is, however, questionable. A better accuracy can be expected by application of more sophisticated analyses based on numerical decomposition (fitting) of the spectra. This method is superior to the amplitude method also when subtraction of the background signal can be

Table 3 Different types of electron (E) and hole (H) centers that generate RIS signals in GG samples

Type of the center	Spectral characteristics	Generated by gamma radiation	Generated by light including UV	References and instrumentation
E1	Values between $g = 1.97$ and $g = 2.00$	Yes	No	McKeever et al. 2019 (X-band Bruker EMX spectrometer, 4119HS cavity, modulation amplitude = 0.15 or 0.8 mT, microwave power = 27 mW); Wieser et al. 2015 (microwave power of 5 and 30 mW); Sholom et al. 2019 (X-band Bruker EMX spectrometer, 4119HS cavity, modulation amplitude = 0.15 mT; microwave power = 27 mW
E2		No	Yes	
E3		Yes*	Yes*	
E4		Yes*	Yes*	
E5		No	Yes	
H1	Multiline structure with a splitting constant of 1.4 mT with $g \approx 2.01$–2.02 (hyperfine splitting by boron ^{11}B, ^{10}B)	Yes	No	
Boron-oxygen hole centers (BOHC)				
H2	$g = 2.01$	Yes	No	
Non-bridging oxygen hole center (NBOHC)				
H3	$g = 2.02$	Yes	Lack of information	
Oxygen hole center (OHC)				

*Short-living (decay time 6 days)

applied, because of difficulties in accurate determination of background signal intensity due to inter-sample variations. Those adverse effects cause variations in the ΔBG and ΔL, which in turn results in a bias of the ΔA value (Eq. 1). In particular, the amplitude method may lead to large errors if unrevealed spectral components generated by light are present (see sub-section "Effect of light"). Variations in BG and baseline drifts can be eliminated by the fitting procedures. Nevertheless, when the analyzed samples are characterized by a similar native background (e.g. if they are from the same manufactured batch) and have a similar history of light exposure, the results obtained with the amplitude method can be of a similar accuracy as those obtained with spectra decomposition. This is shown in Fig. 6 presenting EPR spectra of four samples of GG glass irradiated with different doses (Fig. 6a), and showing the dose dependence of the determined RISs: four (A_1, A_2, A_3 and A_4) based on the amplitude method (determined at different g ranges) and one based on numerical decomposition of the spectra (matrix method) —those data were measured by the present authors in the intercomparison project reported by Fattibene et al. (2014). As can be seen in Fig. 6b, the results of the fit procedure and the A_1 and A_2 peak-to-peak amplitudes are very close to each other. The data for the A_3 and A_4 amplitudes are different and they cannot be used for dosimetry below ~ 5 Gy because of their non-monotonic dependence on dose. Apparently, at g positions where A_3 and A_4 amplitudes were measured, the EPR spectra of these samples differed in their background components—most probably the one with 0.8 Gy dose. These differences were efficiently eliminated by the fitting and, in this case, by a proper (or lucky) choice of spectra points used for measurements of the amplitudes A_1 and A_2.

Another method of quantitative analysis of radiation-induced changes in EPR spectra was recently reported by Kortmis and Maltar-Strmecki (2018), Kortmiš and Maltar-Strmečki (2019), who observed a dose-dependent horizontal shift (in g value) of the maximum peak of the EPR spectrum (Fig. 7); this shift was caused by an increase in contribution of the RIS to the total (BG + RIS) spectrum. In soda–lime glasses this shift was exponentially dependent on dose and was very sensitive to the dose in the 0–10 Gy range, resulting in the detection of 0.3 Gy with 20% accuracy.

The radiation sensitivity varies remarkably between different types of glasses (Fig. 8). Generally, it is impossible to compare this parameter, because the different authors did not use any universal definition of this quantity and expressed it in "relative" units. Moreover, in many reports the doses applied or measured are specified without any information regarding what material they refer to: to air (or air kerma), to water, or to the glass itself. For high photon energies those doses do not differ remarkably (Fig. 1), but at lower energies (below 100 keV), the differences in interaction coefficients

Table 4 Detection limits and analytical methods used for the determination of radiation-induces EPR signals (RISs) (The detection limits included in this table and their comparison should be considered as approximate, because they were differently defined by different authors or were given even without any definition)

Detection limit	Dose range examined (confirmed linearity range)	Method of determination of the dosimetric signal (RIS)	Types of glass	References
~1 Gy (dose which induces RIS equal to two standard deviations of the BG in un-irradiated samples)	$3{\cdot}10^4$ Gy (0–200 Gy)	Integration method	Clear fused quartz (CFQ) in bulk form	Ranjbar et al. (1996)
~2 Gy (dose which induces RIS equal to two standard deviations of the BG in un-irradiated samples)	0–22.4 Gy (0–7 Gy)	Integration method	Clear fused quartz (CFQ) in powder form	Ranjbar et al. (1999)
Lack of Information	5 Gy–1 kGy	Integration method and peak-to-peak amplitude	Bioglass (Bio-G)	Hassan et al. (2004)
Lack of information	5 Gy–1 kGy	Integration method and peak-to-peak amplitude	Bioglass (Bio-G)	Hassan et al. (2005)
Lack of information	0–20 Gy	g-shift, peak-to-peak amplitude	Soda-lime glass	Kortmis and Maltar-Strmecki (2018)
0.3 Gy at 20% accuracy	0–10 Gy	g-shift	Soda-lime glass	Kortmiš and Maltar-Strmečki (2019)
2.5 Gy	0–10 Gy	Peak-to-peak amplitude		
5 Gy	5 Gy–20 kGy (5–1 kGy)	Peak-to-peak amplitude	Turkish commercial window glass	Engin et al. (2006)
Lack of information	50–500 Gy (50–500 Gy)	Peak-to-peak amplitude	Laboratory glass: "Thuring", Windscreen, "Jena", "Rasoterm", window glass	Gancheva et al. (2006)
8–21 Gy (calculated according to the method described in Fattibene et al. (2011))	4–30 Gy	Peak-to-peak amplitude	Window glass	Liu et al. (2019)
2 Gy (dose below which the dosimetric signal "is too low to be distinguished from the background signal")	0–50 Gy	Lack of information	Watch glass	Wu et al. (1995)
<2 Gy	0–50 Gy	Lack of information	Watch glass	Wu et al. (1998)
1.3 Gy for photons 1.2 Gy for electrons 1.1 Gy for protons (dose which induces RIS equal to three standard deviations of the BG in un-irradiated samples)	1–20 Gy (1–10 Gy)	Peak-to-peak amplitude	Watch glass	Marrale et al. (2011)
5 Gy (dose which induces RIS equal to three standard deviations of the BG in un-irradiated samples)	1–105 Gy	Peak-to-peak amplitude	Watch glass	Longo et al. (2010)
~1 Gy, 12 Gy in 20 days after irradiation	0.5–135 Gy/(0.5–135 Gy)	Peak-to-peak amplitude	Watch glass	Aydaş et al. (2016)
Lack of information	1–200 Gy (1–200 Gy)	Peak-to-peak amplitude	Watch glass & mobile phone LCDs	Bassinet et al. (2010)
Lack of information	0–100 Gy	Peak-to-peak amplitude	Mobile phone LCDs	Trompier et al. (2011a)

Table 4 (continued)

Detection limit	Dose range examined (confirmed linearity range)	Method of determination of the dosimetric signal (RIS)	Types of glass	References
Average 4.12 Gy, variations in the detection limit from 0.75 Gy to 11.91 Gy between participants (calculated according to the method described in Fattibene et al. (2011))	0–10 Gy (0–10 Gy)	Numerical decomposition by fitting of the spectra—matrix method	Gorilla Glass from mobile phones	Fattibene et al. (2014)
2 Gy at 10–20% accuracy	0–10 Gy	Numerical decomposition by fitting of the spectra—matrix method	Protective glass from different mobile phone screen	Sholom and McKeever (2017)
2 Gy at ~ 20% accuracy	0–20 Gy (0–20 Gy)	Numerical decomposition by fitting of the spectra—matrix method	Gorilla Glass from mobile phones	Sholom et al. (2019)
1.4–2.0 Gy (calculated according to the method described in Fattibene et al. (2011)	0–20 Gy	Numerical decomposition by fitting of the spectra—matrix method	Mobile phone screen glass: Gorilla Glass, Mineral Glass, Tempered Glass and iPhone 6S glass	Juniewicz et al. (2019)
About 2 Gy	(up to the level of kGy)	Lack of information	Lack of information	Trompier et al. (2009)

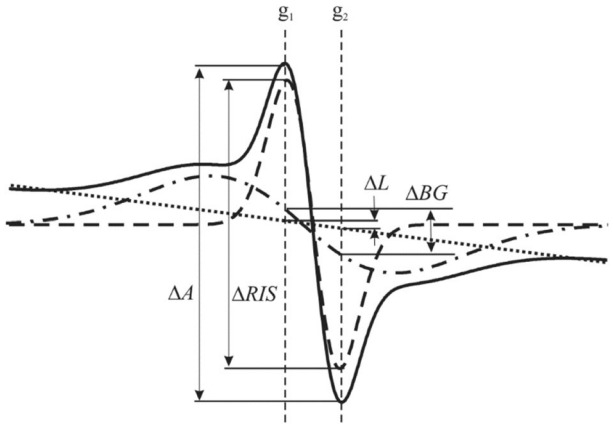

Fig. 5 The peak-to peak amplitude (ΔA) of the experimental spectrum (solid line) is the sum of the background (ΔBG, dashed/dotted line), drift of the baseline (ΔL, dotted line) and the radiation-induces signal (ΔRIS, dashed line) measured at two magnetic field positions marked by the vertical dashed lines denoted by g_1 and g_2

between glass and, for example, water or tissue become relevant. Consequently, comparison of the radiation sensitivity is possible only if the dose response of various types of glasses was investigated with the same analytical procedures. Also, the differences in detection limits presented in Table 4 reflect not only differences in the radiation-induced generation of the detectable paramagnetic centers, but also the precision of the experimental and analytical procedures applied by different researchers.

Practical applicability of a dosimetry method is limited by its sensitivity to ionising radiation, which is characterized by the minimum detectable dose (detection limit). This term was not always precisely defined by researchers either. Definitions used by various authors varied from the imprecise "dose below which the dosimetric signal is too low to be distinguished from the background signal" (Wu et al. 1995), through "the dose value that produces in the irradiated samples an ESR signal equal to the mean value of the zero-dose signal in unirradiated samples plus three standard deviations" (Longo et al. 2010), to its most precise version of the minimal dose which can be detected with a given probability—the latter definition was used in analysis of data measured during the dosimetry intercomparison project (Fattibene et al. 2014). Taking into account these differences in the meaning of the "detection limit", the data collected in the 1st column of Table 4 are not directly inter-comparable and give only a rough assessment on the relative sensitivity of the dosimetry procedures used by the corresponding authors. Nevertheless, those data do allow evaluation of the range of doses for which a given type of glass and the applied analytical procedure can be useful. The minimum detectable dose and accuracy are also limited by inter-sample variations—within one type of watch

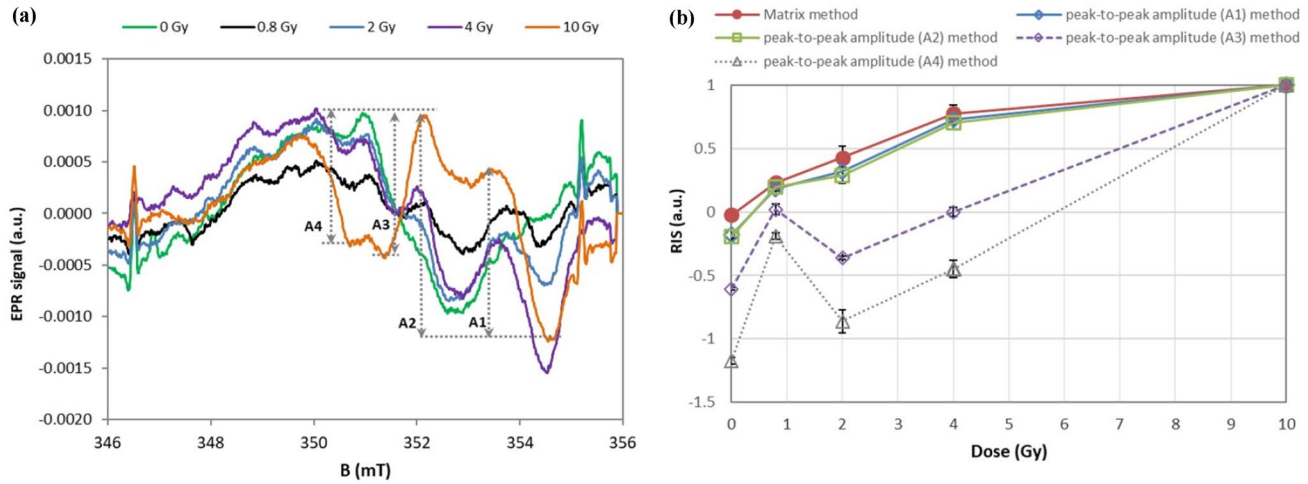

Fig. 6 **a** EPR spectra of five Gorilla Glass samples irradiated in the 0–10 Gy dose range (the sharp peaks at the spectra wings are residuals of Mn^{2+} standard lines). **b** Dose dependences of radiation-induced signals (RISs) expressed as amplitude (A_1, A_2, A_3 and A_4) and as fitted contributions of the model RIS_r spectrum (matrix method). Data were normalized to their respective values at 10 Gy, and connected with lines to guide the eye; error bars represent maximum deviation of the data measured at different orientations of the sample in the EPR cavity

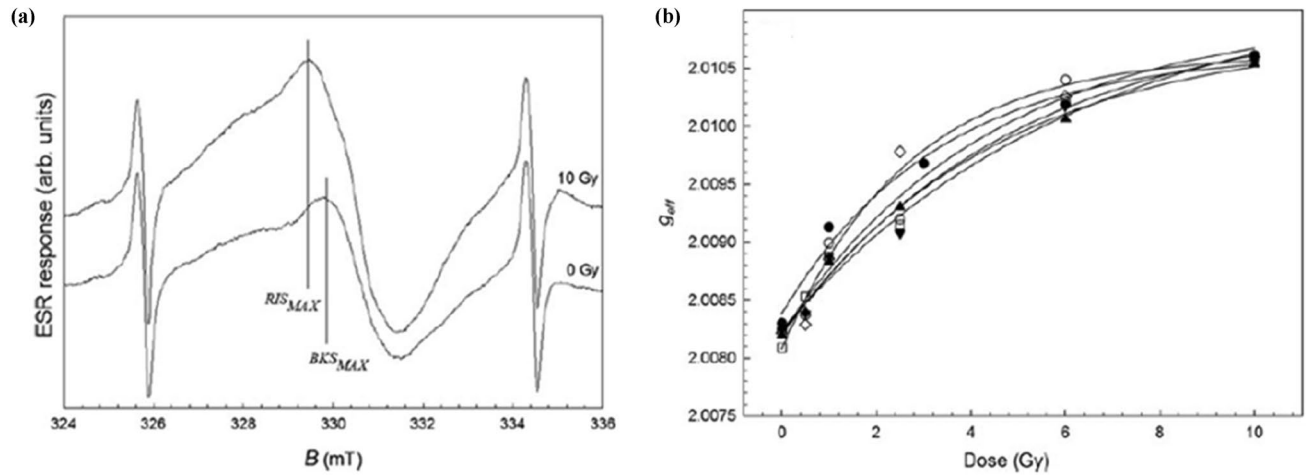

Fig. 7 Shift of the spectra maximum between un-irradiated and irradiated soda-lime glass (**a**) and dependence of corresponding g position on dose (**b**). Reproduced with permission from Kortmiš and Maltar-Strmečki (2019)

glass the scatter in EPR amplitudes can be equivalent to their increase caused by several Gy (Wu et al. 1995; Marrale et al. 2011). Variations in amplitude between different types of glass (from different producers) were even bigger (Wu et al. 1995).

As other dosimetric methods, EPR dosimetry in glass requires calibration of the dosimetric signal (RIS) regardless of what method is applied for its determination. This can be done using other samples of the same type of glass assuming that radiation sensitivity of the RIS and parameters of EPR spectra (line-shapes) of the calibration samples are the same as those of the samples used for dose assessment. An alternative method is based on the "additive dose"—i.e. delivery of known doses to the very same sample (the one also used to measure an unknown dose). This method assures that the same spectral components (BG, RIS) are analyzed during the calibration procedure as in the analysis of the "as-received" sample (the one with unknown dose).

Dose response of the RIS is approximately linear in the low-dose range, which facilitates dosimetric procedures. Sub-linearity due to dose saturation of the signal was observed above several kGy (Teixeira et al. 2005; Wieser and Regulla 1990). A nonlinear dependence was observed in

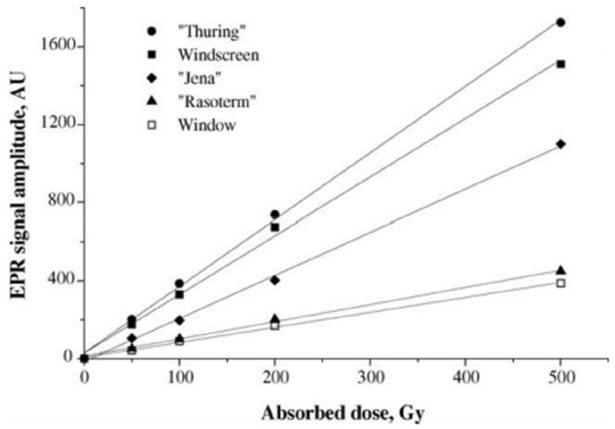

Fig. 8 Dose response of EPR amplitudes in various types of glass (reproduced with permission from Gancheva et al. 2006)

watch glasses when high microwave power and modulation amplitude values were chosen (Marrale et al. 2011).

Generally, it can be concluded that determination of the dosimetric signal in glass samples is more accurate and reliable when using the methods based on signal decomposition and fitting rather than on measurement of amplitudes of the spectral lines. The numerical decomposition and fitting enables a better separation of the dosimetric component from the other background signals, than the amplitude method, but requires knowledge of the model spectra to be used in the signal decomposition and fitting procedures. Studies of Sholom et al. (2019) showed that use of different sets of reference spectra, simulated or experimental, in dose reconstructions in GG samples yielded qualitatively similar results, even at a relatively low nominal dose of 2 Gy.

Stability of RIS

The post-irradiation EPR signal in glass is not long-term stable. This has been mentioned by many authors as a disadvantage of this material in its use in dosimetry. Nevertheless, despite of the fading, the RIS was still detectable after many months after irradiation. For example, Bortolin et al. (2019) reported existence of a visible radiation-induced EPR signal in labware glass one year after irradiation. Trompier et al. (2011a) observed a distinct RIS in LCD glass over two years after irradiation. Juniewicz et al. (2019) monitored the EPR signals in irradiated GG and tempered glass (TG) for almost 19 months (Fig. 9). Several other authors (Bassinet et al. 2010; Juniewicz et al. 2019; McKeever et al. 2019; Liu et al. 2019) monitored the changes in EPR signal through shorter periods of up to hundreds of hours.

Decay kinetics of the RIS varies in different glasses. Due to the complex nature of the superimposing EPR lines, in some glasses the fading results not only in a drop of the signal amplitude, but also in changes in the shape of the spectra measured at different time after irradiation, as can be seen in Fig. 9a, b.

Figure 10 and Table 5 summarize information reported by various authors on the kinetics of fading of the dosimetric signal—expressed here in a form of a Decay Factor (DF) defined as the fraction of the initial RIS measured after a given number of days after irradiation. Often details of storage conditions were not fully specified in the literature. Consequently, the data presented in Fig. 10 are only for those storage conditions for which room temperature (RT) in darkness or in ambient (laboratory) light is specified. If the authors did not specify the storage conditions, it was assumed that the samples were stored at RT in darkness, and the respective data were included in the present analysis of stability. Some of the DF values plotted in Fig. 10 were evaluated by the authors of the present study by interpolation of the original data from plots presented in the referenced

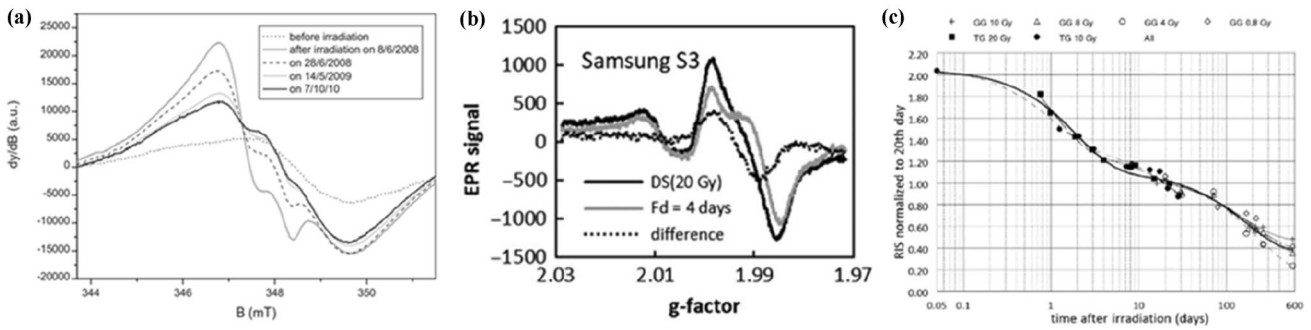

Fig. 9 **a** Changes in a 2-year period in spectra of glass from LCD from mobile a phone irradiated by 50 Gy (Trompier et al. 2011a), **b** changes in spectra of irradiated (20 Gy) GG in four days (McKeever et al. 2019), **c** variations in time of the RIS induced by doses up to 20 Gy in GG and protective tempered glass (TG) (data are normalized to the 20th day after irradiation (Juniewicz et al. 2019))

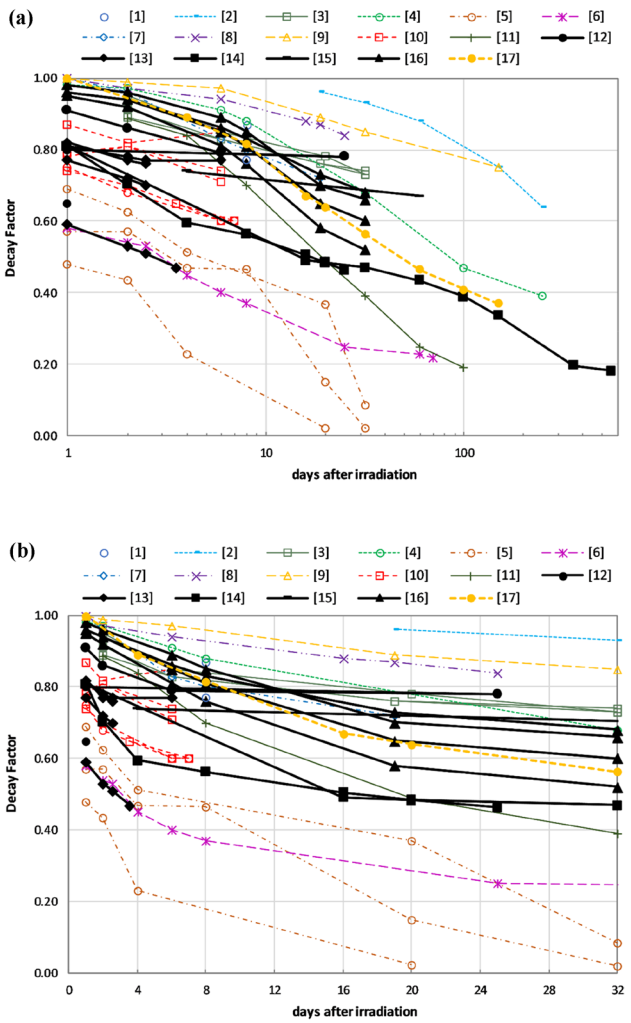

Fig. 10 Data for glasses from mobile phones are marked with thick, black solid lines. **a** Kinetics of fading of the RIS in glasses. The "Decay Factor" represents the fraction of the initial EPR signal (as reported in Engin et al. 2006; Longo et al. 2010; Aydaş et al. 2016; Hassan and Sharaf 2005; Bortolin et al. 2019; Moghaddam et al. 2012) or the RIS (other reports) measured after a given number of days after irradiation. **b** Same data as in (**a**) but up to the 32nd day, with linear horizontal axis. The numbers in brackets in the legends show the respective references as numbered in Table 5

articles. Therefore, the DFs should be considered as approximate. Taking into account the limited precision of the original data and an inter-sample variability of the fading kinetics, the relative accuracy of the present evaluation of the Decay Factors may be within a few percent.

Many of the authors cited in Fig. 10 and Table 5 did not specify the moment of the first, initial EPR measurement, which provided the reference RIS value to calculate the DF for their later measurements. This is an additional factor contributing to the approximate character of the presented estimates. Those uncertainties are reflected by the large scatter of the DF values for day 1 (the intercepts of the lines in Fig. 10a) varying from about 0.5 to 1.0. An initial fast decay (up to the reported 50% after one day, which is equivalent roughly to a decrease of 2% per hour) may lead to large biases, if the time interval between irradiation and first EPR measurement is not accurately reported; not to mention the duration of the irradiation, which at low-dose rates may require a few hours to deliver a dose of dozens of Gy. The data spread in Fig. 10a, b is also due to the variability in types of glass investigated and, potentially, due to differences in doses to which the examined glasses had been exposed. The latter effect (i.e., the dependence of fading on radiation dose) was not studied so far in EPR glass dosimetry, but was already observed, for example, in irradiated alanine, where the decay of radicals at room temperature is faster in high-dose than in low-dose samples (Sleptchonok et al. 2000, Ciesielski 2006). An increase in fading above ~ 100 Gy of color centers was spectrophotometrically observed in glass by Kriedl and Blair (1956). However, some of the reported data indirectly indicate that the DF in glass does not vary noticeably for samples exposed within the low-dose range (up to 10–20 Gy). This can be inferred from a linearity of dose response curves in calibrations performed at different times after irradiation (Fig. 5 in Fattibene et al. 2014; Fig. 5 in Juniewicz et al. 2019). A detailed analysis (not presented here) of own results shown in Fig. 9c also did not reveal any dose-related differences in fading of RIS below 20 Gy.

Despite of the limitations mentioned above, the present analysis allows for practical conclusions regarding the course of dosimetric procedures. Presentation of the data using the linear scale for the time axis (Fig. 10b) proves that after the first 6–8 days of strong fading (by more than 30% in some mobile phone screens) the decay still continues, but remarkably slows down: for all mobile phone glasses this decay is smaller than 25% in the next 26 days. This is a crucial observation for planning dosimetry procedures, which should be based on a thoughtful, properly scheduled calibration of the RIS on the basis of the determined DF parameter, to account for the fading phenomena. In consequence of the early, rapid decay, the accuracy of accidental EPR glass dosimetry in the first 6–8 days after exposure can be strongly limited. This aspect was accounted for by organizers of the "EPR dosimetry intercomparison using smart phone touch screen glass" (Fattibene et al. 2014), who recommended keeping at least five day intervals between irradiation of the samples and their EPR measurements. It is plausible that the large fluctuation of results obtained by participants in group B in this intercomparison project could be caused by variations in scheduling of the measurements. It is noted that repeated measurements using the same type of samples done by one laboratory while strictly obeying timing (30 and 60 days after irradiation) resulted in a significant improvement of the results (Fattibene et al. 2014).

Table 5 References for data in Fig. 10a, b

Type of glass examined	Doses studied	Type of radiation	References	Line No in Fig. 10a, b (in the labels at top)
Labware glass (blood test tubes)	1000 Gy	Gamma ^{60}Co	Bortolin et al. (2019)	1
Bioglass	5–1000 Gy	Gamma ^{60}Co	Hassan et al. (2005)	2
Clear fused quartz (from EPR sample tubes)	5.46 kGy, 16.09 kGy 37.5 kGy	Electrons 10 MeV	Ranjbar et al. (2009)	3
Turkish commercial window glass	2000 Gy	Gamma ^{60}Co	Engin et al. (2006)	4
Window Glass	30 Gy	Gamma ^{137}Cs	Liu et al. (2019)	5
Window glass powder	20 kGy	Electron beams 10 MeV	Moghaddam et al. (2012)	6
Watch glass	1–105 Gy	Protons 60 MeV	Longo et al. (2010)	7
Watch glass	1–20 Gy	X-rays 6 MV	Marrale et al. (2011)	8
Watch glass	fluence: $2.7{\cdot}10^{11}$ cm^{-2}	Neutrons from ^{241}Am-Be	Marrale et al. (2012)	9
Watch glass	0–50 Gy	Gamma ^{60}Co	Wu et al. (1995)	10
Watch glass	50 Gy	Gamma ^{60}Co	Aydaş et al. (2016)	11
Displays of mobile phones and wristwatches Type I, II	0–100 Gy	Gamma ^{60}Co and ^{137}Cs	Bassinet et al. (2010)	12
LCDs glass from mobile phones Type I, II, III	100 Gy	Gamma ^{60}Co and ^{137}Cs	Trompier et al. (2011a)	13
GG, TG glasses	0–20 Gy	Photons 6 MV	Juniewicz et al. (2019)	14
GG	20 Gy	Beta ^{90}Sr/^{90}Y	McKeever et al. (2019)	15
Gorilla glass coming from touchscreens phones A, B, C and D	10 Gy	Gamma ^{137}Cs	De Angelis et al. (2015)	16
Mineral eyeglass	5 Gy–10 kGy	Gamma ^{60}Co	Karaaslan and Engin (2021)	17

Increased temperature and exposure to light during storage may speed up the decay of RIS in glass. Juniewicz et al. 2020 reported that five minutes of sunlight can reduce twofold the RIS, and other authors also observed an accelerated decay of the RIS components under the presence of laboratory light (Wieser et al. 2015; Fattibene et al. 2014). More information on effects of temperature and light are given in the sub-section "Effect of light" further below.

Effects of physical factors on EPR signal in glass

Effect of cleaning and crushing of the samples

The placement of glass samples inside an EPR spectrometer cavity usually necessitates crushing or braking larger glass pieces into small ones with sizes from fractions of millimeters up to a few millimeters, or cutting them into elongated rods of a few mm in width and a few cm in length. The glass has to be cleaned from any casual impurities, which can introduce unwanted EPR signals. In this context it is important to note that structural elements of larger and thicker glass layers are firmly interconnected by a glue. For example, the glasses in touch screens of mobile phones or smartwatches are typically covered by a protective glass layer reducing their vulnerability to cracks and scratches. In order to eliminate any residues of the glue used, the samples are usually cleaned with water and ethanol, which potentially can affect the EPR signals. Trompier et al. (2011a) reported lack of any effect of ethanol on EPR in display windows of mobile phones, with the exception of a removal of signals produced by crushing of one type of examined glass. This effect could be associated with elimination of mechanically induced surface radicals by ethanol. Juniewicz et al. (2019) also reported lack of effect of 10 min water treatment on EPR signal in irradiated (20 Gy) mineral glass. Similarly, Liu et al. (2019) did not observe any influence of alcohol and water on the EPR signal in window glass. These observations are consistent with the low permeability of glass to liquids and its chemical resilience, the features which limit any potential chemical interactions on its surface.

Mechanical stress in solids can generate paramagnetic centers contributing to background EPR signals. Actions such as grinding or crushing have been proven to increase the EPR background signal, for example in tooth enamel (Sholom et al. 1998) or in bones (Ciesielski et al. 2014). In glass, Trompier et al. (2009, 2011a) and Bassinet et al. (2010) noted that crushing samples into grains larger than 315 μm does not induce any additional components in their

EPR signals. However, when the glass was ground to fine powder (< 315 µm), generation of additional signals was observed (Fig. 11). Trompier et al. (2011a) reported that the mechanically induced EPR signal decayed by about 30% within 8 h after crushing at room temperature. This signal was easily removed by ethanol, which indicates its origin from surface effects. Usually the size of grains or pieces of glass inside an EPR sample tube that provide sufficient measurement reproducibility (by averaging out potential deviations caused by anisotropy) are larger than 315 µm. Juniewicz et al. (2019) reported lack of any effects of crushing to such submillimeter grains. An alternative solution to the problem of anisotropic sample geometry is the use of larger (i.e., a few mm in size) pieces of glass and reduction of any anisotropic effects by averaging spectra measured at different orientation of the sample tube in the cavity.

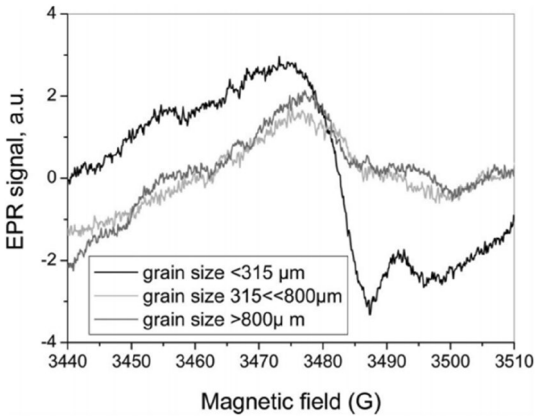

Fig. 11 Effect of glass sample crushing on EPR signals in an un-irradiated watch. Reproduced with permission from Bassinet et al. (2010)

Effect of temperature

Increase in temperature often causes speeding up of chemical reactions and can, therefore, be an important factor influencing the kinetics of the decay of EPR signals, including those generated by ionising radiation. Such temperature effects can be discussed from two perspectives: (1) effects of little elevated environmental temperatures, which can affect the accuracy of dosimetry due to speeding up the RIS decay, and (2) effects of very high temperatures applied deliberately to the samples, to anneal any unwanted signals (for example, to reconstruct the sample-specific background signal). In normal conditions of using personal items, ceramics, kitchen vessels, window glass, etc., temperatures usually do not exceed 100 °C. Much higher temperatures can be used to study annealing effects up to about 300 °C (Engin et al. 2006; Hassan and Sharaf 2005).

With regard to the first, low temperature range, the results published by Wu et al. (1995) show that in watch glass irradiated to 0–50 Gy the reduction in EPR signal over seven days varied from about 20% at 4 °C to about 60% at 40 °C, respectively (corresponding to DFs of 0.8 and 0.4). Engin et al. (2006) studied effects of thermal annealing for window glass irradiated up to 500 Gy. In their study the signal intensity at g = 2.0128 did not change up to 50 °C in 15 min isochronal annealing and dropped by about 70% at 100 °C (Fig. 12a). The decay at other temperatures and times of annealing are presented in Fig. 12b, showing that 50 min of storage resulted in DF ≈ 0.75 and DF ≈ 0.50 at 60 and 90 °C, respectively. Hassan et al. (2005) reported for a bioglass a remarkable change in DF from about 0.5 to 0.03 within 2 h storage at 70 and 150 °C. Hence, the storage temperature can be a significant factor affecting accuracy of dosimetry.

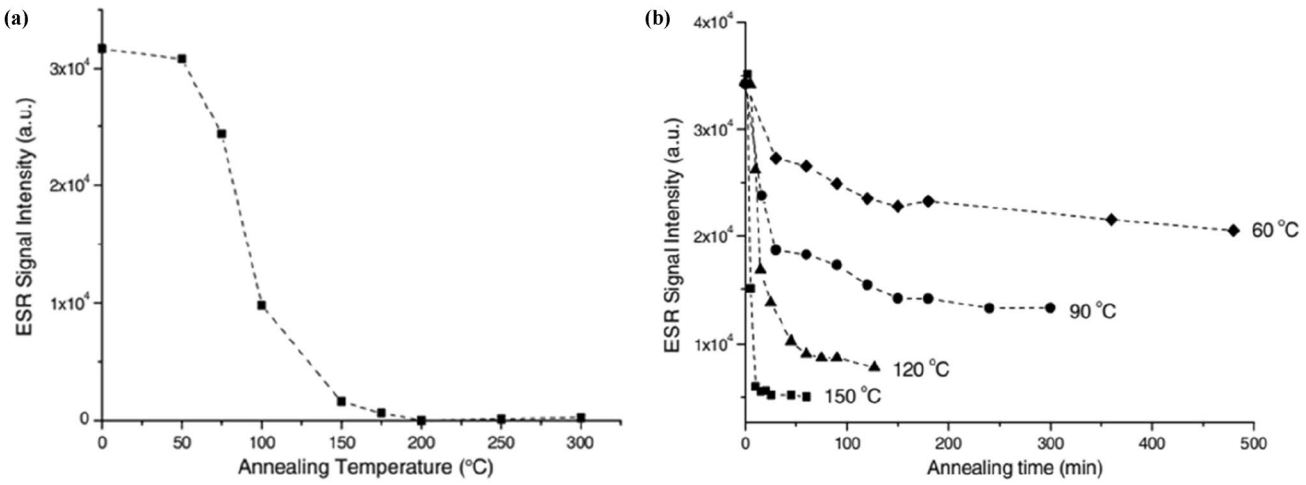

Fig. 12 Window glass irradiated to 500 Gy. **a** Effect of isochronal 15 min annealing on EPR signal **b** decay of EPR signal as a function of time of heating and temperature (reproduced with permission from Engin et al. 2006)

Wu et al. (1995) observed that one hour of annealing at 200 °C of an irradiated watch glass eliminated the radiation-induced component (RIS). Consequently, they suggested that annealing can be considered as a treatment of irradiated samples allowing to restore their original, native background. Gancheva et al. (2006) confirmed applicability of such a method for various types of window glasses. They found that the difference in EPR signals between irradiated samples and the same samples annealed for 40 min at 200 °C showed a linear dependence on dose from 50 up to 500 Gy. Consequently, thermal treatment of irradiated glasses at 300 °C was proposed for their re-use as dosimeters (Gancheva et al. 2006). Elimination of RIS by 20 min annealing at 200 °C was also observed by Bassinet et al. (2010) and Liu et al. (2019).

Much higher temperatures were necessary to bleach out the RIS in fused quartz. For example, Ranjbar et al. (1996) reported on a total reduction of the dosimetric signal due to irradiation with 16 Gy in clear fused quartz after 20 min annealing above 700 °C; at 200 °C the RIS faded by only 30%. A complete decay of RIS (at $g = 2.0025$ and $g = 1.9676$) in glass test tubes irradiated by 1 kGy followed by annealing to 400 °C was also reported by Bortolin et al. (2019). McKeever et al. (2019) reported rapid fading of EPR background signal in GG at about 350–375 °C, which coincided with the temperature range of the TL glow peak.

Unfortunately, the insensitivity of the native background signal to heating—a necessary feature allowing for bleaching out the RIS to restore the sample's original background—is not typical for all types of glasses. Trompier et al. (2011a) annealed glass from phones' LCDs screens for 20 min at 200 °C and obtained various effects:

(1) in one sample the signal decreased to a level lower than that before irradiation and annealing, while maintaining its shape (Fig. 13a),
(2) while in another sample the annealing caused induction, in both irradiated and non-irradiated samples, of an additional EPR line attributable to the generation of additional paramagnetic centers (Fig. 13b).

This diversity in effects of high temperatures on background signals is a disadvantage in applications of glass for fortuitous dosimetry, when the background signal in irradiated samples is unknown and the measured spectra are composed from unknown contributions of the radiation-induced and the native signals. If elimination of the radiation-induced component by annealing is accompanied by changes in the sample's background, then the determination of the RIS becomes problematic. This is particularly the case when the heating affects the shape of the native signal, because any variations only in its magnitude can be accounted for by the numerical fitting procedures. Consequently, appropriateness of the determination of the background signal by annealing of irradiated samples should be verified with other unirradiated samples of the same type of glass.

At low storage temperatures (−18 °C) fading of the RIS slows down in comparison to its fading at room temperature, as was shown by Liu et al. (2019).

Kortmis and Maltar-Strmecki (2018) reported an increase in radiosensitivity of EPR signals in gamma-irradiated soda–lime glasses, if measured at low temperatures. The authors demonstrated, that in glass irradiated in a dose range of 1–20 Gy the EPR amplitude measured at 200 K increased by 30–80%, respectively, compared to the room temperature (300 K) signal readout. The authors suggested to perform

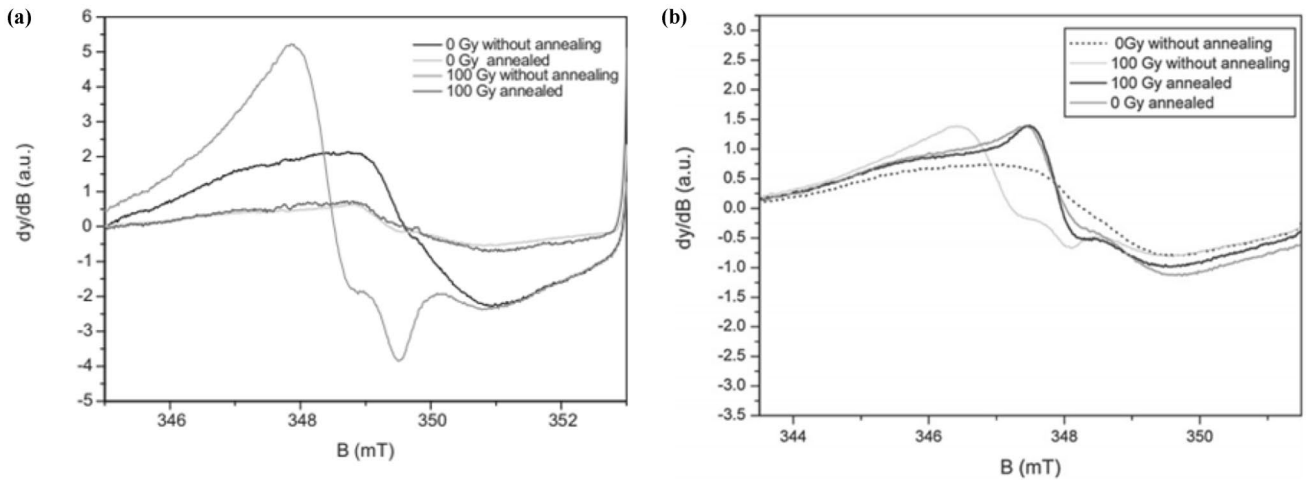

Fig. 13 Effect of annealing at 200 °C on EPR spectra of two glasses from LCD **a** elimination of the radiation-induced signal (RIS) and decrease of background (BG) signal, **b** induction of a spectral component different than RIS and original BG (reproduced with permission from Trompier et al. 2011a)

EPR measurements at low temperature to improve the dose detection limit.

Effect of light

Light is a widespread physical factor always present in the environment. Therefore, its potential influence on EPR signals in glass has to be determined in order to avoid any biases caused by exposure of irradiated samples to light. Effects of light were investigated in several studies on EPR dosimetry in glass. In general, potential effects of light on EPR dosimetry can result from changes (1) in the background signal including generation of spectral lines other than those assigned to the RIS and (2) in the RIS by influencing its fading or by generating spectral lines identical to those assigned to the RIS. Taking into account the energy of light photons such effects can be expected rather for shorter wavelengths (UV) than for longer wavelength (visible light). Engin et al. (2006) reported lack of any effects on background signals as well as on the RIS (at $g = 2.0128$) induced by 100 Gy despite exposures of window glass to visible light from a fluorescent lamp for up to eight months. In addition, these authors did not observe any change in EPR signal in samples exposed for one year to daylight. Also, Juniewicz et al. (2020) reported lack of effects of an intense (110 W/m^2) light from fluorescent bulbs (which produced light without UV component) on the EPR signal from an iPhone screen glass irradiated to 10 Gy. However, an induction of a spectral component assigned to an E2 electron center in GG exposed for 95 days to laboratory light (of wavelength > 365 nm) was reported by Wieser et al. (2015).

Effects of light on spectra of un-irradiated glass and on radiation-induced signals in glass were reported also by other authors, who observed such effects for artificial light from UV lamps or sunlight. Reports of De Angelis et al. (2015) showed induction of EPR lines assigned to the E1 center by exposures of GG to UV (254 nm, 15 min) or sunlight (for three days). Amplitudes of these light-induced signals were similar in magnitude to those of the RIS generated by several Gy.

There is ample evidence that generation of paramagnetic centers in glass by UV light can strongly contribute to BG signals. A strong argument for this was given by McKeever et al. (2019), who reported a significant reduction in the BG intensity (by ~ 80%) after etching samples of screen glass from a phone with 40% HF, where the acid removed the surface layer of the glass, which was affected by UV. They also observed a higher intensity of the BG component in EPR signals of GG samples cut from edge regions of another mobile phone, as compared to EPR signals from center parts of the screen. The authors attributed this to the curing of the adhesive between glass layers by exposure to UV light during the production processes. Illumination of this glass with 254 nm light resulted in generation of two spectral components: one was stable and similar to that generated by 302 nm light, and the other was an unstable singlet at $g = 1.994$. Light of 365 nm was much less efficient in its effects on EPR spectra than light with shorter wavelength.

Exposure of un-irradiated mineral glass to direct sunlight and UV lamps caused changes in the shape of the spectrum at g < 2.00 (Fig. 14a). An additional paramagnetic center with an EPR line at $g \approx 2.00$ was also observed, especially in the sample exposed to sunlight (Fig. 14b).

Numerical decomposition of the spectra of irradiated and then illuminated glass samples into their native (BG) and light-induced signals (LIS) showed that the EPR intensity of

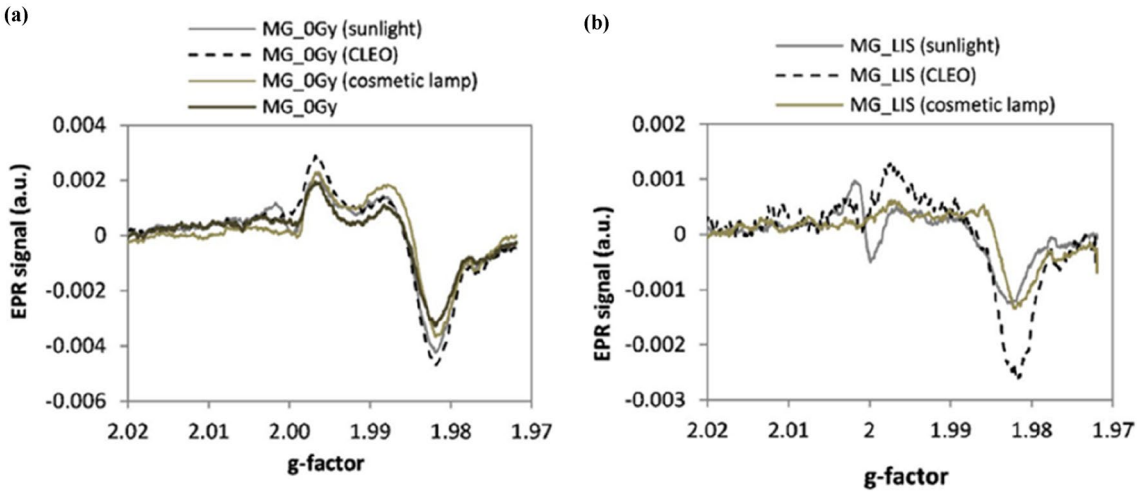

Fig. 14 **a** Changes in background (BG) spectra caused by exposure of glass from mobile phone screens to light including a UV component: sunlight, Phillips CLEO lamp and cosmetic lamp. **b** Light-induced signals (LIS) obtained as differential spectra from those in (**a**) (reproduced with permission from Juniewicz et al. 2020)

spectral components assigned to the native background did not change remarkably with illumination, leading to hypothesis that the light did not interact with those paramagnetic centers in glass responsible for the native signal, but produced additional centers which generate the LIS.

The RIS decays faster under illumination by UV than without illumination. Liu et al. (2019) reported a complete decay of RIS in irradiated (30 Gy) window glass exposed for 25–100 h to sunlight. The fading was similar in samples kept in the dark or exposed to indoor light, and was much slower than in those exposed to sunlight. Juniewicz et al. (2020) showed, that exposures of glass from mobile phones (mineral glass, GG, tempered glass) to light with a UV component caused significant fading of the dosimetric signal (RIS). Specifically, even a few minutes of exposure to light with a UV component caused a 20–60% decrease in the RIS determined by spectra decomposition (i.e., fitting with the matrix method). Samples of tempered glass used as protection for mobile phone screens, were less sensitive to light and showed an about 50% RIS decay after 30 min of exposure to UV.

Gorilla Glass also exhibits a sensitivity to both ionising radiation and light, having a characteristic shape of the EPR spectral line for all three components, i.e., the BG, RIS, and LIS signals, where the later was attributed to the E2 electron center (Wieser et al. 2015; Sholom et al. 2019). The effect of UV exposure on GG spectra and their three main signal components is presented in Fig. 15. A correlation between the fading of RIS and the LIS generated by light from a CLEO UV lamp (Philips) are shown for this glass in Fig. 16.

The plausible presence of LIS in screen glasses of used mobile phones—for example due to their exposure to sunlight—demonstrates the need to base EPR dosimetry on procedures that take into account the LIS component. Ignoring this component may result in significant inaccuracy of the reconstructed RIS and, consequently, in an overestimation of the actual RIS by up to 90%, as was shown for high light fluences by Juniewicz et al. (2020). The correlation between the RIS and LIS shown in Fig. 16c can potentially be used to introduce corrections accounting for the light-induced fading of RIS. A similar correlation between RIS and LIS was also observed for mineral glass from mobile phones (Juniewicz et al. 2020).

Finally, it was also shown that an exposure of mineral glass to sunlight before its irradiation with X-rays did not affect noticeably its radio-sensitivity (Juniewicz et al. 2020).

Conclusion

Results of the studies discussed in this brief review confirm applicability of EPR signals in glasses for fortuities dosimetry of ionising radiation following unexpected, accidental exposures of humans and their closest environment to doses of a few Gy. In particular, dosimetry based on glasses from ubiquitous utility items kept close to the body, like mobile phones and wrist watches, allows to achieve a sensitivity of detection on the level of 1–2 Gy, which is sufficient for triage of exposed individuals before planning further medical actions. However, there are two crucial requirements to be fulfilled, in order to obtain reliable results of the EPR dosimetry. The first is implementation of a proper correction in analytical procedures accounting for rapid fading of the dosimetric signal during the first 6–10 days after irradiation.

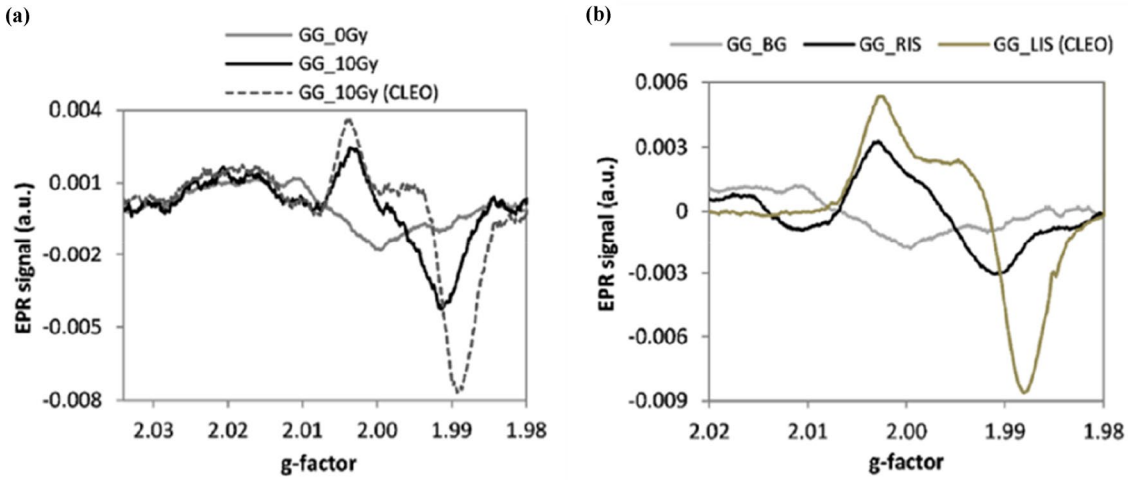

Fig. 15 **a** EPR spectra demonstrating the effect of irradiation of a Gorilla Glass (GG) sample with 10 Gy X-rays, and the effect of a subsequent 45 min illumination with a Philips CLEO UV lamp. **b** Three components of EPR spectra for the GG sample: background signal (BG), radiation-induced signal (RIS), and light-induced signal (LIS) determined in a separate experiment for use as model spectra in the matrix method (reproduced with permission from Juniewicz et al. 2020)

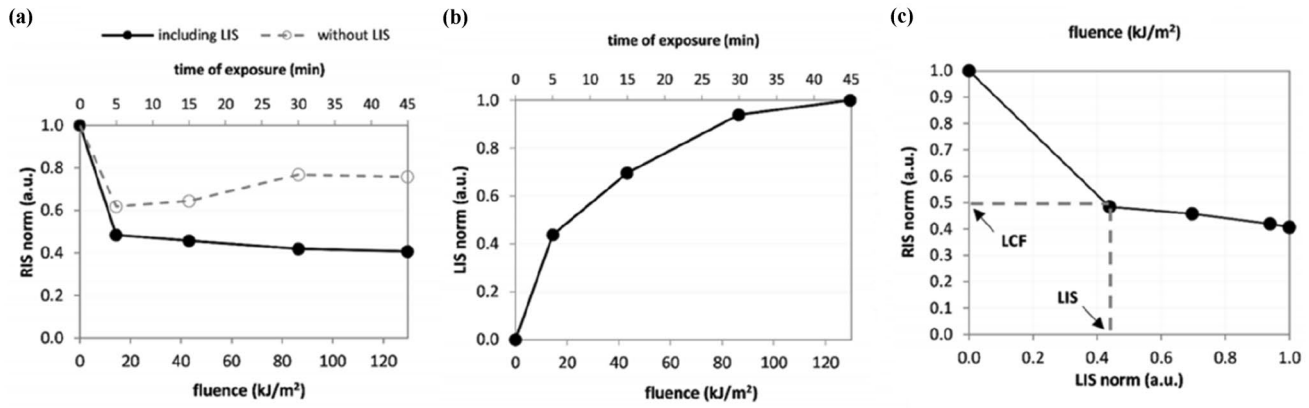

Fig. 16 **a** Light-induced decay of the radiation-induced signal (RIS)—decomposition by the matrix method including presence of a light-induced signal (LIS) (the solid line) and ignoring presence of the LIS (dashed line), (**b**) LIS (**c**) correlation between RIS and LIS and determination of the light correction factor (LCF) (reproduced with permission from Juniewicz et al. 2020)

The second is taking into account potential exposures of the irradiated glass to light, particularly to the UV component of sunlight. Depending on the method used for determination of the dosimetric signal (amplitude or numerical decomposition), neglecting the light effects can introduce remarkable over- or underestimation of the reconstructed doses.

Declaration

Conflict of interest The Authors have no conflict of interests to declare that are relevant to the content of this article.

References

Ainsbury EA, Bakhanova E, Barquinero JF, Brai M, Chumak V, Correcher V, Darroudi F, Fattibene P, Gruel G, Guclu I et al (2011) Review of retrospective dosimetry techniques for external ionizing radiation exposures. Radiat Prot Dosim 147(4):573–592

Alexander GA, Swartz HM, Amundson SA, Blakely WF, Buddemeier B, Gallez B, Dainiak N, Goans RE, Hayes RB, Lowry PC (2007) BiodosEPR-2006 meeting: acute dosimetry consensus committee recommendations on biodosimetry applications in events involving uses of radiation by terrorists and radiation accidents. Radiat Meas 42(6–7):972–996

Aydaş C, Yüce ÜR, Engin B, Polymeris GS (2016) Dosimetric and kinetic characteristics of watch glass sample. Radiat Meas 85:78–87

Bassinet C, Trompier F, Clairand I (2010) Radiation accident dosimetry on glass by TL and EPR spectrometry. Health Phys 98(2):400–405

Beinke C, Siebenwirth C, Abend M, Port M (2021) Contribution of biological and EPR dosimetry to the medical management support of acute radiation health effects. Appl Magn Reson. https://doi.org/10.1007/s00723-021-01457-5

Boizot B, Petite G, Ghaleb D, Calas G (1998) Radiation induced paramagnetic centres in nuclear glasses by EPR spectroscopy. Nucl Instrum Meth b 141(1–4):580–584

Bortolin E, De Angelis C, Quattrini MC, Barlascini O, Fattibene P (2019) Detection of ionizing radiation treatment in glass used for healthcare products. Radiat Prot Dosim 186(1):78–82

Cerezo L (2011) Radiation accidents and incidents. What do we know about the medical management of acute radiation syndrome? Rep Pract Oncol Radiother 16(4):119

Ciesielski B (2006) Combined effects of high doses and temperature on radiation-induced radicals and their relative contributions to EPR signal in gamma-irradiated alanine. Radiat Prot Dosim 120(1–4):184–190

Ciesielski B, Kaminska J, Emerich K (2011) Analysis of various modifications in spectra analysis on accuracy of dose reconstructions in EPR dosimetry in tooth enamel. Radiat Meas 46(9):783–788

Ciesielski B, Krefft K, Penkowski M, Kaminska J, Drogoszewska B (2014) Effects of water treatment and sample granularity on radiation sensitivity and stability of EPR signals in X-ray irradiated bone samples. Radiat Prot Dosim 159(1–4):141–148

De Angelis C, Fattibene P, Quattrini MC, Della Monaca S, Trompier F, Wieser A, Brai M, Ciesielski B, De Angelis C, Della Monaca S et al (2015) Variability of the dosimetric EPR response of Gorilla Glass touchscreen to dose and to light. Presented at the 2015 EPR BioDose conference, Hanover, USA, October 4–8, 2015; Poster P8-W

Desrosiers MF (1991) In vivo assessment of radiation exposure. Heath Phys 61(6):859–861

Discher M, Greiter M, Woda C (2014) Photon energy dependence and angular response of glass display used in mobile phones for accident dosimetry. Radiat Meas 71:471–474

Discher M, Hiller M, Woda C (2015) MCNP simulations of a glass display used in a mobile phone as an accident dosimeter. Radiat Meas 75:21–28

Engin B, Aydas C, Demirtas H (2006) ESR dosimetric properties of window glass. Nucl Instrum Methods Phys Res b 243(1):149–155

Fattibene P, Callens F (2010) EPR dosimetry with tooth enamel: A review. Appl Radiat Isot 68(11):2033–2116

Fattibene P, Wieser A, Adolfsson E, Benevides LA, Brai M, Callens F, Chumak V, Ciesielski B, Della Monaca S, Emerich K (2011) The 4th international comparison on EPR dosimetry with tooth enamel: part 1: report on the results. Radiat Meas 46(9):765–771

Fattibene P, Trompier F, Wieser A, Brai M, Ciesielski B, De Angelis C, Della Monaca S, Garcia T, Gustafsson H, Hole EO (2014) EPR dosimetry intercomparison using smart phone touch screen glass. Radiat Environ Biophys 53(2):311–320

Flood AB, Bhattacharyya S, Nicolalde RJ, Swartz HM (2007) Implementing EPR dosimetry for life-threatening incidents: factors beyond technical performance. Radiat Meas 42(6–7):1099–1109

Gancheva V, Yordanov ND, Karakirova Y (2006) EPR investigation of the gamma radiation response of different types of glasses. Spectrochim Acta A 63(4):875–878

Griscom DL (1980) Electron spin resonance in glasses. J Non-Cryst Solids 40(1–3):211–272

Griscom DL, Sigel GH, Ginther RJ (1976) Defect centers in a pure-silica-core borosilicate-clad optical fiber: ESR studies. J Appl Phys 47(3):960–967

Hasanuzzaman M, Rafferty A, Sajjia M, Olabi AG (2016) Properties of glass materials. In: Reference module in materials science and materials engineering. Elsevier Inc. https://doi.org/10.1016/B978-0-12-803581-8.03998-9

Hassan GM, Sharaf MA (2005) ESR dosimetric properties of some biomineral materials. Appl Radiat Isot 62(2):375–381

Hassan GM, Sharaf MA, Desouky OS (2004) A new ESR dosimeter based on bioglass material. Radiat Meas 38(3):311–315

https://www.nrc.gov/reading-rm/basic-ref/glossary/lethal-dose-ld.html. Access December 2021

https://www.statista.com/statistics/274774/forecast-of-mobile-phone-users-worldwide. Access December 2021

International Commission on Radiation Units and Measurements (2019) ICRU report 94, methods for initial-phase assessment of individual doses following acute exposures to ionizing radiation

ISO 13304-2:2020, Radiological protection—minimum criteria for electron paramagnetic resonance (EPR) spectroscopy for retrospective dosimetry of ionizing radiation—part 2: ex vivo human tooth enamel dosimetry (2020)

Ivannikov AI, Sanin D, Nalapko M, Skvortsov VF, Stepanenko VF, Tsyb AF, Trompier F, Zhumadilov K, Hoshi M (2010) Dental enamel EPR dosimetry: comparative testing of the spectra processing methods for determination of radiation-induced signal amplitude. Health Phys 98(2):345–351

Juniewicz M, Ciesielski B, Marciniak A, Prawdzik-Dampc A (2019) Time evolution of radiation-induced EPR signals in different types of mobile phone screen glasses. Radiat Environ Biophys 58(4):493–500

Juniewicz M, Marciniak A, Ciesielski B, Prawdzik-Dampc A, Sawczak M, Boguś P (2020) The effect of sunlight and UV lamp exposure on EPR signals in X-ray irradiated touch screens of mobile phones. Radiat Environ Biophys 59(3):539–552

Karaaslan H, Engin B (2021) ESR dosimetric properties of gamma irradiated different origin eyeglass samples. Appl Radiat Isot. https://doi.org/10.1016/j.apradiso.2021.109987

Kinoshita A, Calcina CSG, Sakamoto-Hojo ET, Camparato ML, Cesar Picon C, Baffa O (2002) ESR and FISH dose estimation in an accidental case of partial body irradiation with gamma radiation. Adv ESR Appl 18:211–213

Kortmis MV, Maltar-Strmecki N, Maltar-Strmecki N (2018) ESR response of soda-lime glasses irradiated with gamma radiation in the 0.5–20.0 Gy range. Radiat Eff Defect S 173(11–12):978–985

Kortmiš MV, Maltar-Strmečki N (2019) Dose reconstruction from ESR signal of gamma-irradiated soda-lime glass for triage application. Radiat Prot Dosim 186(1):88–93

Krefft K, Drogoszewska B, Kaminska J, Juniewicz M, Wołąkiewicz G, Jakacka I, Ciesielski B (2014) Application of EPR dosimetry in bone for ex vivo measurements of doses in radiotherapy patients. Radiat Prot Dosim 162(1–2):38–42

Kriedl NJ, Blair GE (1956) Recent developments in glass dosimetry. Nucleonics (US) Ceased publication 1956, 14

Kulka U, Abend M, Ainsbury E, Badie C, Barquinero JF, Barrios L, Beinke C, Bortolin E, Cucu A, De Amicis A, Domínguez I (2017) RENEB–running the European Network of biological dosimetry and physical retrospective dosimetry. Int J Radiat Biol 93(1):2–14

Le Gac A, Boizot B, Jégou C, Peuget S (2017) Aluminosilicate glasses structure under electron irradiation: an EPR study. Nucl Instrum Methods Phys Res B 407:203–209

Liu YL, Huo MH, Ruan SZ, Su KJ, Zhang WY, Jiao L (2019) EPR dosimetric properties of different window glasses. Nucl Instrum Methods B 443:5–14

Longo A, Basile S, Brai M, Marrale M, Tranchina L (2010) ESR response of watch glasses to proton beams. Nucl Instrum Methods Phys Res B 268(17–18):2712–2718

López M, Martín M (2011) Medical management of the acute radiation syndrome. Rep Pract Oncol Radiother 16:138–146

Marciniak A, Ciesielski B, Czajkowski P, Krefft K, Boguś P, Prawdzik-Dampc A, Lipniewicz J (2018) EPR dosimetry in nail samples irradiated in vivo during total body irradiation procedures. Radiat Meas 116:24–34

Marciniak A, Ciesielski B, Juniewicz M, Prawdzik-Dampc A, Sawczak M (2019) The effect of sunlight and UV lamps on EPR signal in nails. Radiat Environ Biophys 58(2):287–293

Marrale M, Longo A, D'oca MC, Bartolotta A, Brai M (2011) Watch glasses exposed to 6 MV photons and 10 MeV electrons analysed by means of ESR technique: a preliminary study. Radiat Meas 46(9):822–826

Marrale M, Longo A, Brai V, Tomarchio E (2012) ESR response of watch glasses to neutron irradiation. Nuclear Instrum Methods Phys Res 292:30–33

McKeever SWS, Sholom S, Chandler JR (2019) A comparative study of EPR and TL signals in Gorilla® glass. Radiat Prot Dosim 186(1):65–69

Moghaddam AR, Shamsaei M, Amraei R (2012) Preliminary study of window silicate glass powder for EPR dosimetry with 10-MeV electron beam irradiation. Nucl Instrum Meth B 274:135–138

Muralidhara RS, Kesavulu CR, Rao JL, Anavekar RV, Chakradhar RPS (2010) EPR and optical absorption studies of Fe^{3+} ions in sodium borophosphate glasses. J Phys Chem Solids 71:1651–1655

Padlyak B (2000) Radiation-induced paramagnetic centers in Bioglass®. Opt Appl 30(4):709–717

Port M, Kulka U, Wojcik A, Barquinero F, Endesfelder D, Moquet J, Oestreicher U, Siebenwirth C, Terzoudi G, Trompier F, Vral A, Abend M (2021) Reneb inter-laboratory study on biological and physical dosimetry employing eight assays. In: 67th annual international meeting connected by science, October 3–6, 2021, S12-05

Pukhkaya V, Trompier F, Ollier N (2014) New insights on P-related paramagnetic point defects in irradiated phosphate glasses: impact of glass network type and irradiation dose. J Appl Phys 116(12):123517

Ranjbar AH, Charles MW, Durrani SA, Randle K (1996) Electron spin resonance and thermoluminescense dosimetry of clear fused quartz: its possible use for personal, high dose and high temperature dosimetry. Radiat Prot Dosim 65(1–4):351–354

Ranjbar AH, Durrani SA, Randle K (1999) Electron spin resonance and thermoluminescence in powder form of clear fused quartz: effects of grinding. Radiat Meas 30:73–81

Ranjbar AH, Aliabadi R, Amraei R, Tabasi M, Mirjalily G (2009) ESR response of bulk samples of clear fused quartz (CFQ) material to high doses from 10 MeV electrons: Its possible application for radiation processing and medical sterilization. Appl Radiat Isot 67(6):1023–1026

Rea ME, Gougelet RM, Nicolalde RJ, Geiling JA, Swartz HM (2010) Proposed triage categories for large-scale radiation incidents using high-accuracy biodosimetry methods. Health Phys 98(2):136–144

Romanyukha A, Mitchell CA, Schauer DA, Romanyukha L, Swartz HM (2007) Q-band EPR biodosimetry in tooth enamel microsamples: feasibility test and comparison with X-band. Health Phys 93(6):631–635

Ruano-Ravina A, Wakeford R (2020) The increasing exposure of the global population to ionizing radiation. Epidemiology 31(2):155–159

Schauer DA, Desrosiers MF, Kuppusamy P, Zweier JL (1996) Radiation dosimetry of an accidental overexposure using EPR spectrometry and imaging of human bone. Appl Radiat Isot 47(11–12):1345–1350

Sholom S, McKeever SWS (2017) Developments for emergency dosimetry using components of mobile phones. Radiat Meas 106:416–422

Sholom SV, Haskell EH, Hayes RB, Chumak VV, Kenner GH (1998) Influence of crushing and additive irradiation procedures on EPR dosimetry of tooth enamel. Radiat Meas 29(1):105–111

Sholom S, Wieser A, McKeever SWS (2019) A comparison of different spectra deconvolution methods used in EPR dosimetry with Gorilla glasses. Radiat Prot Dosim 186(1):54–59

Sleptchonok OF, Nagy V, Desrosiers MF (2000) Advancements in accuracy of the alanine dosimetry system. Part 1. The effects of environmental humidity. Radiat Phys Chem 57(2):115–133

Teixeira MI, Ferraz GM, Caldas LV (2005) EPR dosimetry using commercial glasses for high gamma doses. Appl Radiat Isot 62(2):365–370

Trompier F (2012) Institute for Radiological Protection and Nuclear Safety (IRSN), France. Personal communication at International Workshop on Radiation Dosimetry in Glass, Multibiodose/EURADOS, IRSN, Paris

Trompier F, Sadlo J, Michalik J, Stachowicz W, Mazal A, Clairand I, Rostkowska J, Bulski W, Kulakowski A, Sluszniak J, Gozdz S, Wojcik A (2007) EPR dosimetry for actual and suspected overexposures during radiotherapy treatments in Poland. Radiat Meas 42:1025–1028

Trompier F, Bassinet C, Wieser A, De Angelis C, Viscomi D, Fattibene P (2009) Radiation-induced signals analysed by EPR spectrometry applied to fortuitous dosimetry. Ann Inst Super Sanita 45(3):287–296

Trompier F, Della Monaca S, Fattibene P, Clairand I (2011a) EPR dosimetry of glass substrate of mobile phone LCDs. Radiat Meas 46:827–831

Trompier F, Bassinet C, Della Monaca S, Romanyukha A, Reyes R, Clairand I (2011b) Overview of physical and biophysical techniques for accident dosimetry. Radiat Prot Dosim 144(1–4):571–574

Trompier F, Fattibene P, Woda C, Bassinet C, Bortolin E, De Angelis C, Della Monaca S, Viscomi D, Wieser A (2012) Retrospective dose assessment in a radiation mass casualty by EPR and OSL in mobile phones In: Proceedings of the 13th IRPA international congress, Glasgow, May 14–18, 2012, pp 13–18

Trompier F, Burbidge C, Bassinet C, Baumann M, Bortolin E, De Angelis C, Eakins J, Della SM, Fattibene P, Quattrini MC (2017) Overview of physical dosimetry methods for triage application integrated in the new European network RENEB. Int J Radiat Biol 93(1):65–74

Wieser A, Regulla DF (1990) Ultra high level dosimetry by ESR spectroscopy of crystalline quartz and fused silicate. Radiat Prot Dosim 34(1–4):291–294

Wieser A, Fattibene P, Trompier F, Brai M, Ciesielski B, De Angelis C, Della Monaca S, Garcia T, Gustafsson H, Hole EO (2015) Analysis of the EPR spectrum of gamma exposed gorilla glass presented at EPR BioDose conference, Hanover, USA, October 4–8, 2015, Poster P7-W

Wu K, Sun CP, Shi YM (1995) Dosimetric properties of watch glass: a potential practical ESR dosemeter for nuclear accidents. Radiat Prot Dosim 59(3):223–225

Wu K, Guo L, Cong JB, Sun CP, Hu JM, Zhou ZS, Wang S, Zhang Y, Zhang X, Shi YM (1998) Researches and applications of ESR dosimetry for radiation accident dose assessment. Radiat Prot Dosim 77(1–2):65–67

frontiers | Frontiers in Public Health

TYPE Original Research
PUBLISHED 17 November 2022
DOI 10.3389/fpubh.2022.1063769

OPEN ACCESS

EDITED BY
Nadica Maltar-Strmečki,
Rudjer Boskovic Institute, Croatia

REVIEWED BY
Hasan Tuner,
Balikesir University, Turkey
Robert Hayes,
North Carolina State University, United States
Hiroshi Yasuda,
Hiroshima University, Japan

*CORRESPONDENCE
Agnieszka Marciniak
amarciniak@gumed.edu.pl

†These authors have contributed equally to this work and share first authorship

SPECIALTY SECTION
This article was submitted to Radiation and Health, a section of the journal Frontiers in Public Health

RECEIVED 07 October 2022
ACCEPTED 28 October 2022
PUBLISHED 17 November 2022

CITATION
Marciniak A, Juniewicz M, Ciesielski B, Prawdzik-Dampc A and Karczewski J (2022) Comparison of three methods of EPR retrospective dosimetry in watch glass.
Front. Public Health 10:1063769.
doi: 10.3389/fpubh.2022.1063769

Comparison of three methods of EPR retrospective dosimetry in watch glass

Agnieszka Marciniak[1*†], Małgorzata Juniewicz[1†], Bartłomiej Ciesielski[1†], Anita Prawdzik-Dampc[2] and Jakub Karczewski[3]

[1]Department of Physics and Biophysics, Medical University of Gdańsk, Gdańsk, Poland, [2]Department of Oncology and Radiotherapy, Medical University of Gdańsk, Gdańsk, Poland, [3]Institute of Nanotechnology and Materials Engineering, Faculty of Applied Physics and Mathematics, Gdańsk University of Technology, Gdańsk, Poland

In this article we present results of our follow-up studies of samples of watch glass obtained and examined within a framework of international intercomparison dosimetry project RENEB ILC 2021. We present three methods of dose reconstruction based on EPR measurements of these samples: calibration method (CM), added dose method (ADM) and added dose&heating method (ADHM). The study showed that the three methods of dose reconstruction gave reliable and similar results in 0.5–6.0 Gy dose range, with accuracy better than 10%. The ADHM is the only one applicable in a real scenario, when sample-specific background spectrum is not available; therefore, a positive verification of this method is important for future use of EPR dosimetry in glass in potential radiation accidents.

KEYWORDS

EPR, dosimetry, glass, radiation, dose, annealing

Introduction

The increasing use of ionizing radiation in industry, medicine and other areas of everyday life causes the need to control exposure of people to this factor. Despite of the growing awareness of people and use of various safety measures, radiation accidents may occur, where people may be irradiated with dangerously large doses of ionizing radiation. This raises the need for reliable methods of post-accident dosimetry useful in assessment of scale of the accident and in planning medical assistance to exposed people. One of such retrospective methods is based on electron paramagnetic resonance (EPR), which involves the detection and quantification of EPR signals from stable free radicals generated by ionizing radiation. So far, various materials have been studied, both biological, like tooth enamel, bones or nails (1–5), as well as those present in humans' environment (1, 6–14). Materials that come into close contact with humans, such as the screen of a mobile phone or the glass of a watch, are particularly attractive. They have many advantages for potential retrospective dosimetry, such as widespread availability, resistance to water, chemical inertness (10, 15, 16) and non-invasive sampling. However, the reliability of EPR dosimetry in glass requires consideration of several major

confounding factors. One of them is the necessity of individual approach to each sample due to the differences in spectral characteristics of the native background (BG) signal and the radiation-induced signal (RIS) in different types of glasses. The more that their types are usually difficult to identify by simple methods. This is a significant obstacle in application of this method in a real scenario, when one can examine only the very sample, which had been irradiated in the accident and another, unirradiated samples of the same type of glass are not available. Consequently, the lack of information about the sample's background signal, which is crucial for accuracy of dosimetry, can prevent application of this method. The tests of retrospective EPR dosimetry in glasses presented so far in the literature (6) were carried out in laboratory conditions (i.e., using the CM), when the background signal of the tested glass was available and dose calibration was done by irradiation of unexposed glass of the same type.

Annealing of irradiated glass samples at high temperatures (above 200 °C) in order to recover their BG signal by elimination of the dosimetric component (RIS) have already been proposed by various researchers in: watch glass (17), window glass (16, 18, 19), bioactive glass (Bio-G) (20), fused quartz (21), glass test tubes (22), mineral glass from mobile phone (8) and glass from phones' LCDs screens (10). However, applicability of this method, which can be successfully applied only, if the annealing bleaches out the RIS and does not affect the shape of BG signal, has not been yet verified experimentally.

This article presents results of verification of the procedure of dose reconstruction using three methods for watch glasses irradiated with an unknown dose of ionizing radiation: (1) calibration method (CM), (2) added dose method (ADM) and (3) added dose&heating method (ADHM).

In a real scenario of a radiation accident, it is the most probable that retrospective dosimetry would have to be based only on the samples irradiated in the accident, without a possibility to use unirradiated glass samples of the same type for determination of the BG signal and for calibration of the RIS. Therefore, in a real scenario the ADHM can be the only applicable method. In this article we compare results of retrospective dosimetry obtained with the three mentioned above methods.

Materials and methods

Samples

The examined watch glass samples were delivered by organizers of international inter-comparison project RENEB ILC 2021 (23) in which we participated.

The elemental composition of the watch glass, as determined by Energy Dispersive Spectroscopy (EDS) at the Institute of Nanotechnology and Materials Engineering of the Gdańsk University of Technology, was: 27.5% Si, 11.0% Na, 2.5% Mg, 1.0% Al, 1.0% K, 3.0% Ca and 54.0% O. The measurement uncertainty was 0.5% for all elements except oxygen, for which the uncertainty was 3.0%.

Before EPR measurements the glasses were cut into small pieces, crushed in agate mortar and sieved to the final grain size in the interval of 0.5–2 mm. It was reported, that such crushing did not generate any EPR signal in glass (1, 10, 15).

EPR measurements and spectrometer settings

The EPR measurements were carried out at room temperature with a Bruker EMX-6/1 spectrometer in X-band with a cylindrical cavity of type 4119HS W1/0430 using the following acquisition parameters: 350.5 mT central magnetic field; 9.88 GHz microwave frequency; 32 mW microwave power; 100 kHz modulation frequency; 0.5 mT modulation amplitude; 163.84 ms time constant and 81.92 sweep time, 5 averaged scans per one spectrum. The 150–180 mg samples were positioned in the central region of the EPR cavity in a quartz EPR tube of 4 mm inner diameter. Each sample was measured at three orientations of the sample tube in the cavity and the spectra were averaged. Intracavity standard sample (Mn^{2+} in MgO) was measured simultaneously with all samples and can be seen as two sharp lines at the spectra wings in the presented signals (Figures 3, 5, 6A).

Data analysis

Quantitative analysis of the spectra (alignment and normalization of their amplitudes to the standard's lines and sample mass, subtractions of the empty tube spectrum, averaging, numerical decompositions of the spectra) was carried out using Microsoft Office Excel 2016. Numerical fitting/decomposition of the experimental spectra into the BG and RIS components, as described in Marciniak et al. (12), was performed using the Reglinp procedure in Excel.

Irradiations

All samples were irradiated at room temperature with single doses in a Maxishot SPE X-ray cabin (Yxlon, Hamburg, Germany) using 3 mm beryllium and 3 mm aluminum filters, an accelerating potential of 240 kV with half value layer (HVL) 0.630 ± 0.025 mm of copper[1]. The examined samples were

1 Abend Michael. Bundeswehr Institute of Radiobiology, Munich. Information distributed to participants of the RENEB 2021 Interlaboratory Comparison project; 2021.

10.3389/fpubh.2022.1063769

of two types: blinded (with the doses revealed to participants only after reporting of the results), which were exposed to X-rays to doses 0 Gy, 1.2 Gy, and 3.5 Gy, and calibration samples irradiated with known doses of 0.0, 0.5, 1.0, 2.0, 3.0, and 6.0 Gy – in terms of kerma in air.

Annealing of the samples

Annealing of unirradiated and irradiated samples was performed in a drying oven VWR VENTI-Line with Forced Convection (VL 53, VL 115) at temperature of 200 °C and in a furnace at 250 °C.

Calibration method

The spectra decomposition was performed using the model BG signal measured in an unirradiated (0.0 Gy) sample of the same glass type and the model RIS, which was determined as difference between spectra of the 6.0 Gy and 0.0 Gy calibration samples. Magnitudes of the RIS components determined in the blinded samples were implemented into the calibration lines (represented by liner regression of data points in Figure 4) to reconstruct the unknown doses. The rate of decay of the RIS in time was determined by repetition of measurements of the irradiated samples in time (inset in Figure 4). This decay rate was applied to account for different periods between irradiation and EPR measurements of the blinded and calibration samples, as shown in the Results.

Added dose method

Added dose method (ADM) is applicable when the BG signal is known and the very sample with the unknown dose is used to perform the RIS vs. dose calibration by its additional irradiation with a known dose, instead of the calibration based on separate, dedicated calibration samples.

The radiation sensitivity of the samples was individually calibrated by their re-irradiation with 6 MVp photons from Clinac 2300 (Department of Oncology and Radiotherapy, Medical University of Gdańsk, Poland). The added calibration dose (D_{cal}) was (6.0 ± 0.1) Gy in terms of absorbed dose to water, which is equivalent to (5.17 ± 0.10) Gy in glass [this water-to-glass dose conversion was based on mass absorption coefficients and stopping powers from NIST website (https://www.nist.gov)].

In the spectra decomposition the model RIS was represented by the differential spectrum, i.e., the difference between the samples' EPR spectra measured after and before re-irradiation of the samples with the added dose D_{cal}; the model BG was represented by the spectrum measured in the unirradiated (0.0 Gy) sample.

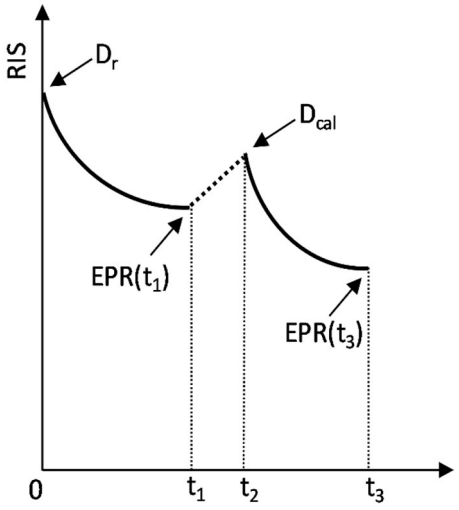

FIGURE 1
Schematic representation of the added dose method. The sample was irradiated at $t = 0$ with the unknown dose D_r, measured at $t = t_1$, re-irradiated at t_2 with the added calibration dose D_{cal} and measured again at $t = t_3$. The arrows marked as $EPR(t_1)$ and $EPR(t_3)$ indicate the two moments of EPR measurements: at t_1 and t_3, which yield two measured RISes: $RIS\,(D_r)$ and $RIS(D_r + D_{cal})$, respectively.

The procedure of ADM is graphically presented in Figure 1.

The unknown dose K_{air} in terms of kerma in air can be reconstructed as follows:

$$RIS(D_r) = k(t_1) \cdot c \cdot D_r \quad (1)$$

$$RIS(D_r + D_{cal}) = k\,(t_3) \cdot c \cdot D_r + k(t_3 - t_2) \cdot c \cdot D_{cal} \quad (2)$$

where:

D_r – the unknown dose in glass;

c – proportionality constant dependent on settings of EPR spectrometer and the spectra decomposition procedure – those conditions were the same for all measurements.

$RIS(D_r)$ – the value of the dosimetric signal generated by the unknown dose D_r, measured before re-irradiation of the samples;

$k\,(t)$ – a function representing decay of the RIS in time t; a single exponential decay was assumed, i.e., by the function $k\,(t) = a_0 + a_1 \cdot e^{-\frac{t}{a_2}}$, with $a_0 = 0.10607$, $a_1 = 0.09368$ and $a_2 = 20.48925$ (inset in Figure 4) for time t given in days. The numerical values for a_0, a_1 and a_2 were obtained from dependence of the slope of the calibration lines on time. Taking into account direct proportionality between the RIS and dose (as shown in Figure 4), relative changes in the RIS are the same, as relative changes in the slope. However, the changes in the slope (which is a resultant of several data points for various samples

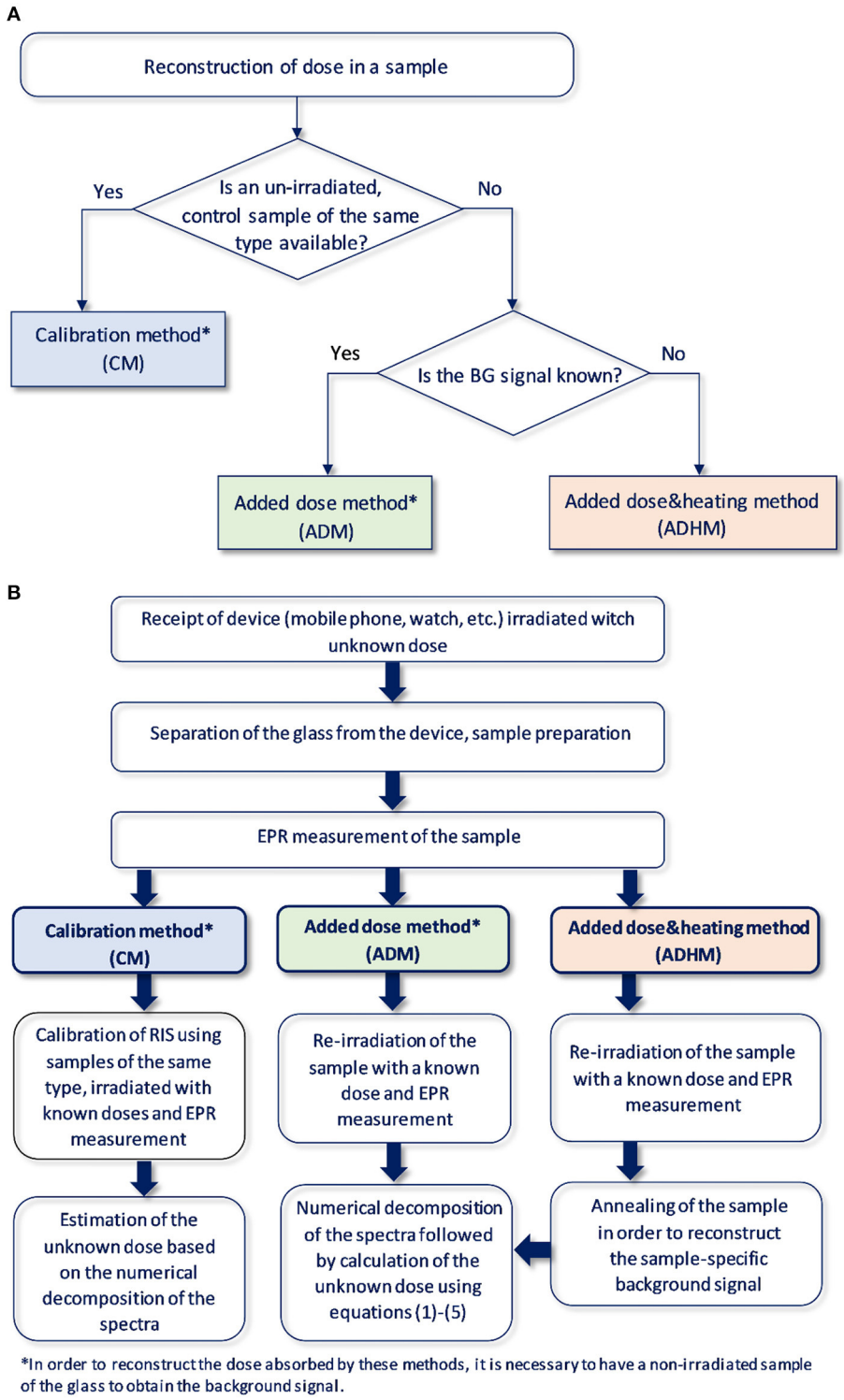

FIGURE 2
(A) Logical diagram for selection of the method of reconstructing the absorbed dose in the glass depending on the available information and the tested material. **(B)** Schematic illustration of the dose reconstruction procedure.

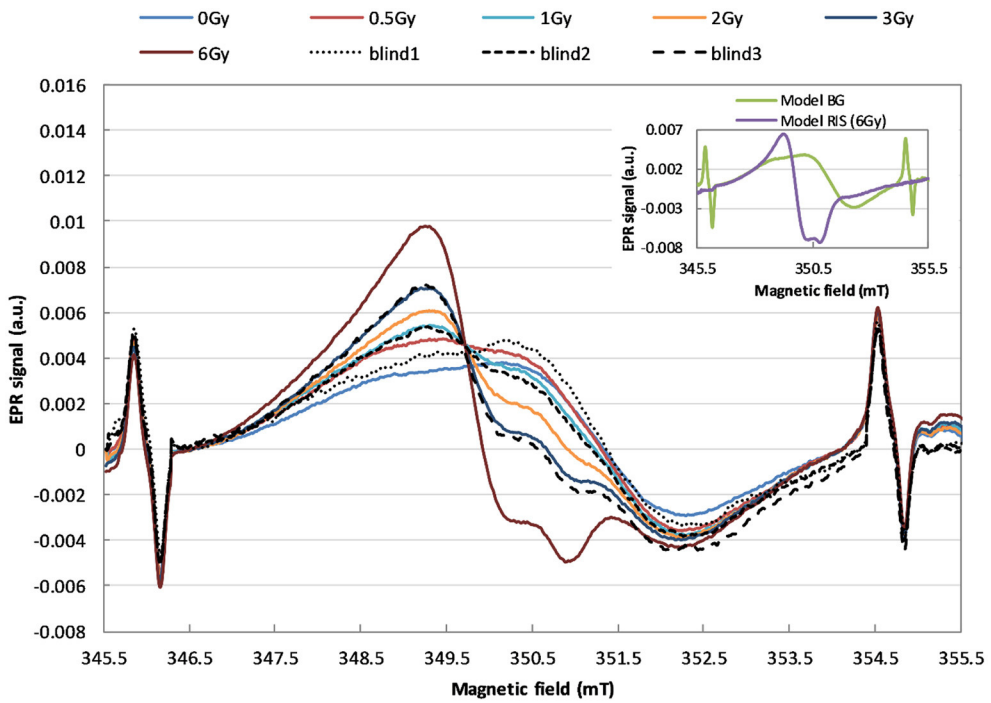

FIGURE 3
EPR spectra demonstrating the effect of irradiation of the watch glass with 240 keV X-rays with doses in the range of 0–6 Gy (in terms of kerma in air). The solid lines refer to the calibration samples, the dashed and dotted lines refer to the blind samples.

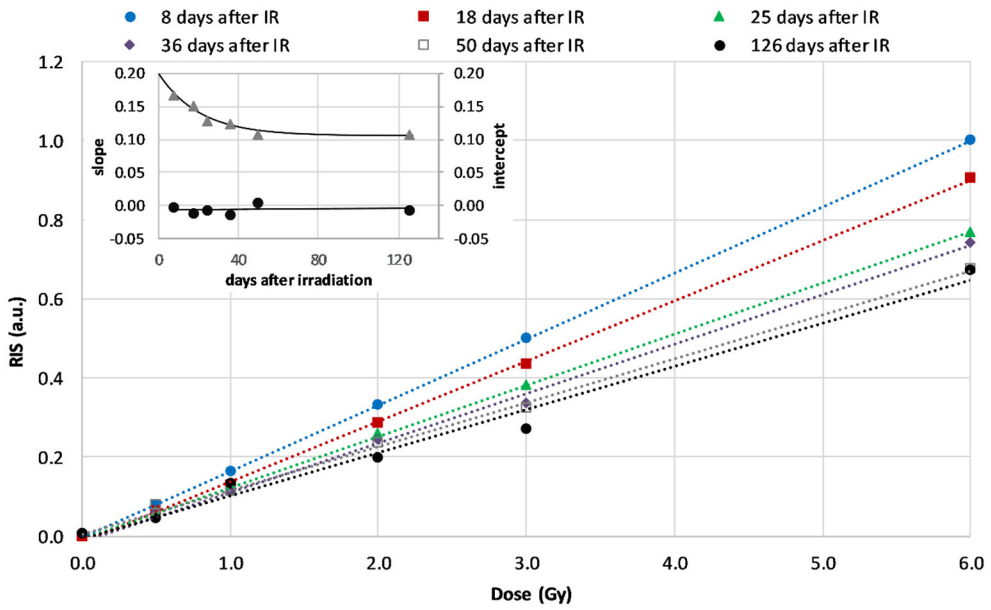

FIGURE 4
Calibration lines for WG measured at 8th, 18th, 25th, 36th, 50th, and 126th day after irradiation (dashed lines are linear regressions of the data). The inset shows time dependence of the slopes (the rate of decay of the RIS, triangles) and intercepts (circles) of the regression lines in the first 126 days after irradiation.

10.3389/fpubh.2022.1063769

with different doses) gives a better statistics in the calculated rate of decay $k(t)$, than calculations of the $k(t)$ based on monitoring decay of RIS in just one dose or sample.

D_{cal} - the known added dose ($D_{cal} = 5.17\ Gy$ in glass);

$RIS(D_r + D_{cal})$ – the value of the dosimetric signal measured after re-irradiation of the glass samples with the added calibration dose D_{cal}.

The solution of those two equations yields:

$$D_r = D_{cal} \cdot \frac{RIS\,(D_r) \cdot k\,(t_3 - t_2)}{RIS(D_r + D_{cal}) \cdot k\,(t_1) - RIS(D_r) \cdot k\,(t_3)} \quad (3)$$

Under electronic equilibrium conditions, the dose D_r in glass can be expressed in terms of kerma in air K_{air}:

$$D_r = \left(K^{glass}_{air}\right)_{240kV} \cdot K_{air} \quad (4)$$

where the proportionality factor $\left(K^{glass}_{air}\right)_{240kV} = 2.43$ represents ratio of mass absorption coefficients of glass and air, calculated using data from NIST Standard Reference Database 124 and 126 (https://www.nist.gov) for air and the elements of glass at 66 keV (i.e., the photon energy with HVL= 0.63 mm Cu). Finally one gets:

$$K_{air} = \frac{D_{cal}}{\left(K^{glass}_{air}\right)_{240kV}} \cdot \frac{RIS(D_r) \cdot k(t_3 - t_2)}{RIS\left(D_r + D_{cal}\right) \cdot k(t_1) - RIS(D_r) \cdot k(t_3)} \quad (5)$$

Added dose&heating method

In this method (ADHM) the dose was reconstructed by samples' re-irradiation, as described above for the ADM, with the difference that the BG spectrum in the decomposition procedure was approximated by bleaching out the RIS in the irradiated samples by their annealing at 200 °C or at 250 °C for 4–60 min.

A summary of the above outlined dose reconstruction procedures is shown schematically in the Figure 2.

Results

EPR spectra of the six calibration samples (0.0, 0.5, 1.0, 2.0, 3.0, and 6.0 Gy) and three blind samples (0.0, 1.2, and 3.5 Gy) are presented in Figure 3.

The two model spectral components, BG and RIS, which overlap with various relative contributions (depending on the dose) in those spectra, are shown in the inset in Figure 3.

TABLE 1 Comparison of the reconstructed doses using calibration method (CM), added dose method (ADM) and added dose&heating method (ADHM).

Samples	Real K_{air} [Gy]	Dose estimate by CM [Gy]	Dose estimate by ADM [Gy]	Dose estimate by ADHM [Gy]
Blind 1	0	−0.05	0.63	
Blind 2	1.2	1.03	1.39	
Blind 3	3.5	3.16	3.70	3.19
Cal dose 0.5	0.5		0.47	
Cal dose 1.0	1.0		1.07	
Cal dose 3.0	3.0		3.12	

The gray shadow indicates empty fields in the table (with no data).

The doses in the blind samples #1, #2, and #3 were determined with two methods based on knowledge of the BG signal, which was measured in an unirradiated glass sample: (1) the calibration method (CM) based on calibration of the RIS using the six calibration samples irradiated by organizers of the RENEB ILC with 240 kV X-rays (the same radiation as used for the blind samples), (2) the method of added dose (ADM) using re-irradiation of the samples with 6 Gy (in terms of dose in water) by 6 MV X-rays from the Clinac. In the added dose&heating method (ADHM), the BG spectrum used in numerical decomposition was approximated by EPR spectra from the irradiated samples, in which the RIS was bleached out by annealing at 200 or 250 °C.

Calibration method

Figure 4 shows the dose dependence of the RIS for the WG calibration samples measured 8, 18, 25, 36, 50, and 126 days after irradiation. The decay of RIS in time caused changes in the course of the calibration lines, mainly a drop in their slope while intercept of the regression lines shown in Figure 4 did not change (as shown in the inset). The dashed lines represent linear regression of the data. The uncertainty of the plotted data was less than 1%, therefore the error bars are not shown in Figure 4.

The dependence of the course of those lines (their slopes and intercepts) on time after irradiation was applied to reconstruct the doses in samples measured at days different than those reflected in Figure 4. The blind doses reported in the RENEB ILC were determined from measurements performed on 7^{th} and 11^{th} day and their averaged values are given in the third column of Table 1.

Added dose method

From the values of the dosimetric signals [$RIS(D_r)$ and $RIS(D_r + D_{cal})$] determined in EPR spectra measured before

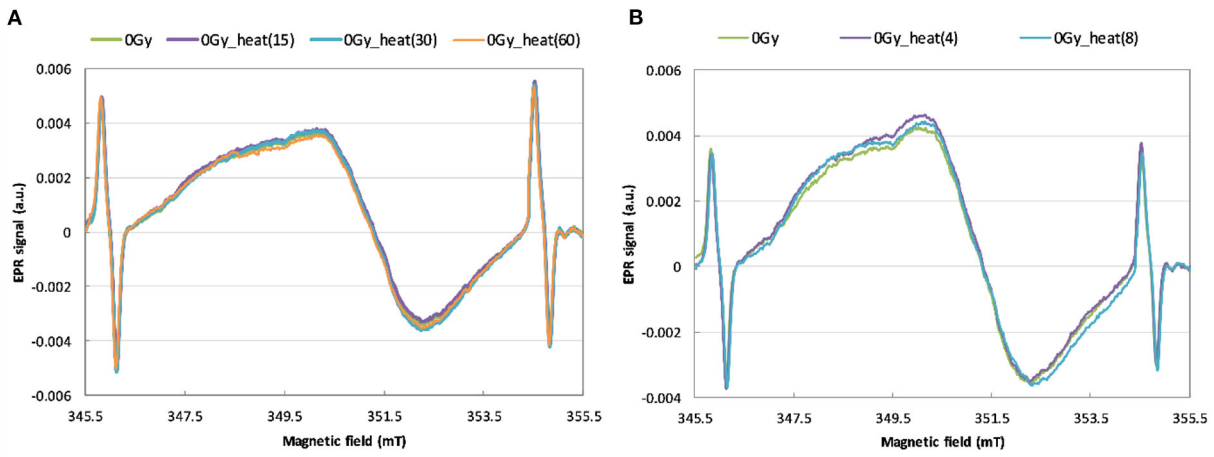

FIGURE 5
EPR spectra of unirradiated WG samples before and after annealing for 15, 30 and 60 min at 200 °C **(A)** and for 4 and 8 min at 250 °C **(B)**.

and after re-irradiation with the known dose (D_{cal}) the unknown doses were reconstructed using equations (1)–(5).

The fourth column of Table 1 presents doses reconstructed by the ADM following re-irradiation of the samples with $D_{cal} = 5.17\ Gy$ after 41 days (for the 0.5 Gy, 1 Gy and 3 Gy calibration samples) and 407 days (for the three blind samples) after the first irradiation of those samples by the 240 kV X-rays (during the RENEB ILC). Those re-irradiations were followed by EPR measurements on the next day – i.e. in the equation (5) the values of t were $t_1 = 8$, $t_2 = 41$, and $t_3 = 42$ days for the 0.5 Gy, 1 Gy, and 3 Gy calibration samples and $t_1 = 407$, $t_2 = 407$, and $t_3 = 408$ for the blind samples.

Added dose&heating method

In order to use the heating method for reconstruction of an unknown dose, it is necessary to check whether the heating of a non-irradiated sample affects the intensity and shape of its EPR signal. Figures 5A,B show the effects of annealing of the unirradiated WG samples on their EPR spectra.

Figure 6 shows the effect of annealing at 200 °C and at 250 °C on spectra of the WG samples irradiated by 6 MVp photons with dose 3.1 *Gy* in glass. The changes in the EPR signal upon annealing up to 45 min is shown in Figure 6A. The corresponding decrease in the RIS component in time of the heating is shown in Figure 6B.

The EPR signal from the irradiated and annealed sample (spectra shown in Figure 6A) was used instead of the original BG (i.e., from unirradiated glass) in the numerical decomposition to reconstruct the dose by the calibration method (CM) and added dose method (ADM) for the three blind samples. The results are presented in Table 2 (columns 3–8). The real delivered doses are given in the second column (in terms of kerma in air).

The dose reconstruction procedure by ADHM method, with recovery of the BG signal by annealing, was performed for one blind sample (Blind 3). It was first re-irradiated with a calibration dose $D_{cal} = 5.17\ Gy$, measured and then heated for 10 min at 250 °C for determination of its BG signal. As a result, the dose of 3.19 Gy was reconstructed, as shown in the last column of Table 1.

Discussion

As can be noticed in Figure 3, X-rays cause evident changes in the shape of EPR lines in the exposed WG samples. Analysis of the spectra presented in inset of Figure 3 proves that shape of the radiation-induced component is spectrally different than the BG signal. This indicates sensitivity of this type of glass to ionizing radiation and its potential applicability in retrospective dosimetry.

The dose dependence of the RISs for the WG samples measured up to 126 days after their irradiation for the purpose of calibration, are presented in Figure 4. The dose dependence is linear within the studied dose range (0–6 Gy). The rapid decay of slope of those calibration lines within the first 30 days after irradiation reflects a rapid decay of RIS. This is in accordance with observations of Juniewicz et al. (15), who also reported rapid decay of RIS within the first 10 days after irradiation. The greatest decay (about 30%) of the RIS was observed up to 50 days after irradiation. The signals measured 4 and 13 months later (on 126^{th} and 408^{th} day after irradiation) did not differ significantly from those measured on the 50^{th} day.

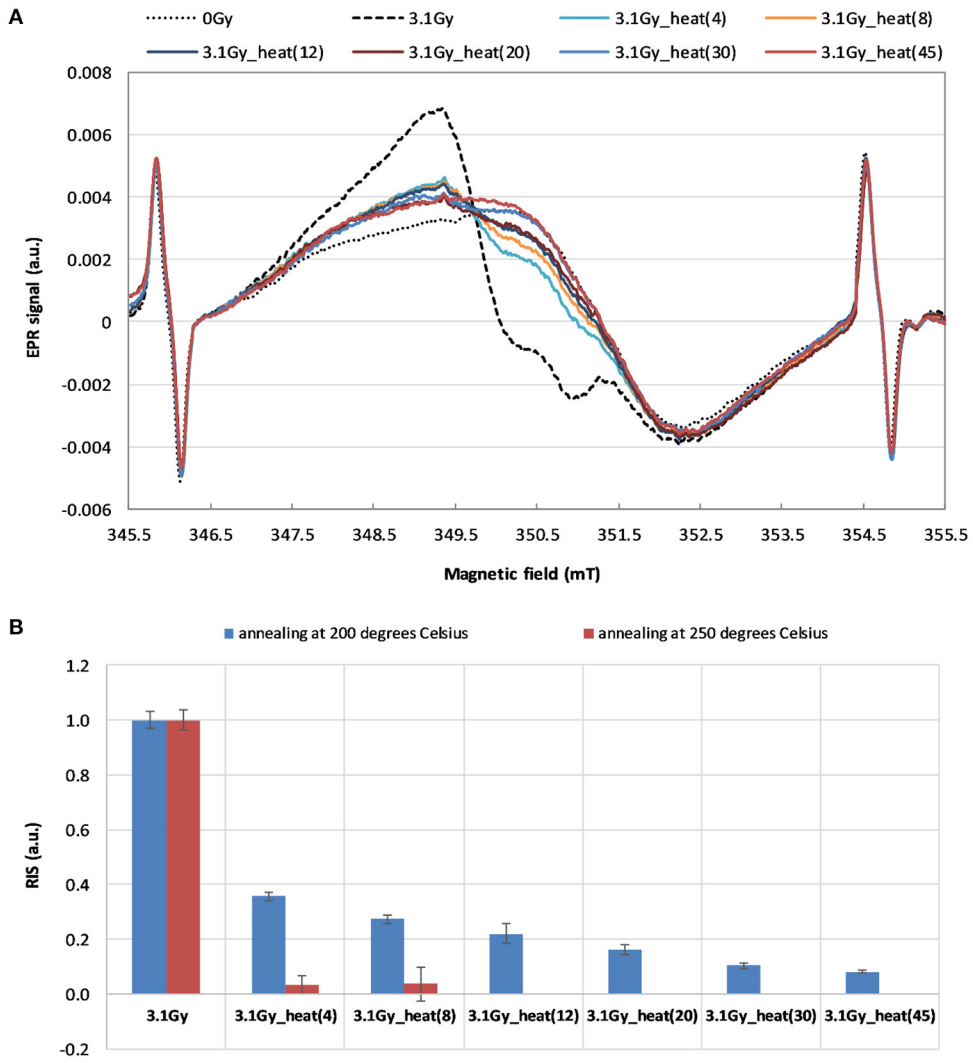

FIGURE 6
(A) The effect of time of annealing at 200 °C on the EPR spectra of the irradiated sample (3.1 Gy 232 in glass). **(B)** The dependence of the RIS component on duration of the annealing at 200 °C (for 4, 8, 12, 233 20, 30 and 45 min) and at 250 °C (for 4 and 8 min). The spectra in **(A)** and the data in **(B)** were marked according to headings of the respective columns in Table 2.

As can be noticed in Figure 5, no changes in shape and intensity of the spectra were observed after annealing up to 200 °C and 250 °C of the unirradiated watch glass samples. In contrary to our results obtained for WG, McKeever et al. (24) observed a rapid decay of the BG signal in Gorilla Glass samples at about 350–375 °C. Also Trompier et al. (10) observed an additional, heat-induced spectral component in spectra of glass substrates from mobile phones – in both irradiated and non-irradiated samples.

The data presented in Figures 6A,B shows that the 45 min of annealing at 200 °C reduces the RIS signal by more than 90%. Only 4 min of annealing the irradiated WG sample at 250 °C caused almost complete elimination of the RIS component (Figure 6B). Our results are consistent with the results described by Wu et al. (17) for watch glass, who showed that heating at 200 °C for one hour completely removed the dosimetric component. The results obtained in this study confirm a lack of influence of the annealing on the native BG signal of watch glass – neither on its shape nor intensity. The observed elimination of the RIS component in the irradiated samples' spectra by their annealing, together with resistance of the BG signal to annealing, are very advantageous features of the examined watch glass. This gives a unique possibility of reconstructing the dose absorbed in a real radiation accident, when the native background signal (BG) of the tested sample, which is necessary for accurate dose reconstruction, is not available. The ultimate verification of this

10.3389/fpubh.2022.1063769

TABLE 2 Comparison of the doses (in terms of kerma in air) reconstructed for 3 blind samples using a model BG signal recovered by heating of irradiated (3.1 Gy) sample for 4–45 min at 200 °C and for 4 and 8 min at 250 °C (a) by calibration method and (b) by added dose method.

(a) Calibration method

Samples	K_{air} [Gy]						
	Real dose	Reconstructed dose using a model BG signal recovered by heating time (min)					
		heat (4)	heat (8)	heat (12)	heat (20)	heat (30)	heat (45)
Annealing at 200 °C							
Blind 1	0	−1.7	−1.3	−1.1	−0.8	−0.6	−0.5
Blind 2	1.2	−0.4	0	0.2	0.5	0.7	0.8
Blind 3	3.5	1.8	2.1	2.4	2.6	2.8	2.9
Annealing at 250 °C							
Blind 1	0	−0.3	−0.4				
Blind 2	1.2	1.0	0.9				
Blind 3	3.5	3.1	3.1				

(b) Added dose method

Samples	K_{air} [Gy]						
	Real dose	Reconstructed dose using a model BG signal recovered by heating time (min)					
		heat (4)	heat (8)	heat (12)	heat (20)	heat (30)	heat (45)
Annealing at 200 °C							
Blind 1	0	−2.81	−2.03	−1.54	−0.87	−0.40	−0.12
Blind 2	1.2	−1.45	−0.69	−0.23	0.34	0.71	0.94
Blind 3	3.5	1.58	2.27	2.68	3.23	3.57	3.76
Annealing at 250 °C							
Blind 1	0	0.43	0.40				
Blind 2	1.2	1.35	1.32				
Blind 3	3.5	4.13	4.07				

The gray shadow indicates empty fields in the tables (with no data).

approach in dose reconstruction is presented in Tables 1, 2 by comparison of the real and reconstructed doses.

From the data presented in Table 1 it can be concluded that the CM and ADM methods of dose reconstruction gave similar results. The reconstructed doses, with exception of the sample Blind 1 measured with ADM, differed at most by 0.34 Gy (about 10% in sample Blind 3, CM) from the real doses. The worst result was obtained for the sample Blind 1 using the ADM - the discrepancy between the real dose (0.0 Gy) and the reconstructed dose (0.63 Gy) resulted from very noisy spectra of this sample. The dose reconstructed by heating method in the Blind 3 sample was 3.19 Gy. An almost identical result was obtained with the calibration method (3.16 Gy).

Table 2 shows the doses reconstructed for the three blind samples using the calibration and the added dose procedures while EPR spectra measured in the annealed sample were used as the model BG signal instead of the original background from an unirradiated sample. As it could be expected, with increase in time of annealing the reconstructed doses were approaching the real ones. Annealing for 4 min at 250 degrees or for 20 min at 200 degrees allowed for reliable reconstruction of the dose in the sample Blind 3 (with 9% deviation from the real dose). It should be emphasized, that only the ADHM method can be used in a real scenario, when one has only one glass sample to measure, the one irradiated during the accident, and its specific BG spectrum is unknown.

Summarizing the presented results, it can be concluded that, the results obtained with the three tested methods show similar accuracy of about 0.3 Gy, sufficient for a reliable triage of people exposed in radiation accidents. Background signal of the examined watch glass was resistant to temperatures up to 250 °C, which gives the possibility to use the heating method to recover the background signal from irradiated samples in a real scenario. The ADHM is the only one, which allows to reconstruct absorbed dose if only one glass sample, the one irradiated during the accident, is available. Applicability of this method for other types of glasses requires verification of the background stability at high temperature. Moreover, as it results from previous reports (24, 25), an important factor disturbing a reliable dose reconstruction in glasses may be the effect of UV light. Therefore, additional research is necessary to assess applicability of the annealing in EPR dosimetry in glasses exposed to UV light.

Data availability statement

The raw data supporting the conclusions of this article will be made available by the authors, without undue reservation.

Author contributions

AM, MJ, and BC: EPR measurements, work concept, data analysis, and writing the manuscript. AP-D: reirradiation of samples and dosimetry. JK: Energy Dispersive Spectroscopy (EDS) measurement of elemental composition of watch glass samples. All authors contributed to the article and approved the submitted version.

Funding

This work was supported by Medical University of Gdańsk, Internal Grant ST-70.

Conflict of interest

The authors declare that the research was conducted in the absence of any commercial or financial relationships that could be construed as a potential conflict of interest.

Publisher's note

References

1. Trompier F, Bassinet C, Wieser A, De Angelis C, Viscomi D, Fattibene P. Radiation-induced signals analysed by EPR spectrometry applied to fortuitous dosimetry. *Ann Inst Super Sanita.* (2009) 45:287–96. Available online at: https://pubmed.ncbi.nlm.nih.gov/19861734/

2. Krefft K, Drogoszewska B, Kaminska J, Juniewicz M, Wołakiewicz G, Jakacka I, et al. Application of EPR dosimetry in bone for ex vivo measurements of doses in radiotherapy patients. *Radiat Prot Dosim.* (2014) 162:38–42. doi: 10.1093/rpd/ncu214

3. Kaminska J, Ciesielski B, Drogoszewska B, Emerich K, Krefft K, Juniewicz M. Verification of radiotherapy doses by EPR dosimetry in patients' teeth. *Radiat Meas.* (2016) 92:86–92. doi: 10.1016/j.radmeas.2016.07.005

4. Fattibene P, Callens F, EPR. dosimetry with tooth enamel: a review. *Appl Radiat Isot.* (2010) 68:2033–116. doi: 10.1016/j.apradiso.2010.05.016

5. Marciniak A, Ciesielski B. EPR dosimetry in nails—A review. *Appl Spectrosc Rev.* (2016) 51:73–92. doi: 10.1080/05704928.2015.1101699

6. Fattibene P, Trompier F, Wieser A, Brai M, Ciesielski B, De Angelis C, et al. EPR dosimetry intercomparison using smart phone touch screen glass. *Radiat Environ Biophys.* (2014) 53:311–20. doi: 10.1007/s00411-014-0533-x

7. Teixeira MI, Da Costa ZM, Da Costa CR, Pontuschka WM, Caldas LVE. Study of the gamma radiation response of watch glasses. *Radiat Meas.* (2008) 43:480–2. doi: 10.1016/j.radmeas.2007.11.029

8. Bassinet C, Trompier F, Clairand I. Radiation accident dosimetry on glass by Tl and EPR spectrometry. *Health Phys.* (2010) 98:400–5. doi: 10.1097/01.HP.0000346330.72296.51

9. Trompier F, Bassinet C, Clairand I. Radiation accident dosimetry on plastics by EPR spectrometry. *Health Phys.* (2010) 98:388–94. doi: 10.1097/01.HP.0000346334.78268.31

10. Trompier F, Della Monaca S, Fattibene P, Clairand I, EPR. dosimetry of glass substrate of mobile phone LCDs. *Radiat Meas.* (2011) 46:827–31. doi: 10.1016/j.radmeas.2011.03.033

11. Trompier F, Bassinet C, Della Monaca S, Romanyukha A, Reyes R, Clairand I. Overview of physical and biophysical techniques for accident dosimetry. *Radiat Prot Dosim.* (2011) 144:571–4. doi: 10.1093/rpd/ncq341

12. Marciniak A, Ciesielski B, Juniewicz M, EPR. dosimetry in glass: a review. *Radiat Environ Biophys.* (2022) 61:179–203. doi: 10.1007/s00411-022-00970-w

13. Kortmiš MV, Maltar-Strmečki N. Dose reconstruction from ESR signal of gamma-irradiated soda-lime glass for triage application. *Radiat Prot Dosim.* (2019) 186:88–93. doi: 10.1093/rpd/ncy290

14. Kortmiš MV, Maltar-Strmečki N. ESR response of soda–lime glasses irradiated with gamma radiation in the 05–200 Gy range. *Radiat Effects Defects Solids.* (2018) 173:978–85. doi: 10.1080/10420150.2018.1513003

15. Juniewicz M, Ciesielski B, Marciniak A, Prawdzik-Dampc A. Time evolution of radiation-induced EPR signals in different types of mobile phone screen glasses. *Radiat Environ Biophys.* (2019) 58:493–500. doi: 10.1007/s00411-019-00805-1

16. Liu YL, Huo MH, Ruan SZ, Su KJ, Zhang WY, Jiao L, et al. dosimetric properties of different window glasses. *Nucl Instrum Meth B.* (2019) 443:5–14. doi: 10.1016/j.nimb.2019.01.022

17. Wu K, Sun CP, Shi YM. Dosimetric properties of watch glass: a potential practical ESR dosemeter for nuclear accidents. *Radiat Prot Dosim.* (1995) 59:223–225. doi: 10.1093/oxfordjournals.rpd.a082654

18. Engin B, Aydas C, Demirtas H, ESR. dosimetric properties of window glass. *Nucl Instrum Methods Phys Res b.* (2006) 243:149–55. doi: 10.1016/j.nimb.2005.08.151

19. Gancheva V, Yordanov ND, Karakirova Y. EPR investigation of the gamma radiation response of different types of glasses. *Spectrochim Acta A.* (2006) 63:875–878. doi: 10.1016/j.saa.2005.10.019

20. Hassan GM, Sharaf MA. ESR dosimetric properties of some biomineral materials. *Appl Radiat Isot.* (2005) 62:375–81. doi: 10.1016/j.apradiso.2004.08.013

21. Ranjbar AH, Charles MW, Durrani SA, Randle K. Electron spin resonance and thermoluminescense dosimetry of clear fused quartz: its possible use for personal, high dose and high temperature dosimetry. *Radiat Prot Dosim.* (1996) 65:351–4. doi: 10.1093/oxfordjournals.rpd.a031659

22. Bortolin E, De Angelis C, Quattrini MC, Barlascini O, Fattibene P. Detection of ionizing radiation treatment in glass used for healthcare products. *Radiat Prot Dosim.* (2019) 186:78–82. doi: 10.1093/rpd/ncz014

23. Port M, Kulka U, Wojcik A, Barquinero F, Endesfelder D, Moquet J, et al. Reneb inter-laboratory study on biological and physical dosimetry employing eight assays, Radiation Research Siciety. In: *67th Annual International Meating: Connected by Science.* (2021).

24. McKeever SWS, Sholom S, Chandler JR. A comparative study of EPR and TL signals in Gorilla® glass. *Radiat Prot Dosim.* (2019) 186:65–69. doi: 10.1093/rpd/ncy243

25. Juniewicz M, Marciniak A, Ciesielski B, Prawdzik-Dampc A, Sawczak M, Boguś P. The effect of sunlight and UV lamp exposure on EPR signals in X-ray irradiated touch screens of mobile phones. *Radiat Environ Biophys.* (2020) 59:539–52. doi: 10.1007/s00411-020-00858-7